

Aus der Abteilung Immunbiochemie  
Mannheim Institute for Innate Immunoscience (MI3)  
der Medizinischen Fakultät Mannheim  
Direktorin: Prof. Dr. rer. nat. Adelheid Cerwenka

**Interaction of endothelial cells and innate lymphoid cells in  
hepatic inflammation and cancer**

Inauguraldissertation  
zur Erlangung des Doctor scientiarum humanarum (Dr. sc. hum.)  
der  
Medizinischen Fakultät Mannheim  
der Ruprecht-Karls-Universität  
zu  
Heidelberg

vorgelegt von  
Sophia Georgia Paraskevi Papaioannou

aus  
Mainz, Deutschland

2024

Dekan: Prof. Dr. med. Sergij Goerd  
Referentin: Prof. Dr. rer. nat. Adelheid Cerwenka

# TABLE OF CONTENTS

	Page
1 INTRODUCTION .....	1
1.1 The immune system .....	1
1.1.1 Innate lymphocytes.....	3
1.1.2 NK cells .....	4
1.1.3 Tissue-resident ILC1s.....	7
1.2 The Liver .....	9
1.2.1 Liver Sinusoidal Endothelial Cells (LSECs) .....	10
1.2.2 Immune cells in the liver .....	12
1.2.3 Liver pathologies.....	14
1.3 Chemotaxis and extravasation of immune cells .....	15
2 THE AIM OF THE STUDY .....	17
3 MATERIALS AND METHODS .....	19
3.1 Materials.....	19
3.1.1 Laboratory equipment.....	19
3.1.2 Chemicals and biological reagents .....	19
3.1.3 Cell culture media and solutions.....	20
3.1.4 Cell culture consumables.....	21
3.1.5 Kits.....	22
3.1.6 Buffers and solutions .....	23

3.1.7	Antibodies for flow cytometry .....	25
3.1.8	Antibodies for functional assays .....	28
3.1.9	Oligonucleotide primers .....	29
3.1.10	Tumor cell lines .....	29
3.1.11	Mouse lines .....	30
3.1.12	Software .....	30
3.2	Methods.....	31
3.2.1	Preparation of single cell suspensions.....	31
3.2.2	Magnetic Cell Sorting (MACS) for LSEC purification .....	32
3.2.3	Fluorescence activated cell sorting (FACS) .....	33
3.2.4	Cell counting .....	34
3.2.5	Primary cell culture .....	34
3.2.7	Collection of cell supernatants .....	36
3.2.8	Cell cytotoxicity assay.....	36
3.2.9	Migration Assay .....	37
3.2.10	Flow cytometry .....	38
3.2.11	Flow cytometric analysis.....	39
3.2.12	RNA extraction .....	39
3.2.13	cDNA Synthesis and quantitative real-time-PCR (qPCR).....	39
3.2.14	Quantification of chemokine concentration .....	40
3.2.15	Mouse genotyping .....	41
3.2.16	Experimental mouse models .....	41
3.2.17	Statistical analysis .....	43

4 RESULTS.....	45
4.1 Interaction of LSECs and NK cells in hepatic inflammation .....	45
4.1.1 NK cells, but not ILC1s, are accumulating in the inflamed liver tissue.....	45
4.1.2 NK cells and LSECs are activated during endotoxemia.....	48
4.1.3 LSECs secrete leukocyte-attracting chemokines.....	50
4.1.4 NK cells are the major source of IFN- $\gamma$ in the liver .....	54
4.1.5 NK cells express the chemokine receptor CXCR3.....	56
4.1.6 LSECs attract NK cells by engaging CXCR3 .....	58
4.1.7 The effect of CXCR3 and VCAM-1 on NK cell recruitment to the liver of LPS-treated animals .....	60
4.1.8 Endothelium-derived CXCL10 supports NK cell recruitment to the inflamed liver .....	62
4.2 Interaction of LSECs and innate lymphocytes in hepatic metastasis.....	67
4.2.1 Effect of tumor cells on LSEC phenotype .....	67
4.2.2 LSECs change their cytokine and chemokine profile in response to tumor cell secreted factors .....	68
4.2.3 LSECs reduce NK cell-mediated killing of target cells in a contact-dependent manner .....	70
4.2.4 Effect of LSECs on NK cell phenotype .....	72
4.2.5 Effect of distant, subcutaneous tumors on LSEC phenotype .....	73
4.2.6 Cytokine and chemokine expression by different tumor cell lines.....	76
4.2.7 LSECs and NK cells in hepatic metastases .....	77

5 DISCUSSION .....	79
5.1 Alterations of LSECs in inflammation and metastasis .....	79
5.1.1 The response of LSECs to inflammatory mediators.....	79
5.1.2 LSECs in hepatic cancer and metastasis .....	81
5.2 NK cells and ILC1s in inflammation and metastasis .....	84
5.2.1 NK cells are the major producers of IFN- $\gamma$ in LPS-induced endotoxemia .....	84
5.2.2 NK cells and ILC1s in the liver tumor microenvironment .....	86
5.3 The crosstalk of LSECs and innate lymphocytes .....	88
5.3.1 LSECs regulate NK cell and ILC1 phenotype and function.....	88
5.3.2 Feedback regulation of innate lymphocytes and LSECs mediated by IFN- $\gamma$ .....	90
5.3.3 LSECs support the chemotaxis of NK cells and ILC1s .....	91
6 SUMMARY .....	93
7 REFERENCES .....	95
8 ABBREVIATIONS.....	111
9 CURRICULUM VITAE .....	115
10 ACKNOWLEDGEMENTS.....	117

# 1 INTRODUCTION

## 1.1 The immune system

The immune system is responsible for the defense and combat against pathogens (e.g. bacteria, viruses, fungi and parasites), stressed or transformed cells, and harmful molecules. It comprises a network of cells, tissues and organs that work together to protect the body. Its primary function is to eliminate foreign pathogens, while maintaining a tolerance to normal and healthy tissue. The immune system is divided in two main branches: The innate and the adaptive immune system.

The innate immune system provides an immediate defense mechanism acting through barriers (e.g. mechanical, physical and microbiological), as well as cellular and non-cellular components, such as phagocytes, Natural Killer (NK) cells, and antigen presenting cells (APCs), or the complement, respectively. Upon penetration of pathogens through the barriers, they get recognized and fought by innate immune cells, which include phagocytes (macrophages and dendritic cells), granulocytes (neutrophils, eosinophils, basophils, mast cells), and innate lymphocytes. They express Pattern Recognition Receptors (PRRs), such as Toll-like receptors (TLRs), which recognize Pathogen-Associated Molecular Patterns (PAMPs) and Damage-Associated Molecular Patterns (DAMPs), which are molecular signatures indicative of pathogens or cellular damage, respectively (Li and Wu, 2021). Upon recognition, PRRs initiate intracellular signaling cascades that trigger immune responses, including the production of cytokines, chemokines, and anti-microbial factors. For example, TLR4 mediates the recognition of lipopolysaccharide (LPS), a component of the outer membrane of Gram-negative bacteria (Miyake, 2007). APCs, including macrophages and dendritic cells, capture and process peptides to present antigens via the major histocompatibility complex (MHC) class I and II. Exo- and endogenous particles are endocytosed by APCs by receptor-mediated endocytosis, macropinocytosis or phagocytosis and lysed by the proteasome or the lysosome (Blum et al., 2013). Peptides generated by proteasomal proteolysis are loaded onto MHC I molecules in the endoplasmatic reticulum, whereas peptides generated by lysosomal proteolysis are loaded onto MHC II molecules in the late endosome. Loaded MHC

molecules are then translocated to the membrane and present the antigen to T cells, thereby bridging the innate and the adaptive immune system.

The adaptive immune system offers a more tailored and specific defense mechanism through T cells and B cells, with the ability to recognize and remember specific pathogens (Bonilla and Oettgen, 2010). They develop in primary lymphoid organs (thymus and bone marrow) and traffic to secondary lymphoid organs (spleen and lymph nodes), where they recognize antigens either directly by circulating pathogens or from antigen-presenting APCs. After recognition of antigens, T cells and B cells undergo a process of activation and differentiation. T cells can be divided into CD4<sup>+</sup> and CD8<sup>+</sup> T cells, and can only be activated by recognition of antigens via the T cell receptor (TCR). CD4<sup>+</sup> T cells recognize antigens presented by APCs via MHC II, whereas CD8<sup>+</sup> T cells recognize antigens presented via MHC I. For activation, T cells additionally receive co-stimulation via CD28 by the co-stimulatory molecules CD80 or CD86, expressed by APCs. Depending on the cytokine stimulus as a third signal, CD4<sup>+</sup> T cells then polarize into T helper (Th) cells (Th1, Th2, or Th17 cells), or regulatory T cells (Treg), and CD8<sup>+</sup> T cells differentiate to cytotoxic T cells (Mosmann et al., 1986; Zhu et al., 2010). B cells can get activated via the B cell receptor (BCR) via crosslinking to its specific antigen, and a second signal received from Th cells (den Haan et al., 2014). They are then able to differentiate into plasma cells and produce antibodies that can mark and neutralize antigens via Immunoglobulin (Ig) M, IgD, IgG, IgA and IgE. The first exposure to an antigen primarily leads to the production of low affinity IgM. During affinity maturation and class switching, B cells can produce other Ig isotypes which show a higher affinity. The primary response to an antigen gives rise to memory T and B cells, which can act more quickly to a second exposure.



### 1.1.1 Innate lymphocytes

Innate lymphocytes include NK cells, three innate lymphoid cell (ILC) subsets and lymphoid tissue-inducer (LTi) cells that all differentiate from the common lymphoid progenitor (CLP) and an Id2-expressing common innate lymphoid progenitor (CILP) in the fetal liver and bone marrow (BM) (Figure 1.1) (Diefenbach et al., 2014). Innate lymphocytes are the first line of defense and reflect the innate counterpart to T cells. NK cells differentiate from an NK precursor (NKP) and require the transcription factors T-bet and eomesodermin (Eomes) for their development and maturation. They are circulating in the periphery and patrol lymphoid and non-lymphoid tissues (Gasteiger et al., 2015). They can secrete Interferon- $\gamma$  (IFN- $\gamma$ ) and tumor necrosis factor alpha (TNF- $\alpha$ ) after activation, and can exert cytotoxic functions.

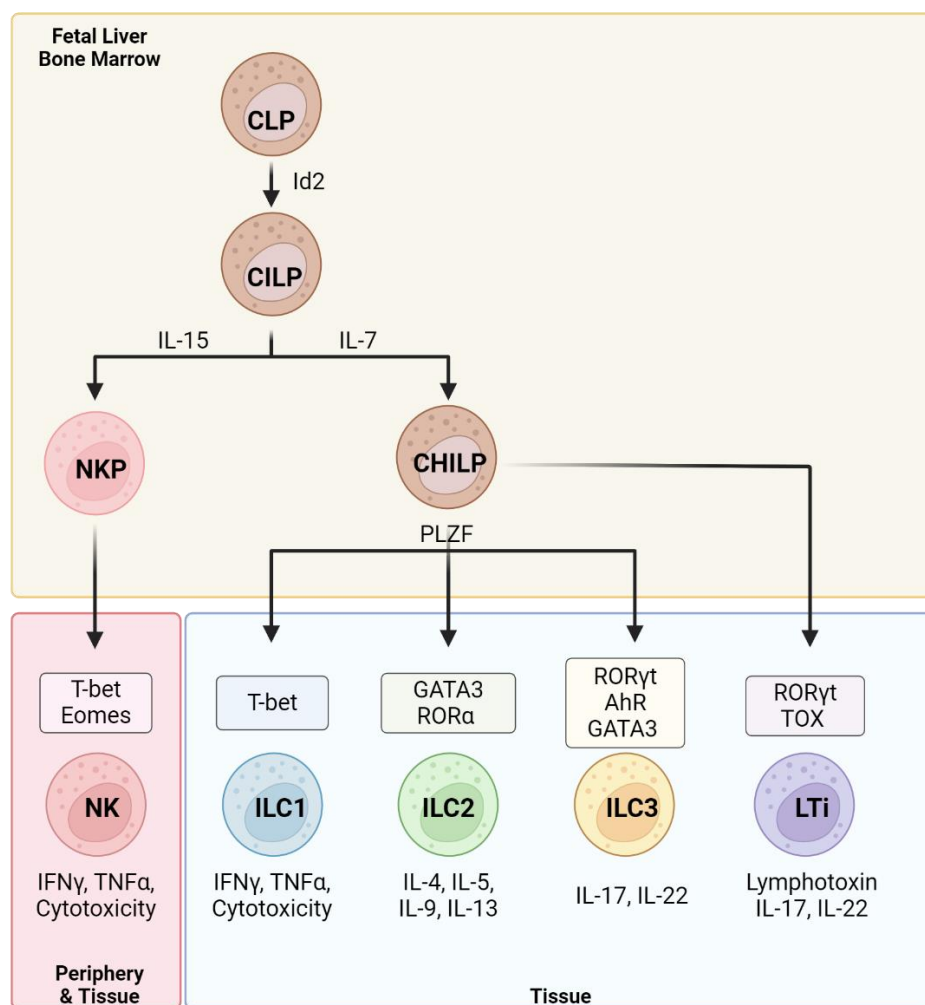


**Figure 1.1 Lineage of innate lymphocytes.** CLP, common lymphoid progenitor; CILP, common innate lymphoid progenitor; NKP, NK progenitor; CHILP, common helper-like innate lymphoid progenitor. (Figure adapted and modified from (Hams et al., 2015))

ILCs develop from a common helper-like ILC progenitor (CHILP) to the distinct classes: ILC1, ILC2 and ILC3, and are tissue-resident (Figure 1.1) (Klose et al., 2014; Spits et al., 2013). They mirror Th cells in the expression of transcription factors and production of cytokines (McKenzie et al., 2014; Robinette et al., 2015). ILC1s share many features with NK cells, as they too express T-bet, but not Eomes, produce IFN- $\gamma$ , and TNF- $\alpha$ , and can exert cytotoxicity. ILC2s express GATA3 and ROR $\alpha$ , and produce the type 2 cytokines IL-5 and IL-13. ILC3 differentiation requires the transcription factor ROR $\gamma$ t. They secrete the cytokines IL-17 and IL-22. LT $\alpha$ i cells can produce lymphotoxin, and are involved in the formation of secondary lymphoid organs. By producing distinct cytokines, ILCs play a crucial role in the initiation of early immune responses against infections, regulation of the adaptive immune system, development of lymphoid tissue, and promotion of tissue homeostasis and repair.

### **1.1.2 NK cells**

Natural Killer (NK) cells circulate throughout the body as part of the innate immune system's surveillance mechanism. Their primary function is to identify and eliminate abnormal cells, such as virus-infected and transformed cells, without the need for prior sensitization or antigen presentation. By circulating in the bloodstream and lymphatic system, NK cells can quickly respond to any potential threat in various tissues and organs. This widespread distribution allows them to patrol the body efficiently, providing a rapid and immediate response to pathogens and abnormal cells, thus contributing to the overall defense against infections and malignancies.

During maturation, murine NK cells follow a series of CD11b and CD27 surface marker expression, dividing them into four subsets. Immature CD11b<sup>lo</sup>CD27<sup>lo</sup> NK cells have a high proliferative potential, but few cytotoxic function. CD11b<sup>lo</sup>CD27<sup>hi</sup> NK cells express Ly49 receptors and the chemokine receptor CX3CR1, whereas CD11b<sup>hi</sup>CD27<sup>hi</sup> NK cells where shown to have the most potent effector functions. Mature NK cells show a CD11b<sup>hi</sup>CD27<sup>lo</sup> expression profile with high effector functions (Chiossone et al., 2009; Hayakawa and Smyth, 2006; Kim et al., 2002).

NK cell activation is regulated by a balance between activating and inhibitory receptors binding to ligands on the target cells (Figure 1.2). The integration of the receiving signals determines, whether the NK cell engages its effector functions (Lanier, 2005). The Ly49 receptor family in mice, which are functionally counterparts of the human killer cell immunoglobulin-like receptors (KIRs), and NKG2A receptor on NK cells primarily recognize self-MHC I molecules in a peptide-dependent, but not peptide-specific manner (Hanke et al., 1999; Karlhofer et al., 1992). Engagement of these receptors inhibits NK cells, thereby preventing the killing of healthy cells. In addition they play a crucial role in licensing of developing NK cells to prevent hyporesponsiveness (Kim et al., 2005). Conversely, activating receptors, such as Ly49H, NKG2D, and NK1.1 and NKp46 engage with stress-induced ligands or viral proteins on target cells, and can trigger NK cell activation (Paul and Lal, 2017). For instance, NKG2D ligands include Rae1, Mult1, and H60, which are upregulated on stressed or infected cells, while Ly49H specifically recognizes the mouse cytomegalovirus (MCMV) protein m157 (Carayannopoulos et al., 2002; Cerwenka et al., 2001; Diefenbach et al., 2000; Dokun et al., 2001; Takada et al., 2008).

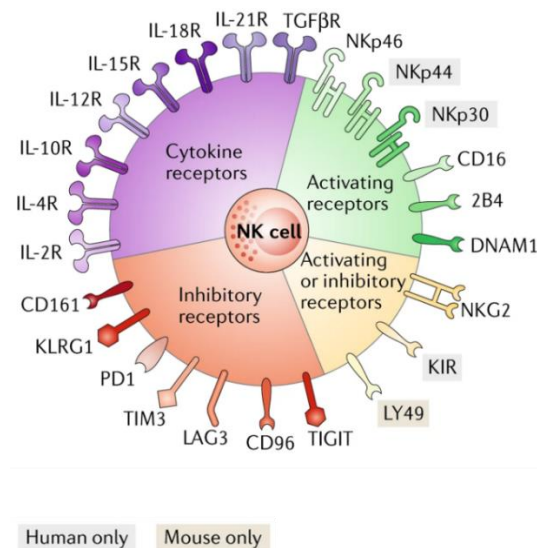


**Figure 1.2 Cell surface receptors expressed by human and murine NK cells.** (Adapted and modified from (Chiossone et al., 2018))

Additionally, NK cells express activating receptors, such as DNAM-1, and the inhibitory receptors CD96, and TIGIT. They bind to their respective ligand CD155, which can be expressed on target cells (Shibuya et al., 1996; Wang et al., 1992; Yu et al., 2009). DNAM-1 and TIGIT have counterbalancing functions, with DNAM-1 amplifying NK cell

anti-tumor responses, and TIGIT limiting IFN- $\gamma$  production and cytotoxicity (Lozano et al., 2012; Stanietsky et al., 2013). Similarly, DNAM-1 and CD96 were also shown to compete for its ligand, with CD96 dampening cytokine responses and IFN- $\gamma$  production in inflammation and metastatic disease (Chan et al., 2014). NK cells have been reported to be suppressed by tumor cells expressing programmed death ligand 1 (PD-L1), and  $\alpha$ PD-1/ $\alpha$ PD-L1 therapies have been shown to improve anti-tumoral and anti-viral functions of NK cells, but the underlying mechanism is yet poorly characterized, as the expression of PD-1 on NK cells seems to be limited and specific to the microenvironment (Bezman et al., 2017; Hsu et al., 2018; Lee et al., 2019; Norris et al., 2012).

The activation, survival and effector functions of NK cells are positively regulated by cytokines, such as IL-2, IL-12, IL-15 and IL-18 (Mao et al., 2016; Zwirner and Domaica, 2010). Individually, each cytokine was shown to stimulate NK cells, while their combination amplified NK cell activation even further (Nielsen et al., 2016). The surface receptors for IL-2, IL-12, IL-15 and IL-18 were shown to be expressed by both NK cells and ILC1s (Robinette et al., 2015). IL-2 and IL-15 promote NK survival through the induction of Bcl-2 (Fehniger et al., 1999), support NK cell maturation and promote NK cell cytotoxic functions (Zwirner and Domaica, 2010). The IL-2 receptor (IL-2R) is a heterotrimeric receptor, comprised of the three subunits IL-2R $\alpha$  (CD25), IL-2R $\beta$  and IL-2R $\gamma$ . Two of these subunits, the IL-2R $\beta$  and the IL-2R $\gamma$  chains, together with the IL-15R $\alpha$  chain, also form the receptor for IL-15. Thus, mice lacking IL-2R $\beta$  or IL-2R $\gamma$  display reduced numbers of NK cells in peripheral tissues (DiSanto et al., 1995; Ohteki et al., 1997; Suzuki et al., 1997). IL-15 can be trans-presented as a complex together with IL-15R $\alpha$  by stromal cells and dendritic cells to NK cells expressing the IL-2R $\beta$  and the IL-2R $\gamma$  chains, then merging together and triggering downstream signaling cascades (Anton et al., 2020; Dubois et al., 2002). IL-12 is a potent cytokine to activate NK cells, leading to IFN- $\gamma$  and TNF $\alpha$  production (Vignali and Kuchroo, 2012). Moreover, it has been shown that IL-18 primes NK cells for a heightened response to IL-12 (Chaix et al., 2008), and that IL-12/15/18 have synergistic effects to induce elevated and prolonged production of IFN- $\gamma$  by NK cells (Lusty et al., 2017). *In vitro* pre-activation of NK cells with a combination of IL-12/15/18 resulted in long-lasting effector functions (Cooper et al., 2009). Moreover, the adoptive transfer of IL-12/15/18 pre-activated NK cells, in combination with radiotherapy, resulted in control of established tumors *in vivo* (Ni et al., 2012). A pre-clinical trial also showed that

adoptively transferred, IL-12/15/18 pre-activated NK cells proliferated in acute myeloid leukemia patients and demonstrated clinical benefits (Romee et al., 2016). Thus, the combined action of cytokines on NK cell activation has attracted interest in cancer immunotherapies as promising approaches to counteract the immunosuppressive conditions within tumors.

NK cell activation is attributed with the upregulation of surface receptors. For instance, CD25, the IL-2R $\alpha$  chain, is upregulated in response to IL-2 and IL-12, promoting the response of NK cells to these cytokines, and being indicative of a high proliferative potential (Clausen et al., 2003). CD69 was shown to mediate NK cell cytotoxicity, support NK cell proliferation and the production of TNF $\alpha$  (Borrego et al., 1999; Clausen et al., 2003). During adenoviral infections of mice, hepatic CD11c<sup>+</sup> innate lymphocytes produced IFN- $\gamma$  and showed lytic activity against target cells (Burt et al., 2008).

Upon engagement with activating ligands outnumbering the inhibitory signals, and in combination with cytokine stimuli, NK cells exhibit effector functions such as cytokine secretion (e.g. IFN- $\gamma$ , TNF- $\alpha$ ) and release of cytotoxic granules resulting in target cell lysis. Cytotoxic granules contain perforin and granzymes (Lieberman, 2003; Pardo et al., 2002). Perforin is a pore-forming protein, which allows granzymes to enter into the target cell. Granzymes, such as granzyme A, B or K, activate caspase-dependent or -independent pathways in the target cell, leading to apoptosis. Another killing mechanism utilized by NK cells is mediated via TNF receptor ligands, such as Fas ligand (FasL) or TNF-related apoptosis inducing ligand (TRAIL) (Dostert et al., 2019). Binding to their respective receptor, expressed by target cells, induces caspase-mediated apoptosis.

### **1.1.3 Tissue-resident ILC1s**

In contrast to NK cells, ILC1s are commonly found in barrier tissues, such as the mucosal surfaces of the intestine, lungs, and skin, where they contribute to immune responses against pathogens and maintain tissue integrity (Gasteiger et al., 2015). In addition to barrier tissues, ILC1s have also been identified in lymphoid organs including the spleen and lymph nodes, as well as in non-lymphoid tissues, such as the liver and adipose tissue (Figure 1.3A) (Gasteiger et al., 2015; Peng et al., 2013). Like NK cells,

ILC1s express the activating NK cell receptors NKp46 and NK1.1 and the transcription factor T-bet (Figure 1.3B). However, ILC1s develop independently of Eomes, and do not express Ly49 receptors, suggesting that they do not exert “missing self” functions (Daussy et al., 2014; Klose and Artis, 2020; Klose et al., 2014). Hepatic ILC1s express CD49a and can be furthermore characterized by the expression of CD200R and the chemokine receptor CXCR6 (Peng et al., 2013; Robinette et al., 2015; Sojka et al., 2014). Functionally, ILC1s can produce IFN- $\gamma$ , TNF $\alpha$  and GM-CSF, and exert cytotoxic functions via TRAIL (Takeda et al., 2005) (Figure 1.3C). It has been shown that tissue-resident ILC1s represent an early source of IFN- $\gamma$ , and limit early MCMV replication and metastatic seeding (Ducimetiere et al., 2021; Weizman et al., 2017). A recent study characterized differentiation stages of ILC1s in the liver. At an early developmental stage ILC1s are preferentially cytokine-producing, and gradually confer to Tcf<sup>lo</sup>CD127<sup>lo</sup> ILC1s with cytotoxic functions (Friedrich et al., 2021).

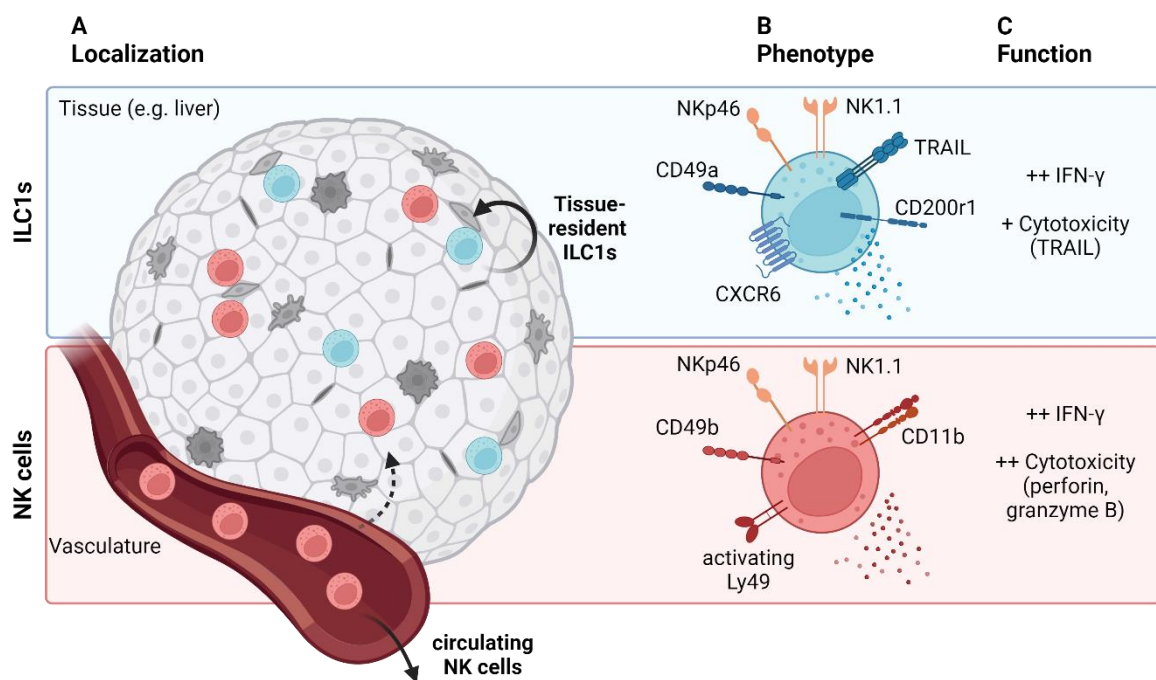


**Figure 1.3 Heterogeneity of NK cells and ILC1s in their (A) localization, (B) phenotype and (C) function.**  
(Figure adapted and modified from (Adams and Sun, 2018))

## 1.2 The Liver

The liver is the largest solid organ in the human body and performs multifaceted functions vital for maintaining homeostasis and health. For instance, it purifies blood from toxins, metabolizes nutrients and drugs, produces bile important for digestion, stores vitamins and minerals, and helps with the production and regulation of hormones.

Structurally, the liver is divided into lobes, which further divide into functional units named lobules (Figure 1.4). Each lobule comprises hepatocytes arranged around a central vein, with portal triads at the corners (Lorente et al., 2020; Panwar et al., 2021). The portal triads consist of the hepatic artery, portal vein and the bile duct. The hepatic artery delivers oxygen-rich blood from the heart, whereas the portal vein supplies nutrient-rich blood from the gastrointestinal tract. This unique dual blood supply branches into smaller vessels, forming sinusoids within the liver lobules, which drain into the central vein.

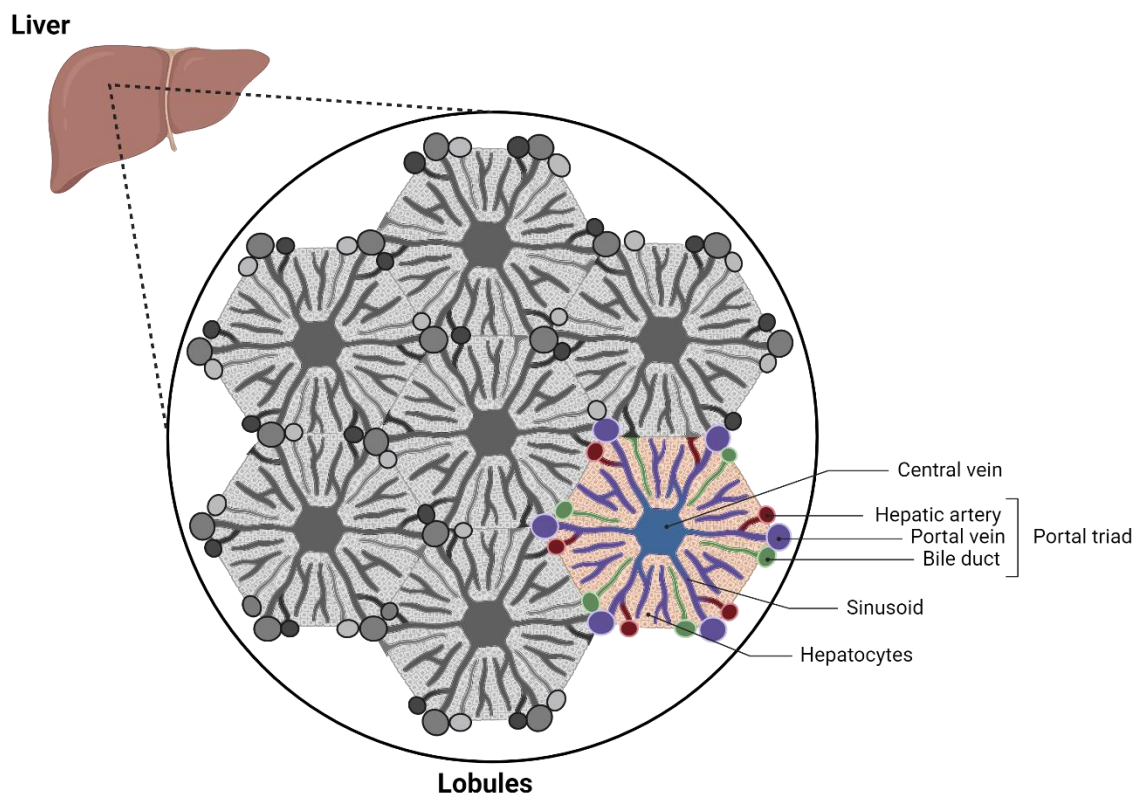


**Figure 1.4 Anatomy of the liver lobules.** (Figure adapted and modified from (Reisner, 2015))

The sinusoids are specialized capillaries, lined by a discontinuous and fenestrated endothelial cell (EC) layer, which facilitates nutrient exchange between the blood and the peri-sinusoidal space, named space of Dissé (Racanelli and Rehermann, 2006). Hepatocytes extend their microvilli to the space of Dissé and take up macromolecules and harmful substances to metabolize them. Hepatocytes regulate carbohydrate, lipid, and protein metabolism, maintain glucose levels, synthesize lipids, and process amino acids (Gong et al., 2022). Moreover, they serve as a storage for glycogen, vitamins (e.g. vitamins A, D, E, K), and minerals (e.g. iron), releasing them into circulation when needed. Hepatocytes metabolize drugs, alcohol and environmental toxins, enabling detoxification and excretion of these substances from the body.

Various factors, such as viral infections, excessive alcohol consumption, obesity and genetic disorders, can compromise liver function, leading to diseases like cirrhosis, fatty liver disease, and liver cancer (Osha et al., 2017). These conditions impair the liver's ability to perform its essential functions, resulting in systemic complications and morbidity.

### **1.2.1 Liver Sinusoidal Endothelial Cells (LSECs)**

Liver sinusoidal endothelial cells (LSECs) are the specialized ECs lining the sinusoids. They exhibit structural and functional features that distinguish them from ECs found in other vascular beds. Unlike other ECs forming continuous layers in other organs, LSECs lack a basement membrane and therefore form a discontinuous surface supported by collagen and proteoglycans. Moreover, they are characterized by 50-200 nm sized membranous pores, forming fenestrations that serve as sieve plates (Figure 1.5) (Wisse et al., 1985). These enable the exchange of solutes, nutrients and macromolecules between the sinusoidal lumen and the space of Dissé (Braet and Wisse, 2002; Szafranska et al., 2021). Moreover, liver-resident lymphocytes and circulating naïve CD8<sup>+</sup> T cells were shown to interact with hepatocytes by extending cell surface protrusions through the fenestrations of LSECs (Warren et al., 2006).



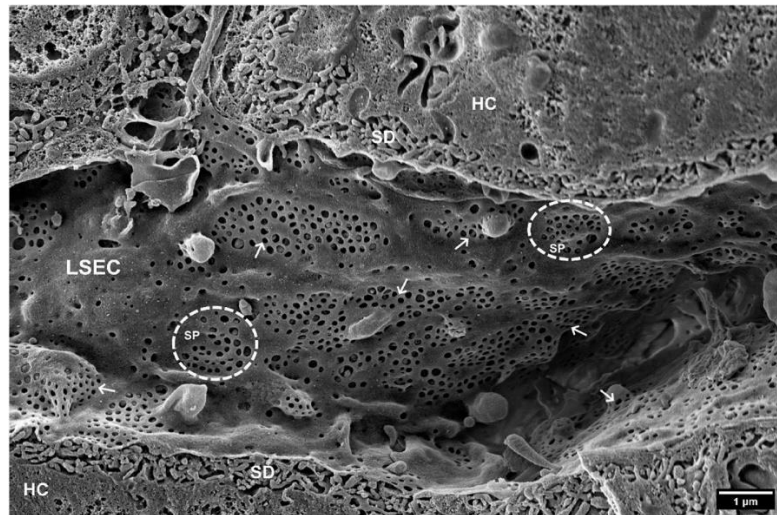


**Figure 1.5 The hepatic sinusoid.** Scanning electron microscopy image of a sinusoid from a murine liver. Liver Sinusoidal Endothelial Cells (LSECs) harbor multiple fenestrations (arrows) arranged into sieve plates (SP, dotted line circles). SD, space of Dissé; HC, hepatocytes. (Figure adapted from (Szafranska et al., 2021))

Modifications in the fenestrations were observed during hypoxia and aging (Cogger et al., 2003; McLean et al., 2003). Complete loss of fenestrations and the formation of a basal membrane characterize the dedifferentiation of LSECs to typical capillary ECs, therefore termed as “capillarization” (Poisson et al., 2017; Schaffner and Poper, 1963). Capillarization is observed in response to liver injury and is associated with the development and progression of fibrosis in chronic liver diseases (Baiocchi et al., 2019; Fukuda et al., 1986; Marrone et al., 2016; Pasarin et al., 2012; Xu et al., 2003).

LSECs assist in the clearance of endogenous and foreign macromolecules with a diameter of up to 200 nm from the blood. They have high endocytic functions due to the expression of the scavenger receptors Stabilin1 (Stab1) and Stab2, mannose receptors, lymphatic vessel endothelial hyaluronan receptor 1 (Lyve-1), and the C-type lectin receptors called liver/lymph node-specific ICAM3-grabbing non-integrin (LSIGN), DCSIGN and liver sinusoidal endothelial cell lectin (LSECtin), as well as the Fc-gamma receptor 1b2 (Bhandari et al., 2021; Pandey et al., 2020; Shetty et al., 2018). After scavenging substances like collagen, hyaluronan, LDL-cholesterol, small immune complexes or exogenous antigens, they rapidly endocytose these via clathrin-mediated endocytosis. Additionally, LSECs also express a variety of TLRs, including TLR4 (Wu et al., 2010; Yao et al., 2016). They were shown to rapidly clear LPS from the blood via HDL-mediated scavenge by Stab1 and Stab2, and develop LPS-induced tolerance after repeated challenge, which results in reduced leukocyte

adhesion due to the downregulation of ICAM-1 (Uhrig et al., 2005). However, when concentrations of LPS in the blood increase, LSECs can get activated via TLR4 and produce the pro-inflammatory cytokines IL-1 $\alpha$ , IL-1 $\beta$ , IL-6, IL-10, IL-15 and TNF- $\alpha$  (Cabral et al., 2021; Uhrig et al., 2005; Yao et al., 2016). LSECtin can bind mannose residues on blood-borne pathogens (Liu et al., 2004). Its additional function is binding to CD44, which is expressed, among others, on activated immune cells. It was shown that this interaction results in inhibition of activated T cells, thereby controlling local inflammation and preventing liver damage (Tang et al., 2009).

Within the liver, conventional APCs, including KCs and dendritic cells, as well as unconventional APCs like hepatocytes, hepatic stellate cells (HSCs), and LSECs, participate in antigen presentation (Horst et al., 2016). LSECs were shown to present antigens to T cells via MHC I and MHC II, but they display a low expression of co-stimulatory molecules (Knolle et al., 1999; Lohse et al., 1996). Under physiological conditions, the antigen presentation serves to induce tolerance to harmless antigens, thereby preventing unwanted adaptive immune responses and maintain liver homeostasis. For instance, presentation of antigens by LSECs via MHC II was shown to result in the differentiation of CD4<sup>+</sup> T cells to Treg rather than Th1 cells (Wiegard et al., 2005). Likewise, antigen presentation via MHC I to CD8<sup>+</sup> T cells lead to T cell tolerance characterized by absence of effector functions, supported by B7-H1 binding to PD-1 (Diehl et al., 2008). However, at high antigen concentrations, LSECs induced the differentiation of CD8<sup>+</sup> T cells to effector T cells (Schurich et al., 2010). Therefore, the antigen presentation function of LSECs is crucial not only for maintaining liver immune tolerance, but also for orchestrating immune responses, highlighting their dual role in liver homeostasis versus host defense.

### **1.2.2 Immune cells in the liver**

Within its complex architecture, a diverse array of immune cells orchestrate a delicate balance between tolerance and defense, crucial for maintaining hepatic homeostasis. Hepatic immune cells reside in the liver parenchyma and in the portal tracts, or crawl along the sinusoids (Figure 1.6) (Racanelli and Rehermann, 2006). Kupffer cells, liver-resident macrophages, predominantly populate the periportal zone and patrol the liver along the sinusoidal endothelium. They phagocytose debris and microorganisms, endocytose endo- and exogenous substances from the blood, and present antigens to

T cells. Similarly, conventional dendritic cells and plasmacytoid dendritic cells populate the liver to screen for antigens, and exit the liver via the central vein or the space of Disse and the lymphatic drainage to transport the antigens to the draining lymph node (Matsuno et al., 1996). However, hepatic dendritic cells were described to be immature and poor in T cell stimulation in comparison to other dendritic cells, probably due to the exposure to the tolerogenic hepatic environment (De Creus et al., 2005; Kudo et al., 1997). The liver is enriched in innate immune cells, including innate lymphocytes and natural killer T (NKT) cells (Racanelli and Rehermann, 2006). NK cells and liver-resident ILC1s comprise approximately 30 % of all hepatic lymphocytes (Robinette et al., 2015; Tian et al., 2013). The liver shows a reversed ratio among the conventional T cell subsets, with CD8<sup>+</sup> T cells outnumbering CD4<sup>+</sup> T cells, and a dominance of effector memory T cells (Norris et al., 1998). It was demonstrated that CD8<sup>+</sup> T cells were preferentially retained within the liver, where they develop into an effector memory phenotype or undergo apoptosis (Thomson and Knolle, 2010). Moreover, the liver favors the differentiation of CD4<sup>+</sup> T cells to Th2 and Tregs rather than Th1, to support the liver microenvironment with regulatory type 2 cytokines, such as IL-10, TGF $\beta$  and IL-4, respectively. Thus, under steady-state conditions, conventional APCs (KCs and dendritic cells) and unconventional APCs (LSECs, HSCs and Hepatocytes) in the liver induce T cell tolerance by clonal elimination, induction of T cell anergy and an enhanced induction of Tregs (Zheng and Tian, 2019).

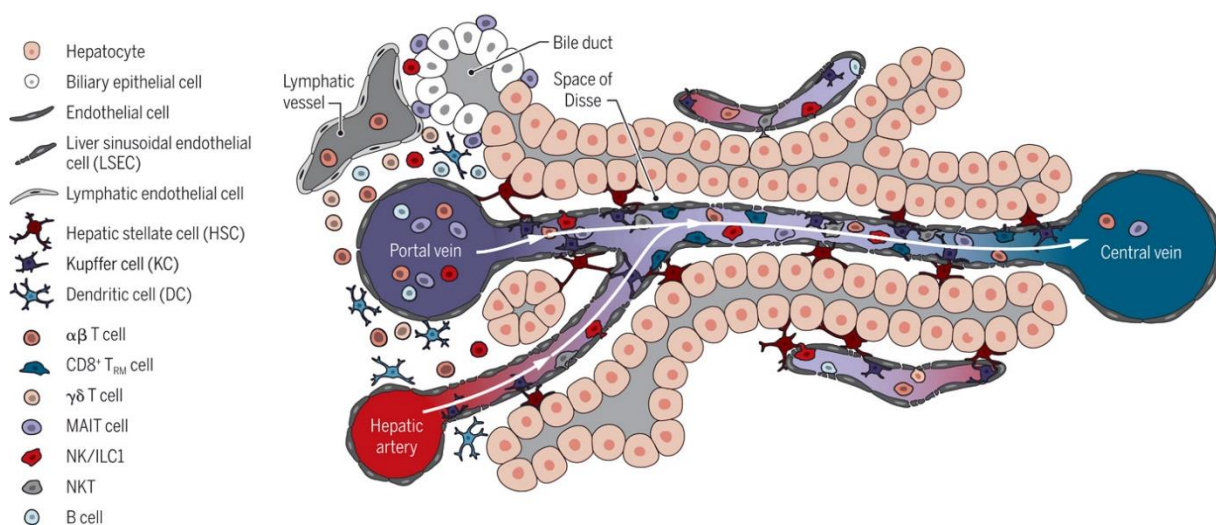


**Figure 1.6 Location of immune cells in the liver.** (Figure adapted from (Ficht and Iannacone, 2020))

### **1.2.3 Liver pathologies**

The immune response triggered by LPS can become dysregulated and lead to sepsis, which is characterized by a systemic inflammatory response syndrome (SIRS). The uncontrolled release of inflammatory mediators in sepsis can lead to widespread tissue damage, organ dysfunction, and potentially life-threatening complications such as septic shock. Severe sepsis lacks specific therapies, resulting in high mortality rates of approximately 20-50 % of patients (Karlsson et al., 2009). LPS-induced hepatic injury is observed during endotoxemia, but also in various liver conditions including cirrhosis, autoimmune hepatitis, and primary biliary cirrhosis. Early infiltration of neutrophils and monocytes to the liver can cause vascular dysfunction and damage (McDonald et al., 2013; Triantafyllou et al., 2018).

Hepatocellular carcinoma (HCC) is the most common type of primary liver cancer, originating from transformed hepatocytes. HCC typically occurs in the setting of chronic liver disease, such as cirrhosis due to hepatitis B or C infection, excessive alcohol consumption, non-alcoholic fatty liver disease, or other factors that cause liver damage (Rossetto et al., 2019). Moreover, the liver is a common site for metastasis from primary tumors, including colorectal cancer, pancreatic cancer, breast cancer and melanoma (Tsilimigras et al., 2021). Factors such as high vascularization, the tolerogenic environment, and metabolic activity contribute to the liver's vulnerability to metastatic colonization.

During these hepatic pathologies, LSECs undergo pathological changes, leading to vascular dysfunction, inflammation, and progression of fibrosis and cancer (Poisson et al., 2017). Targeted therapies aimed at restoring LSEC barrier function, and promoting their immunological functions represent potential strategies for treating liver diseases and improving disease outcomes.

### **1.3 Chemotaxis and extravasation of immune cells**

The directed migration of leukocytes across a chemokine gradient is termed chemotaxis. Chemotaxis plays a crucial role in directing leukocytes towards sites of infection, inflammation, and tumors. The nomenclature for chemokines and their receptors is based on the arrangement of the two first N-terminal cysteine residues and are therefore divided into four main families: CC, CXC, CX3C, and XC ligands and their respective G protein-coupled receptors (Miller and Mayo, 2017; Zlotnik and Yoshie, 2000). For example, for CCL2 the first two cysteine residues are adjacent, whereas for CXCL10 the first two cysteine residues are separated by one amino acid. XCL1 comprises only one N-terminal cysteine-residue, and in CX3CL1 3 amino acids separate the N-terminal cysteine residues.

NK cells express a variety of chemokine receptors, which guide their migration in response to specific chemokines in organs and tissues. For instance, the retention of immature NK cells within the BM is mediated by the expression of CXCR4 and its ligand CXCL12, which is expressed by osteoclasts and BM-specific mesenchymal stem cells (Bernardini et al., 2008). During maturation, CXCR4 expression is downregulated whereas the expression of CXCR3, CCR1, CX3CR1 and the Sphingosine-1-phosphate receptor 5 (S1P5) are increased, which allows NK cells to egress from the BM and enter the periphery (Bernardini et al., 2013; Walzer et al., 2007). During inflammation, NK cells are mobilized from the BM pool and migrate to the inflamed tissue. The recruitment of BM-derived NK cells to the liver was demonstrated in Concanavalin A-induced liver inflammation and during MCMV infection, where it was mediated by the chemokine CCL3 and its receptors, CCR1 and CCR5 (Salazar-Mather et al., 1996; Wald et al., 2006). Furthermore, it was demonstrated that CD27<sup>+</sup> NK cells expressed CXCR3 and selectively migrated towards its ligand CXCL10 (Hayakawa and Smyth, 2006). CD27<sup>+</sup> NK cells are distributed throughout spleen, lymph nodes, and liver, but were nearly absent in the lung. Moreover, CD27<sup>+</sup>CXCR3<sup>+</sup> NK cells produced higher amounts of IFN- $\gamma$  in response to IL-12 and IL-18 in comparison to CD27<sup>lo</sup>CXCR3<sup>lo</sup> NK cells. Interestingly, CXCR3-expressing CD27<sup>+</sup> NK cells were also shown to infiltrate tumor tissue (Wendel et al., 2008).

Liver sinusoids are characterized by a slow blood flow. Therefore, rolling of leukocytes via selectins as an initial step during extravasation is not necessary (Wong et al., 1997).



LSECs mediate transendothelial migration of leukocytes during liver inflammation, or bacterial and viral infections, via adhesion molecule and chemokine interactions to their respective receptors, and subsequent allowance to squeeze inbetween LSECs (paracellular), through the fenestrations (transcellular), or through the LSEC body (intracellular) after attachment to the endothelium (Figure 1.7) (Shetty et al., 2018).

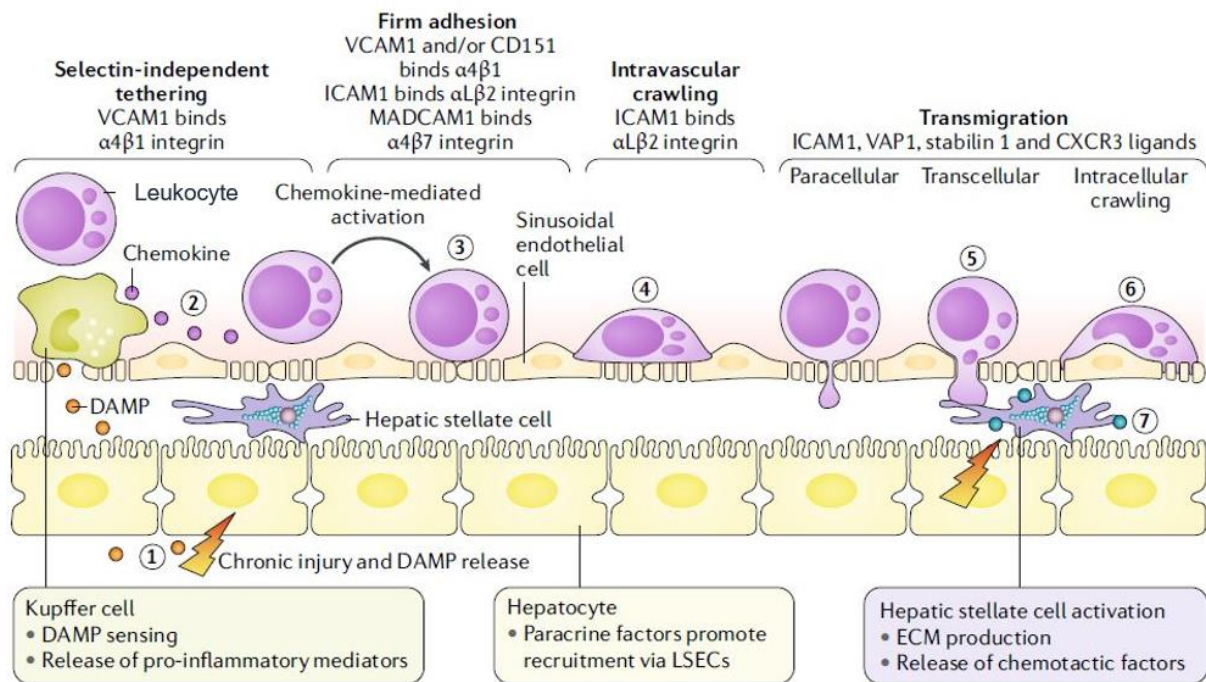


**Figure 1.7 Leukocyte extravasation in the sinusoids.** (1) Infection or damage to the liver parenchyma induces (2) Kupffer cell (KC) and LSEC activation, upregulation of adhesion molecules and chemokine secretion. (3) Leukocytes bind to LSECs via integrins and (4) crawl along the sinusoidal endothelium. (5+6) Paracellular migration (inbetween LSECs), transcellular migration (via fenestrations), or intracellular crawling (through LSEC body) of leukocytes via LSEC-initiated signals. (7) Migration and positioning of leukocytes in the parenchyma by chemokines. CXCR3, CXC-chemokine receptor 3; ECM, extracellular matrix; ICAM1, intercellular adhesion molecule 1; MADCAM1, mucosal addressin cell adhesion molecule 1; VAP1, vascular adhesion protein1; VCAM1, vascular cell adhesion molecule 1. (Figure adapted from (Shetty et al., 2018))

Like this, leukocytes enter into the liver parenchyma, where they participate in the immune responses against infected hepatocytes or damaged tissue. Interestingly, LSECs were shown to not only support monocyte extravasation from the blood stream, but also to enable their return to the bloodstream after their immune surveillance task, a process termed reverse transmigration (Bradfield et al., 2007). This bidirectional migration of cells through the LSEC layer is tightly regulated and essential for maintaining immune homeostasis in the liver while effectively responding to inflammatory insults or infections.

## 2 THE AIM OF THE STUDY

The liver is characterized by a ramified vascular network that is constantly exposed to antigen-rich blood from the gastrointestinal tract. The hepatic blood vessels are lined by liver sinusoidal endothelial cells (LSECs), which screen the blood and clear it from pathogens and endogenous damaging molecules. In addition, LSECs were shown to have immunoregulatory functions by modulating adaptive T cell differentiation and responses. The liver is enriched in innate lymphocytes, comprising mainly natural killer (NK) cells and type 1 innate lymphoid cells (ILC1s), which provide early defense against infections and malignancies by exerting cytotoxicity and secreting pro-inflammatory cytokines. Although they continuously interact with LSECs, the local endothelial functions supporting innate cell responses in the liver remain not fully explored.

Due to the spatial proximity of LSECs and innate lymphocytes in the liver, we postulated that their interaction shapes the inflammatory and anti-tumor responses in the liver. Thus, we aimed to dissect the underlying mechanisms and functional output of these interactions.

In this study, we focused on hepatic inflammation and response to tumor cells, and investigated:

1. Response of the liver endothelium to inflammatory signals and tumor cells
2. Crosstalk of LSECs and innate lymphocytes in the context of acute inflammatory liver injury
3. Regulation of anti-tumor responses of innate lymphocytes by LSECs

To investigate the interplay of LSECs and innate lymphocytes, we utilized *in vitro* culture and co-culture systems, and experimental mouse models of liver inflammation and metastases, including endothelial-specific conditional gene knockout mice. Our discoveries advance the current understanding of the liver microenvironment and aid identifying novel mechanisms of immune-endothelial regulatory circuits in liver inflammatory and anti-tumor responses.





### 3 MATERIALS AND METHODS

#### 3.1 Materials

##### 3.1.1 Laboratory equipment

**Table 3.1 Laboratory equipment**

Product	Company
200 Gel Imaging Workstation	Azure biosystems
C1000 Touch™ Thermal Cycler	Bio-Rad
FACS Aria™ Fusion Cell Sorter	BD Biosciences
GentleMACS™ Octo Dissociator	Miltenyi Biotec
Incubator BD056	BINDER
IVIS200 Imaging System	Caliper Life Sciences
LSR Fortessa™ Cell Analyzer	BD Biosciences
Plate reader Infinite 200 pro	TECAN
QuadroMACS™ Separators	Miltenyi Biotec
QuantStudio™ 5 Real-Time PCR System, 384-well	Applied Biosystems

##### 3.1.2 Chemicals and biological reagents

**Table 3.2 Chemicals and biological reagents**

Product	Company	Catalog no.
7-AAD	Biolegend	420404
D-Luciferin, Potassium Salt	Bio Vision	7903-1G
Lipopolysaccharide E.coli O26:B6	Sigma-Aldrich	L2654
Nuclease-free Water (not DEPC treated)	Ambion Thermo Fisher Scientific	AM9937
Nycodenz	Axis-Shield	1002424
Percoll®	Cytiva	17089101
Recombinant human IL-2	NIH	1104-0890
Recombinant mouse IFN-γ	Peprtech	315-05
Recombinant mouse IL-12	Peprtech	210-12
Recombinant mouse IL-18	MBL	B002-5
Sodium chloride	Sigma-Aldrich	31434-5KG
Zombie Aqua™	Biolegend	423102

$\beta$ -mercaptoethanol (99%)	VWR	97064-588
--------------------------------	-----	-----------

### 3.1.3 Cell culture media and solutions

**Table 3.3 Cell culture media and solutions**

Product	Company	Catalog no.
Cell Dissociation Solution Non-enzymatic (1x)	Sigma-Aldrich	C5914
Detachin Cell Detachment Solution	Genlantis	T100106
Dimethylsulphoxide Hybri Max® (DMSO)	Sigma-Aldrich	D2650
Dulbecco's Modeified Eagle's Medium (DMEM), glucose, L-glutamine, sodium pyruvate, and sodium bicarbonate	Sigma-Aldrich	D6459
Dulbecco's Phosphate Buffered Saline (PBS)	Gibco	1490144
EDTA, 0.5 M, UltraPure™, pH 8,0	Invitrogen	15575020
Fetal Bovine Serum, Origin: EU Approved 10270	Gibco	10270
Gey's Balanced Salt Solution (GBSS)	Pancoll-biotech	P04-48500
Gibco™ RPMI 1640 Medium	Fisher Scientific	11530586
L-Glutamine 200 mM (100x)	Gibco	25030
MACS® BSA Stock Solution	Miltenyi Biotec	130-091-376
Non-essential Amino Acids (100x)	Gibco	11140035
Penicillin/Streptomycin Solution	Gibco	15140
Sodium pyruvate MEM 100mM	Gibco	11360088
Trypsin-EDTA (1x) HBSS, w/o Ca <sup>2+</sup> /Mg <sup>2+</sup> w/ EDTA	Gibco	25300
$\beta$ -mercaptoethanol (50mM)	Gibco	31350010

### 3.1.4 Cell culture consumables

**Table 3.4 Consumables for cell isolation and culture**

Product	Company	Catalog no.
384 well Microplates, black, flat	TECAN	30122299
BD Falcon™ 5mL round bottom tubes with 35µm nylon mesh strainer	Corning	352235
Cell culture flask, T-175	Sarstedt	83.3912.302
Cell culture flask, T-25	Sarstedt	83.3910.302
Cell culture flask, T-75	Sarstedt	83.3911.302
Collagen I, Coated Plate, 24 well	Gibco	A1142802
Collagen I, Coated Plate, 96 well	Gibco	A1142803
Falcon® 100µm Cell Strainer, Yellow, Sterile	Corning	352360
Falcon® 24-well Polystyrene Clear Flat Bottom, not Treated Cell Culture Plate, Sterile	Corning	351147
Falcon® 40 µm Cell Strainer, Blue, Sterile	Corning	352340
Falcon® 70 µm Cell Strainer, White, Sterile	Corning	352350
GentleMACS™ C Tubes	Miltenyi Biotec	130-093-237
MACS LS columns	Miltenyi Biotec	130-042-401
Serological pipette 10 ml, padded	Sarstedt	861254001
Serological pipette 25 ml, padded	Sarstedt	861685001
Serological pipette 5 ml, padded	Sarstedt	861253001
TPP® tissue culture plates, 96 well plate, Round bottom, Polystyrene, Sterile	TPP	Z707899-162EA
RNase-free Microfuge Tubes (1.5 mL)	Ambion Thermo Fisher Scientific	AM12400
6.5 mm Transwell™ with 5 µm Polyester (PET) Membrane Insert, 24 well plate, sterile	Corning	3421

### 3.1.5 Kits

**Table 3.5 Commercial Kits**

Product	Company	Catalog no.
CD146 (LSEC) microbeads, mouse	Miltenyi Biotec	130-092-007
DuoSet ELISA Ancillary Reagent Kit 2	R&D Systems	DY008B
eBioscience™ FoxP3 Transcription factor staining buffer set	eBioscience	00-5523-00
LEGENDplex™ Mouse Proinflammatory Chemokine Panel I and II	Biolegend	740451, 741068
Liver Dissociation Kit, mouse	Miltenyi Biotec	130-105-807
Mouse CXCL10/IP-10/CRG-2 DuoSet ELISA	R&D Systems	DY466-05
MyTaq™ Extract-PCR Kit	Meridian Bioscience	BIO-21127
PowerUp™ SYBR™ Green Master Mix	Applied Biosystem	A25918
ProtoScript® II First Strand cDNA Synthesis Kit	New England Biotechnology	E6560S
RNA Clean and Concentrator - 5	Zymo Research	R1013
RNeasy™ Mini Kit (50 reactions)	Qiagen	74104
RT <sup>2</sup> First Strand Kit	Qiagen	330404
RT <sup>2</sup> Profiler™ PCR Array Mouse Cytokines & Chemokines	Qiagen	PAMM-150Z
RT <sup>2</sup> SYBR Green qPCR Mastermix	Qiagen	330501
TURBO DNA-free™ Kit	Ambion Thermo Fisher Scientific	AM1907

### 3.1.6 Buffers and solutions

**Table 3.6 Buffers and solutions**

Solution	Ingredients
ACK Lysis Buffer	0.829 g Ammoniochloride (NH <sub>4</sub> Cl) 0.1 g Potassium bicarbonate (KHCO <sub>3</sub> ) 0.0038 g EDTA Fill up to 100 mL with ddH <sub>2</sub> O Adjust pH to 7.2-7.4
Cell freezing medium	FCS 10% DMSO
Cell Lysis Buffer for RNA isolation	RLT buffer from Qiagen 1% β-mercaptoethanol (13.8M)
Complete DMEM	DMEM with high glucose 10% FCS 1% Penicillin/Streptomycin
Complete RPMI	RPMI 1640 with high glucose 10% FCS 1% Penicillin/Streptomycin
FACS Buffer	1x PBS 1% FCS 2 mM EDTA 0.02% NaN <sub>3</sub>
Isotonic Percoll solution (freshly prepared)	9 parts stock Percoll 1 part 1.5M NaCl solution
15% Percoll (freshly prepared)	1.5mL isotonic Percoll solution 8.5mL PBS
40% Percoll (freshly prepared)	4mL isotonic Percoll solution 6mL PBS
70% Percoll (freshly prepared)	7mL isotonic Percoll solution 3mL PBS
Liver digestion media for gentleMACS dissociation	DMEM 1% L-glutamine
LSEC culture medium	DMEM with high glucose 10% FCS 1% L-glutamine 1% Non-essential amino acid

	1% Sodium Pyruvate 1% Penicillin/Streptomycin 0.1% $\beta$ -mercaptoethanol (for cell culture)
MACS Buffer	PBS 2% FCS 2 mM EDTA
Migration medium	RPMI 1640 with high glucose 1% BSA 1% L-glutamine 1% Non-essential amino acid 1% Sodium Pyruvate 1% Penicillin/Streptomycin 0.1% $\beta$ -mercaptoethanol (for cell culture)
NK cell culture medium	RPMI 1640 with high glucose 10% FCS 1% L-glutamine 1% Non-essential amino acid 1% Sodium Pyruvate 1% Penicillin/Streptomycin 0.1% $\beta$ -mercaptoethanol (for cell culture)
26% Nycodenz solution (freshly prepared)	10.4g of Nycodenz powder dissolved in GBSS Sterilized filter
Sodium Chloride (NaCl) Solution, 1.5 M	87.66g of sodium chloride in 1 liter water
Sorting Buffer	PBS 1% BSA 2 mM EDTA

### 3.1.7 Antibodies for flow cytometry

*Table 3.7 Conjugated antibodies for flow cytometry*

Antibodies	Clone	Company	Catalog no.
Anti-mouse CD3 APC-Cy7	14A2	Biolegend	100222
Anti-mouse CD3ε BV711	145-2C11	Biolegend	100349
Anti-mouse CD3ε PE-Cy7	145-2C11	Biolegend	100320
Anti-mouse CD4 BV650	RM4-5	Biolegend	100555
Anti-mouse CD8a FITC	53-6.7	Biolegend	100706
Anti-mouse/human CD11b APC	M1/70	Biolegend	101212
Anti-mouse/human CD11b BV650	M1/70	Biolegend	101259
Anti-mouse CD11c PE-Cy7	N418	Biolegend	117318
Anti-mouse CD19 APC-Cy7	6D5	Biolegend	115530
Anti-mouse CD25 PE	PC61	Biolegend	102008
Anti-mouse CD31 BV421	390	Biolegend	102424
Anti-mouse CD45 BV785	30F11	Biolegend	103149
Anti-mouse CD45 PerCP-Cy5.5	30F11	Biolegend	103132
Anti-mouse CD49a PE	Ha31/8	BD	562115
Anti-mouse CD54 (ICAM-1) Alexa Flour 647	YN1/1.7.4	Biolegend	116114
Anti-mouse CD62L PE	MEL-14	Biolegend	104407
Anti-mouse CD69 FITC	H1.2F3	Biolegend	104506
Anti-mouse CD96 APC	3.3	Biolegend	131712

Anti-mouse CD146 PE-Cy7	ME-9F1	Biolegend	134714
Anti-mouse CD155 APC	TX56	Biolegend	131510
Anti-mouse CD200R FITC	OX-110	Biolegend	123910
Anti-mouse CD253 (TRAIL) PE	N2B2	Biolegend	109305
Anti-mouse CXCR3 BV421	CXCR3-173	Biolegend	126529
Anti-mouse CXCR3 PE-Cy7	CXCR3-173	Biolegend	126516
Anti-mouse CXCR6 Alexa Flour 647	SA051D1	Biolegend	151115
Anti-mouse DNAM-1 FITC	10E5	Biolegend	128803
Anti-mouse DR5 PE	MD5-1	Biolegend	119905
Anti-mouse Eomes PE-Cy7	Dan-11mag	Thermo Fisher Scientific	25-4875-82
Anti-mouse Eomes TexasRed	X4-83	BD Horizon	567167
Anti-mouse F4/80 APC-Cy7	BM8	Biolegend	123118
Anti-mouse F4/80 PE/Dazzle 594	BM8	Biolegend	123146
Anti-mouse HVEM APC	C46	BD	564470
Anti-mouse HVEM PE	HMHV-1B18	Biolegend	136304
Anti-mouse H-2Db PE	KH95	BD	553574
Anti-mouse H-2Kb PE	AF6-88.5	BD	561072
Anti-mouse I-A/I-E (MHC II) Alexa Flour 647	M5/114.15.2	Biolegend	107618
Anti-mouse IFN- $\gamma$ PE	XMG1.2	Biolegend	505808
Anti-mouse Ki67 PE	SolA15	Thermo Fisher Scientific	12-5698-82
Anti-mouse KLRG1 FITC	2F1	Southern Biotech	1807-02
Anti-mouse Ly6C FITC	HK1.4	Biolegend	128005
Anti-mouse Ly6G APC-Cy7	1A8	Biolegend	127624



Anti-mouse Ly6G Pacific Blue	1A8	Biolegend	127612
Anti-mouse Lyve-1 PE	FAB2125P	R&D Systems	FAB1155P
Anti-mouse NK1.1 BV785	PK136	Biolegend	108749
Anti-mouse NK1.1 PE	PK136	Biolegend	108708
Anti-mouse NKG2D	CX5	Biolegend	130212
Anti-mouse NKp46 APC	19A1.4	Biolegend	137608
Anti-mouse NKp46 BV421	27A1.4	Biolegend	137612
Anti-mouse PD-L1 PE	10F.9G2	Biolegend	124308
Anti-mouse Siglec F APC-Cy7	E50-2440	BD Biosciences	565527
Anti-mouse Stabilin-2 FITC	34-2	MBL International	D317-A48
Anti-mouse TCRb BV785	H57-597	Biolegend	109249
Anti-mouse Ter119 APC-Cy7	Ter-119	Biolegend	116223
Anti-mouse TIGIT PE-Cy7	1G9	Biolegend	142107
Anti-mouse VCAM-1 APC	429(MVCAM.A)	Biolegend	105712
Armenian Hamster IgG Isotype Control BV421	HTK888	Biolegend	400949
Mouse IgG2a Isotype Control PE	MOPC-173	Biolegend	400212
Mouse IgG1 Isotype Control PE-Cy7	MOPC-21	Biolegend	981816
Mouse IgG2b Isotype Control PE	MPC-11	Biolegend	400312
Rat IgG1 Isotype Control PE	G0114F7	Biolegend	401906
Rat IgG2a Isotype Control APC	54447	R&D Systems	IC006A
Rat IgG2a Isotype Control PE	RTK2758	Biolegend	400508

Rat IgG2b Isotype Control Alexa Flour 647	RTK4530	Biolegend	400626
Rat IgG2b Isotype Control APC	RTK4530	Biolegend	400612
Rat IgG2b Isotype Control FITC	RTK4530	Biolegend	400606
Rat IgG2b Isotype Control PE	RTK4530	Biolegend	400608
Rat IgG2a Isotype Control BV421	RTK2758	Biolegend	400549

### 3.1.8 Antibodies for functional assays

**Table 3.8** List of antibodies for functional assays and in vivo applications

Antibodies	Clone	Concentration	Company	Catalog no.
Armenian Hamster IgG Isotype Control, Functional Grade	eBio299Arm	10 µg/ml	Thermo Fisher Scientific	16-4888-85
InVivoMAb anti-mouse CD106 (VCAM-1), monoclonal	M/K-2.7	200 µg/mouse	Bio X Cell	BE0027
InVivoMAb anti-mouse CXCR3 (CD183), monoclonal	CXCR3-173	200 µg/mouse	Bio X Cell	BE0249
Ultra-LEAF Purified CD16/CD32	93	10 µg/mL	Biolegend	101329
Ultra-LEAF™ Purified anti- mouse CD183 (CXCR3)	CXCR3-173	10 µg/ml	Biolegend	126526

### 3.1.9 Oligonucleotide primers

Primers for PCR genotyping

**Table 3.9 Primers for PCR genotyping**

Gene/Protein	Forward sequence (5' → 3')	Reverse sequence (3' → 5')
VE-Cadherin	CCA GGC TGA CCA AGC TGA G	CCT GGC GAT CCC TGA ACA

Primers for quantitative RT-PCR

**Table 3.10 Primers for qRT-PCR**

Gene/Protein	Forward sequence (5' → 3')	Reverse sequence (3' → 5')
mB2m	TGCTATCCAGAAAACCCCTCA	GGCGGGTGGAAGTGTGTTA
mActb	CAGATGTGGATCAGCAAGCA	GGGTGTAAAACGCAGCTCAGTA
mCxcl10	CCATATCGATGACGGGCCA	CTTTTTCATCGTGGCAATGATCTC

### 3.1.10 Tumor cell lines

**Table 3.11 Tumor cell lines**

Cell line	Cell type	Medium
B16	Mouse melanoma	Complete DMEM
B16F10 Luciferase/tdTomato	Dual reporter mouse melanoma	Complete DMEM
LL/2	Mouse lung carcinoma	Complete DMEM
MC38	Mouse colon carcinoma	Complete DMEM
MC38 Luciferase/tdTomato	Dual reporter mouse colon carcinoma	Complete DMEM
RMA-S	Mouse T cell lymphoma	Complete RPMI

### 3.1.11 Mouse lines

**Table 3.12 Mouse lines**

Mouse line	Scientific name	Source
C57BL/6N	C57BL/6NRj	Janvier Labs
Cdh5 <sup>Cre</sup> CXCL10 <sup>fl/fl</sup>	B6-Cxcl10tm1.1Dple Tg(Cdh5-cre)1Spe/Platt	Provided by Prof. Dr. med. Michael Platten, DKFZ Heidelberg
Rag2 knockout	B6.(MF;129)-Rag2tm1Fwa	Haus 111, UMM
Rag2 knockout Ly5.1	B6.Rag2tm1Fwa Ptprca	Haus 111, UMM

### 3.1.12 Software

**Table 3.13 Software for data analysis**

Software	Source
FlowJo™ version >10.7.1	FlowJo™ LLC
GraphPad Prism 7	GraphPad
LEGENDplex™ Data Analysis Software	Biolegend
Living Image version 4.1	PerkinElmer
pheatmap	Ravio Kolde, RDocumentation
R version >4.1	R core team
RStudio	Posit PBC

## **3.2 Methods**

### **3.2.1 Preparation of single cell suspensions**

Mice were sacrificed by CO<sup>2</sup>-asphyxiation. Spleens and livers were kept in PBS on ice until organ processing. Blood was collected by retroorbital bleeding on heparin and kept at RT until processing.

#### **Blood**

Red blood cells were lysed with 30 ml ACK buffer for 10 minutes. Cells were centrifuged at 1,600 rpm for 10 min and then washed with PBS twice (1,500 rpm for 10 min). Blood mononuclear cells were resuspended in an appropriate amount of PBS and kept on ice.

#### **Spleen**

Spleens were mashed through a 40 µm pore strainer and washed with PBS (1,500 rpm for 10 min). Red blood cells were lysed with 3 ml of ACK buffer per spleen for 3 min and cell suspensions were filtered with a 40 µm strainer. Cells were washed twice with PBS (1,500 rpm for 10 min). Splenocytes were resuspended in PBS and kept on ice.

#### **Liver (for LSEC enrichment)**

Livers were perfused with PBS via the portal vein and resected. The gall bladder and connective tissue were removed. To isolate LSECs for primary cell culture, livers were enzymatically and mechanically digested using the Liver Dissociation Kit (Miltenyi Biotec) according to the manufacturer's protocol. Subsequently, liver tissue was mashed through a 100 µm strainer and washed with cold GBSS (300xg for 10 min at 4 °C). To remove red blood cells, 4 ml of ACK buffer were added per liver and incubated for 4 min at RT. Cells were filtered through a 70 µm strainer and washed with cold GBSS (300xg for 10 min at 4°C). The cell pellet was resuspended in cold GBSS, filtered through a 40 µm strainer and washed. Liver cells were resuspended in 6 ml of cold GBSS, and layered on 26 % Nycodenz solution in GBSS. The gradient was centrifuged at 1,400xg for 18 min at 4 °C (acc: 1, dec: 1). The interphase, enriched with non-parenchymal cells, was collected and washed with cold GBSS (300xg for 10 min at 4 °C). Cells were resuspended in GBSS, counted and prepared for LSEC enrichment using magnetic beads.

**Liver (for simultaneous LSEC and lymphocyte enrichment)**

To enrich for LSECs and liver mononuclear cells, livers were enzymatically and mechanically digested using Enzyme D and Enzyme A from the Liver Dissociation Kit (Miltenyi Biotec) according to the manufacturer's protocol. Enzyme R was excluded from the Enzyme cocktail as the surface receptor NK1.1 was sensitive to the digestion with this Enzyme. After digestion, the liver tissue was mashed through a 100 µm strainer and washed with PBS (300xg for 10 min). To remove red blood cells, 4 ml of ACK buffer were added and incubated for 4 min at RT. Cells were filtered through a 70 µm strainer and washed with PBS (300xg for 10 min). The cell pellet was resuspended in PBS, filtered through a 40 µm strainer and washed. Cells were resuspended with 3 ml of PBS. Isotonic Percoll solution was prepared by diluting Percoll in a 9:1 ratio with 1.5 M NaCl. The isotonic Percoll solution was further diluted to 70% Percoll, 40 % Percoll and 15 % Percoll solution with PBS. To prepare a 70 % - 40 % - 15 % Percoll gradient, 3 ml of each Percoll solution was carefully layered on top of each other. For the isolation of cells for functional assays, the gradient was prepared with 70 % and 40 % of Percoll solution to enrich for liver lymphocytes only. The liver solution was layered on top of the Percoll gradient and centrifuged at 1,400xg for 25 min at RT (acc: 1, dec: 1). The interphase between 15 % and 40 % Percoll solution (enriched with LSECs, Kupffer cells, Monocytes and Neutrophils), and the interphase between 40 % and 70 % Percoll solution (enriched with liver lymphocytes) were collected, and washed twice with cold PBS (1,500 rpm for 10 min at 4 °C). Cells were then resuspended with PBS and counted.

**3.2.2 Magnetic Cell Sorting (MACS) for LSEC purification**

Cell solutions enriched with liver non-parenchymal cells, as prepared described above were resuspended in 98 µl MACS buffer per  $1 \times 10^7$  cells. Cells were incubated with 10 µg/ml anti-mouse CD16/32 for 10 min at 4 °C. To label LSECs, 2 µl of CD146 microbeads (Miltenyi Biotec) were added per  $1 \times 10^7$  cells and incubated for 15 min at 4 °C. Cells were washed with MACS buffer (300xg for 10 min at 4 °C), loaded onto a LS column (Miltenyi Biotec) and purified according to the manufacturer's instructions. The enriched LSECs were washed with MACS buffer (300xg for 10 min at 4 °C) and resuspended in pre-warmed LSEC culture medium. The magnetic purification usually yielded a purity of >90 % of CD146<sup>+</sup>Stab2<sup>+</sup>CD31<sup>+</sup> cells.

### 3.2.3 Fluorescence activated cell sorting (FACS)

Liver cell suspensions prepared as described above were washed and re-suspended in cold PBS at a density of  $5 \times 10^7$  cells/ml. Unspecific antibody binding to Fc receptors was blocked by incubating the cells with 10 µg/ml of anti-mouse CD16/32 for 10 min at 4 °C. Cells were then incubated for 20 min at 4 °C with the following antibody cocktail:

**Table 3.14 Antibody Master Mixes used for cell sorting**

Sorting of	Antigens
NK cells and/or ILC1s	CD45, CD3ε, NK1.1, NKp46, CD200R, CXCR6
LSECs and Immune cells	CD3ε, CD11b, CD19, CD31, CD45, CD146, F4/80, Ly6C, Ly6G, NKp46, NK1.1, Stab2, TCRβ

Afterwards, cells were washed (1,500 rpm for 10 min at 4 °C) and resuspended in cold PBS (NK cells and ILC1s) or Sorting buffer (LSEC and immune cells) at a density of  $5 \times 10^7$  cells/ml. The cell suspension was filtered through a 30 µm pore cell strainer. To exclude dead cells, 7AAD was added before cell sorting. Single, viable cells were sorted as following:

**Table 3.15 Gating strategies for cell sorting**

Sorting of	Gating
NK cells and ILC1s	CD45 <sup>+</sup> CD3ε <sup>neg</sup> NK1.1 <sup>+</sup> NKp46 <sup>+</sup>
NK cells	CD45 <sup>+</sup> CD3ε <sup>neg</sup> NK1.1 <sup>+</sup> NKp46 <sup>+</sup> CD200R <sup>neg</sup> CXCR6 <sup>neg</sup>
ILC1s	CD45 <sup>+</sup> CD3ε <sup>neg</sup> NK1.1 <sup>+</sup> NKp46 <sup>+</sup> CD200R <sup>+</sup> CXCR6 <sup>+</sup>
LSECs	CD45 <sup>neg</sup> Stab2 <sup>+</sup> CD146 <sup>+</sup> CD31 <sup>+</sup>
T cells	CD45 <sup>+</sup> Ly6G <sup>neg</sup> CD19 <sup>neg</sup> CD3ε <sup>+</sup> TCRβ <sup>+</sup>
Monocyte/Kupffer cells	CD45 <sup>+</sup> Ly6G <sup>neg</sup> CD19 <sup>neg</sup> CD11b <sup>+</sup> F4/80 <sup>+</sup>

NK cells and ILC1s for functional assays were sorted into NK cell culture media. LSECs and immune cells were sorted into sorting buffer. The purity of sorted cells was >98 % after each sort.

### 3.2.4 Cell counting

Single cell suspension was mixed with 0.05 % Trypan blue solution (w/v) in a 1:1 ratio and viable cells were counted using a Neubauer chamber (0.1 mm depth). Total number of viable cells was calculated as:

$$Total\ cell\ number\ [\times 10^6] = \frac{cell\ count}{counted\ squares} \times dilution\ factor \times 10^4 \times volume\ (ml)$$

Alternatively, cell suspension was mixed with 0.05 % Trypan blue solution (w/v) in a 1:1 ratio, and 10  $\mu$ l of stained cell solution were added to a CellChip™ and counted using TECAN Spark according to the suppliers' instructions. Total number of cells and viability were calculated as:

$$Total\ cell\ number = (Cell\ number \times viability\ [\%]) \times dilution\ factor \times volume\ (ml)$$

### 3.2.5 Primary cell culture

#### Culture of LSECs

After magnetic purification, LSECs were counted and seeded at  $0.8-1 \times 10^6$  cells/ml in a collagen-coated 24-well or 96-well plate to achieve a confluency of 100 %. After 24 h of culture, the LSEC layer was washed twice with warm PBS to remove dead cells. LSECs were then stimulated with 100 ng/ml of LPS, 100 ng/ml of IFN- $\gamma$  or left unstimulated in LSEC culture medium. For stimulation with tumor cell supernatants, supernatants were diluted 1:2 with fresh LSEC culture medium, and added to the LSEC layer. After 24 h, LSECs were used for co-cultures with NK cells. To detach LSECs, the LSEC layer was washed twice with pre-cooled PBS. Then, 300  $\mu$ l of pre-cooled Detachin™ Cell Detachment Solution were added per well and incubated for 10 min at 37 °C. Detachment of the cells was ensured by observing a round shape of the cells under the microscope. Cells were collected in a 15 ml Falcon containing pre-warmed LSEC culture medium. Wells were washed with cold PBS to collect remaining cells. Collected LSECs were washed twice with PBS by centrifugation (300xg for 10 min at 4 °C) and used for downstream applications.



### **Co-culture of LSECs with NK cells or ILC1s**

LSECs were cultured in a collagen-coated 96-well plate, as described above, and then washed with warm PBS twice. Sorted liver NK cells and ILC1s were counted, resuspended in NK culture medium supplemented with 300 U/ml IL-2 at a concentration of  $0.2 \times 10^6$  cells/ml, and added to the LSEC layer. Cells were co-cultured for 16 h. NK cells and ILC1s were harvested from the wells and used for flow cytometry or for functional analyses.

### **3.2.6 Culture of tumor cells**

#### **Cell thawing**

Cell suspensions in cryovial were thawed in a 37 °C waterbath by gentle shaking for 1-2 min. Thawed cells were diluted with pre-warmed media and transferred to a tube containing 30 ml of warm media. Cells were centrifuged (1,500 rpm for 10 min) and cell pellet was resuspended in appropriate media for culture.

#### **Culture of adherent and suspension tumor cells**

Cells were incubated at 37 °C with 5 % CO<sub>2</sub>. For splitting of adherent cells, media was aspirated and cell layer was washed with PBS. Trypsin-EDTA solution was added and incubated at 37 °C until cells were starting to detach. Pre-warmed media was added and cells were rinsed from the cell culture flask and collected in a tube. Cells were washed with PBS (1,500 rpm for 10 min) and resuspended at the desired density with pre-warmed media. Suspension cells were maintained by feeding them with fresh culture media every 2-3 days until they reached confluency. Then, a portion of the cells was withdrawn and splitted accordingly in media.

#### **Cell freezing**

Cells were collected and washed twice with PBS (1,500 rpm for 10 min). Cells were resuspended in cell freezing medium to a concentration of  $5 \times 10^5$  cells/ml and 1 ml was aliquoted to each cryovial. Cryovials were kept in a freezing container at -80 °C for at least 24 h. Afterwards, cryovials were stored for long term storage in liquid nitrogen.

### 3.2.7 Collection of cell supernatants

LSECs or tumor cells were cultured for 24 h in the respective media. Cell culture supernatants were collected and centrifuged twice (1,500 rpm for 10 min and 3,000 rpm for 10 min). Supernatants were filtered with a 0.33 µm filter, and then used for stimulation or frozen at -80 °C.

### 3.2.8 Cell cytotoxicity assay

Tumor cells were detached with non-enzymatic Cell Dissociation Solution and washed twice with PBS (1,500 rpm for 10 min). Tumor cells were resuspended in NK culture medium supplemented with 300 U/ml IL-2 to a concentration of 0.1x10<sup>6</sup> cells/ml. 12.5 µl (± 1,250 cells/well) were seeded in a black 384-well plate. CellTox™ Green Dye (Promega) was diluted 1:1,000 with NK cell culture medium supplemented with 300 U/ml IL-2, and 25 µl of the diluted dye were added to the wells. As effector cells, NK cells or ILC1s were harvested and counted. Cells were resuspended in NK culture medium supplemented with 300 U/ml IL-2 to a concentration of 0.125-0.25x10<sup>6</sup> cells/ml. 12.5 µl (± 1,250-3,125 cells/well) of NK cells were added to the wells with target cells, corresponding to an Effector-to-Target Ratio of 2.5:1, or as indicated in the Results section. To calculate maximum toxicity, 0.01 % of TritonX was added to target cells. Untreated target and effector cells (Target/Effector only control) and medium control were taken used for background correction. Fluorescence was measured with TECAN Spark every three hours for 48 h inside of a humidity cassette at 37 °C and 5 % CO<sub>2</sub>. Killing of target cells was calculated as

$$\text{Cytotoxicity [\%]} = \frac{(MFI \text{ Effector} + \text{Target}) - MFI \text{ Target Only Control} - MFI \text{ Effector Only Control}}{(MFI \text{ Target max. Toxicity} - MFI \text{ Target Only Control})} \times 100$$

### 3.2.9 Migration Assay

LSECs were purified from livers and cultured in a collagen-coated 24-well plate. If indicated, LSECs were stimulated with IFN- $\gamma$  for 24 h. The LSEC layer was washed with warm PBS, and migration media was added to the wells.  $1.5 \times 10^5$  of sorted liver CD3 $\epsilon^{\text{neg}}$ NK1.1 $^+$ NKp46 $^+$  cells were added into Transwell inserts (5  $\mu\text{m}$  pore size), which was placed above the LSEC layer or over a medium control well. The same amount of cells was incubated in the lower chamber in migration media only (input control). If indicated, lymphocytes were incubated for 10 min with anti-CD16/32 at 4°C, followed by incubation with anti-CXCR3 antibody for 15 min at 4°C. Cells were allowed to migrate for 4 h. Migrated cells were collected from the lower wells, and their numbers were quantified by flow cytometry using counting beads. NK cells were gated as NK1.1 $^+$ NKp46 $^+$ Eomes $^+$  and ILC1s were gated as NK1.1 $^+$ NKp46 $^+$ Eomes $^{\text{neg}}$ . Cell migration was calculated as

$$\text{Cell migration} = \left( \left( \frac{\# \text{ migrated cells}}{\# \text{ of beads}} \right) \times 100 \right) \div \left( \frac{\# \text{ Input cells}}{\# \text{ of beads}} \right)$$

Fold-change was calculated relative to migration towards media, which was set as 1 in every independent experiment.

### **3.2.10 Flow cytometry**

#### **Staining of surface molecules**

Cells were resuspended in cold PBS and distributed to a 96-well plate. For dead cell exclusion, cells were incubated with 30  $\mu$ l cold PBS containing 0.3  $\mu$ l of Aqua Zombie™ for 20 min at RT in the dark. 25  $\mu$ l of FcR-blocking reagent (10% supernatant of  $\alpha$ CD16/CD32-producing hybridoma 2.4G2) was added and cells were incubated for 15 min at 4 °C in the dark, followed by an incubation with fluorochrome-labeled monoclonal antibodies against surface molecules in 50  $\mu$ l of FACS buffer for 20 min at 4 °C in the dark. Cells were washed twice with FACS buffer (2,100 rpm for 4 min at 4 °C). Cells were fixed and afterwards washed and resuspended in 200  $\mu$ l of FACS buffer. If cell fixation was not required, dead cells were excluded by labeling with 7-aminoactinomycin D (7-AAD) directly before acquisition.

#### **Staining of intracellular molecules**

For staining of intracellular antigens, cells were fixed and permeabilized with the Intracellular Fixation & Permeabilization Buffer Set according to the manufacturer's instructions. 25  $\mu$ l of FcR-blocking reagent, diluted 1:1 with Perm buffer, were added and cells were incubated for 15 min at 4 °C in the dark. Antibody cocktail containing fluorochrome-labeled monoclonal antibodies against intracellular molecules in 50  $\mu$ l of Perm buffer was added and incubated for 20 min at 4 °C in the dark. Cells were washed twice with Perm buffer (2,100 rpm for 4 min at 4 °C) and resuspended in 200  $\mu$ l of FACS buffer for flow cytometric analysis.

### 3.2.11 Flow cytometric analysis

Samples were acquired with LSRFortessa or FACS Aria Fusion and data were analyzed with FlowJo v10.7.1. Cell populations were gated as follows:

**Table 3.16 Gating strategies of different cell populations. Lin: CD19, Ly6G, Ter119, F4/80**

Cells	Gating strategy
LSECs	CD45 <sup>neg</sup> Stabilin2 <sup>+</sup> CD146 <sup>+</sup> CD31 <sup>+</sup>
Cultured LSECs	CD45 <sup>neg</sup> CD146 <sup>+</sup>
Kupffer cells	CD45 <sup>+</sup> Stabilin2 <sup>neg</sup> Ly6G <sup>neg</sup> F4/80 <sup>+</sup> CD11b <sup>low</sup>
Infiltrating monocytes	CD45 <sup>+</sup> Stabilin2 <sup>neg</sup> Ly6G <sup>neg</sup> CD11b <sup>+</sup> F4/80 <sup>+</sup>
Neutrophils	CD45 <sup>+</sup> Stabilin2 <sup>neg</sup> Ly6G <sup>+</sup>
ILC1s	CD45 <sup>+</sup> Lin <sup>neg</sup> CD3ε <sup>+</sup> NK1.1 <sup>+</sup> NKp46 <sup>+</sup> Eomes <sup>neg</sup>
NK cells	CD45 <sup>+</sup> Lin <sup>neg</sup> CD3ε <sup>+</sup> NK1.1 <sup>+</sup> NKp46 <sup>+</sup> Eomes <sup>+</sup>
NKT cells	CD45 <sup>+</sup> Lin <sup>neg</sup> CD3ε <sup>+</sup> TCRβ <sup>int</sup> NK1.1 <sup>int</sup>
CD4 <sup>+</sup> T cells	CD45 <sup>+</sup> Lin <sup>neg</sup> CD3ε <sup>+</sup> TCRβ <sup>+</sup> NK1.1 <sup>neg</sup> CD4 <sup>+</sup>
CD8 <sup>+</sup> T cells	CD45 <sup>+</sup> Lin <sup>neg</sup> CD3ε <sup>+</sup> TCRβ <sup>+</sup> NK1.1 <sup>neg</sup> CD8 <sup>+</sup>

### 3.2.12 RNA extraction

Cells were collected in a 1.5 ml tube and washed with sterile PBS (5,000 rpm for 5 min). Pellet was lysed in RLT buffer containing 1 % of β-mercaptoethanol, and vortexed for 2 min. Lysates were stored at -80 °C until further processing. RNA was purified using RNeasy Mini Kit according to the manufacturer's instructions. Genomic DNA was removed by treatment with TURBO DNA-free Kit according to the manufacturer's instructions. RNA concentration was measured with TECAN Spark plate reader.

### 3.2.13 cDNA Synthesis and quantitative real-time-PCR (qPCR)

First strand cDNA was generated from total RNA using ProtoScript® II First Strand cDNA Synthesis Kit. Master Mix, containing respective primers and PowerUp™ SYBR™ Green Mastermix, was added to cDNA, and qPCR was performed in a QuantStudio™ 5 Real-Time 384-well PCR System with the following program: hold stage with 50 °C for 20 min and 95 °C for 2 min, 40 cycles of amplification at 95 °C for 1 s and 60 °C for 30 s, and melt curve stage at 95 °C for 15 s, 60 °C for 1 min and 95 °C for 15 s.

For RT<sup>2</sup> Profiler™ PCR Array of Mouse Cytokines & Chemokines, a total of 400 ng of RNA was reverse-transcribed, and cDNA was obtained using the RT2 First Strand Kit. qPCR was run in a QuantStudio™ 5 Real-Time PCR System, according to the manufacturer's instructions.

Mouse B2m or Actin mRNA were used as reference controls (as indicated in respective Figure legends), and relative mRNA expression was calculated using delta-Ct ( $2^{-\Delta Ct}$ ) method. Transcripts yielding a Ct value >35 were excluded from the analysis.

### **3.2.14 Quantification of chemokine concentration**

#### **Legendplex**

Blood of mice was collected by retroorbital bleeding in a 1.5 ml tube and incubated at 37 °C for 2 h. Clotted blood was removed by centrifugation at 14,000 rpm for 3 min. Serum was transferred in a fresh 1.5 ml tube and stored at -20 °C until performing the assay. Chemokine concentration in serum was assessed using bead-based LEGENDplex™ Kit according to the manufacturer's instructions. Data were analyzed with the LEGENDplex™ Data Analysis Software.

#### **ELISA**

The concentration of murine CXCL10 in supernatants was determined by ELISA according to the manufacturer's instructions.

### **3.2.15 Mouse genotyping**

Cdh5<sup>Cre</sup>CXCL10<sup>fl/fl</sup> mice were kindly genotyped by the group of Prof. Dr. Michael Platten. After performing the experiments, mice were re-genotyped in our laboratory. Tail pieces were collected and lysed using MyTaq™ Extract-PCR Kit according to the manufacturer's instructions. The PCR Mastermix was prepared with the MyTaq™ HS Red Mix and optimized primers. DNA was added to the Master Mix, and a Touchdown PCR was run in a C1000 Touch™ Thermal Cycler. PCR products were separated on a 1.5 % agarose gel and separated bands were visualized with a 200 Gel Imaging Workstation.

### **3.2.16 Experimental mouse models**

#### **LPS-induced acute liver inflammation**

Male mice were injected intraperitoneally with LPS (5 mg/kg of body weight; Escherichia coli strain O26:B6) or with equivalent amount of PBS, and sacrificed 6 h or 16 h post-injection.

If indicated, mice were injected with 200 µg of mouse anti-CXCR3, mouse anti-VCAM-1, or a combination of both monoclonal antibodies, 2 days before and on the day of LPS injection.

#### **Preparation of tumor cells for injection**

MC38 or MC38 Luciferase/tdTomato tumor cells were harvested in the exponential growth phase after 5-7 d of culture using non-enzymatic cell-dissociation buffer, and centrifuged (1,200 rpm for 5 min). Cells were washed with media without FCS (1,200 rpm for 5 min), followed by wash with sterile PBS (1,200 rpm for 5 min).

**Subcutaneous injection of tumor cells**

Tumor cell suspensions were counted and resuspended at a density of  $1 \times 10^7$  cells/ml in PBS. C57BL/6N mice were injected subcutaneously with 100  $\mu$ l of tumor cell suspension ( $\pm 1 \times 10^6$  cells) into the left flank. Tumor growth was assessed every 2 - 3 days with a caliper measuring the height, width and depth of the tumors, and tumor volume was calculated. Mice were sacrificed when the tumors reached a diameter of  $\sim 1.5$  cm.

**Portal vein injection of tumor cells**

MC38 Luciferase/tdTomato cancer cell suspensions were counted and resuspended at a density of  $1 \times 10^6$  cells/ml in PBS. 30 min before surgical procedure, C57BL/6N mice were injected subcutaneously with buprenorphine (0.1 mg/kg of body weight) in 100  $\mu$ l sterile PBS for post-surgical pain management. Mice were anaesthetized with isoflurane, and ointment was applied to the animal's eyes. The abdominal fur of the mice was removed with a razor, followed by removal of remaining hair using hair removal cr me. Laparotomy was performed through midline incision and the intestine was carefully moved to a sterile gauze. The portal vein was exposed and 100  $\mu$ l of tumor cell suspension ( $\pm 1 \times 10^5$  cells) was injected with a 29 G needle. The needle was removed while gentle pressure was applied to the vein with a sterile cotton tip for 5 min. Internal organs were carefully returned to the abdominal cavity and mice were sutured. Buprenorphine was given to the mice every 6-8 h for 48 h for post-surgical pain management.

**In vivo bioluminescence imaging**

To monitor the tumor growth after injection of tumor cells via the portal vein, *in vivo* bioluminescence imaging was performed at day 7, 10 and 14 post-injection. Mice were injected with D-luciferin (150 mg/kg BW) intraperitoneally and anaesthetized with isoflurane. Animals were imaged using an IVIS200 imaging system with an exposure time set to 1 min, small binning and F stop of 1. Quantification of the bioluminescence was performed with the Living Image software.



**3.2.17 Statistical analysis**

For statistical analyses and data visualization, Prism, R, RStudio, and packages ggplot and pheatmap were used. Data were tested for normal distribution using Shapiro-Wilk test, followed by evaluation using an appropriate test indicated in the figure legends. Correction for multiple comparison testing was done when necessary. Experimental results are shown as mean  $\pm$  SEM; n represents numbers of animals or as specified in figure legends. Experimental groups were considered to be significantly different when \*,  $p < 0.05$ , \*\*,  $p < 0.01$ , \*\*\*,  $p < 0.001$  or \*\*\*\*,  $p < 0.0001$ .



## 4 RESULTS

LSECs are positioned within the liver sinusoids, where they can interact with immune cells, blood, and the surrounding tissue. It was recently shown that liver innate NKp46<sup>+</sup> cells (NK cells and ILC1s) locate within the sinusoids in close contact to the blood vessel lining endothelial cells (Ducimetiere et al., 2021). Until now, it remains unclear how vascular cells affect the function of innate lymphocytes during inflammation and malignancies in the liver. Furthermore, it remains elusive how different groups of innate lymphocytes respond to LSEC-mediated signals.

### 4.1 Interaction of LSECs and NK cells in hepatic inflammation

To investigate the interaction of innate lymphocytes and LSECs in hepatic inflammation, we injected mice with LPS to induce a systemic inflammation and acute inflammatory response in the liver. LSECs were shown to rapidly eliminate LPS from the blood, and can be activated via TLR4, which leads to the secretion of pro-inflammatory cytokines and increased expression of adhesion molecules (Amersfoort et al., 2022; Cabral et al., 2021; Uhrig et al., 2005; Yao et al., 2016). It was also shown that IFN- $\gamma$ -secreting NK cells drive LPS-induced mortality in mice, and that NK cells were the major producers of IFN- $\gamma$  in several organs (Chan et al., 2014; Rasid et al., 2016). To study the inflammatory response in the liver, we injected mice with 5  $\mu$ g/kg body weight of LPS and analyzed the liver, spleen and blood 16 h after injection (Figure 4.1A).

#### 4.1.1 NK cells, but not ILC1s, are accumulating in the inflamed liver tissue

We observed a significantly reduced body weight (BW), liver weight and a reduced liver-to-BW ratio in mice injected with LPS in comparison to control mice (Figure 4.1B). Furthermore, the numbers of Neutrophils, Monocytes and Kupffer cells (gated as shown in Figure 4.1C) were increased, whereas the numbers of CD4<sup>+</sup> and CD8<sup>+</sup> T cells (gated as shown in Figure 4.1D) were reduced in livers of LPS injected mice (Figure 4.1E).

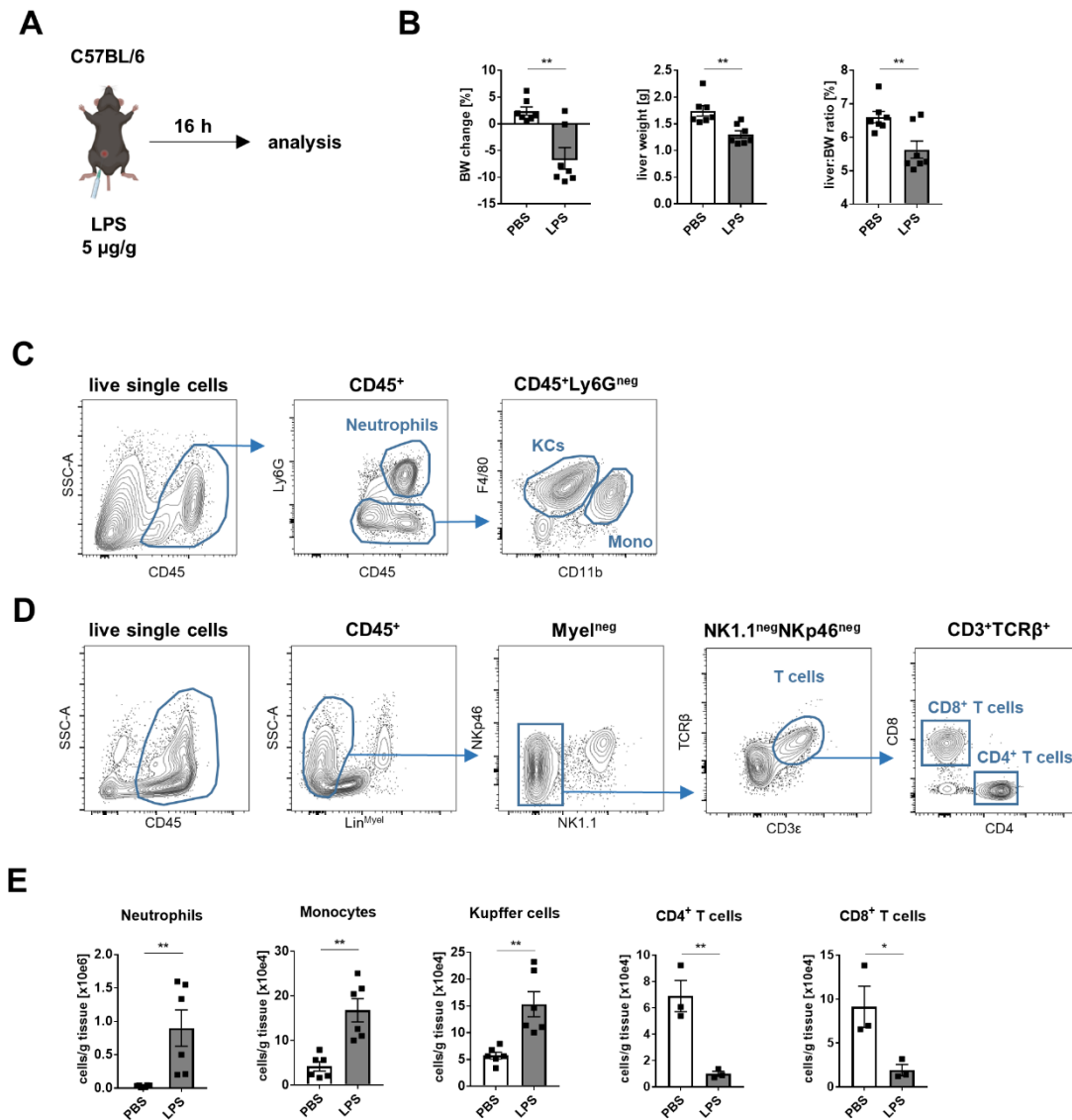
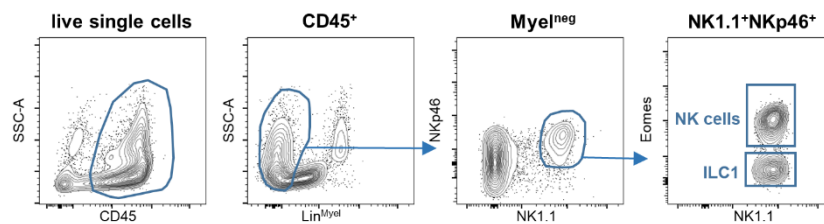


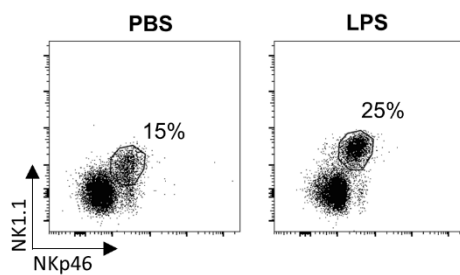
**Figure 4.1 Immune cell distribution in the liver after LPS injection.** (A) Schematic illustration of experimental procedure. (B) Body weight (BW) change relative to initial body weight (left), liver weight (middle) and liver-to-BW ratio (right) after treatment with LPS.  $n = 7-8$  mice from two independent experiments. (C-D) Immune cells were gated as live CD45-expressing single cells. Myeloid cell subsets were gated as Ly6G<sup>+</sup> Neutrophils, Ly6G<sup>neg</sup>CD11b<sup>+</sup>F4/80<sup>dim</sup> Monocytes (Mono) and Ly6G<sup>neg</sup>F4/80<sup>+</sup>CD11b<sup>+</sup> Kupffer cells (KCs) (C). For lymphocytes, myeloid and B cells were excluded (Lin<sup>Myel</sup>:Ly6G, SiglecF, F4/80, CD19), and cells further defined as NK1.1<sup>neg</sup>NKp46<sup>neg</sup>TCRβ<sup>+</sup>CD3ε<sup>+</sup> T cells (CD4<sup>+</sup> or CD8<sup>+</sup>) (D). (E) Cell numbers of indicated immune cell subsets 16 h post-injection of PBS or LPS.  $n = 3-6$  mice from one (T cells) or two (Myeloid cells) experiments. (B+E) Data are shown as mean  $\pm$  SEM, analyzed by unpaired Student's *t*-Test. \*,  $p < 0.05$ ; \*\*,  $p < 0.01$ . Symbols represent individual mice.

Furthermore, we observed an increased frequency of NK1.1<sup>+</sup>NKp46<sup>+</sup> innate immune cells (gated as shown in Figure 4.2A), comprising NK cells and ILC1s, among CD45<sup>+</sup>Lin<sup>neg</sup> cells, and increased numbers in the inflamed livers (Figure 4.2B+C). While Eomes<sup>neg</sup> ILC1s did not increase in proportion among all NK1.1<sup>+</sup>NKp46<sup>+</sup> cells or in numbers, we found that both frequencies and numbers of Eomes<sup>+</sup> NK cells significantly increased in the livers of LPS-injected mice (Figure 4.2D+E).

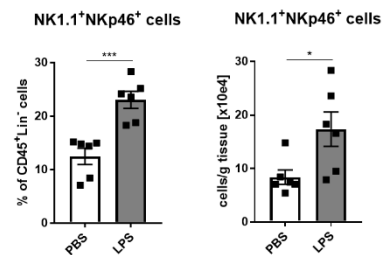
A



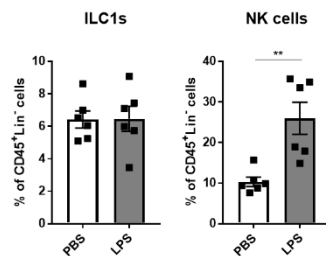
B



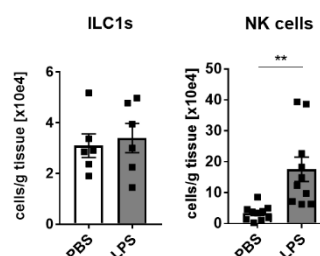
C



D



E



F

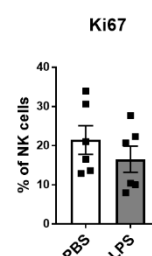


**Figure 4.2 NK cells numbers are increased in the liver after LPS injection.** (A) Immune cells were gated as live CD45-expressing single cells. Myeloid and B cell lineage markers were excluded (Lin<sup>Myel</sup>: Ly6G, SiglecF, F4/80, CD19), and cells further defined as NK1.1<sup>+</sup>NKp46<sup>+</sup> ILCs, NK1.1<sup>+</sup>NKp46<sup>+</sup>Eomes<sup>+</sup> NK cells, NK1.1<sup>+</sup>NKp46<sup>+</sup>Eomes<sup>neg</sup> ILC1s. (B) Representative flow cytometry plots of NK1.1<sup>+</sup>NKp46<sup>+</sup> cells in the liver of PBS- and LPS-injected mice. (C) Proportion and cell numbers of NK1.1<sup>+</sup>NKp46<sup>+</sup> cells in the liver of PBS- or LPS-injected mice. (D+E) Proportion among CD45<sup>+</sup>Lin<sup>-</sup> cells (D) and cell numbers (E) of NK cells and ILC1s in the liver 16 h post-injection of PBS or LPS. (F) Frequency of Ki67-expressing NK cells in the livers of PBS- or LPS-injected mice. (C-F) Data are shown as mean  $\pm$  SEM, analyzed by unpaired Student's *t*-Test. \*, *p*<0.05; \*\*, *p*<0.01; \*\*\*, *p*<0.001. Symbols represent individual mice. *n*=6 mice from 2 independent experiments.

We hypothesized that the increase in NK cell numbers in the liver tissue after LPS injection would occur either due to proliferation or due to active recruitment. However, the frequency of Ki67-expressing NK cells did not increase after LPS injections (Figure 4.2F), indicating that NK cells did not change their proliferative behavior, but were infiltrating the tissue after recruitment.

#### 4.1.2 NK cells and LSECs are activated during endotoxemia

In order to evaluate the activation of NK cells, we assessed the expression of several molecules, previously shown to indicate NK cell activation (Borrego et al., 1999; Burt et al., 2008; Nabekura et al., 2020). After the injection of LPS, hepatic NK cells expressed CD25 and CD69 (Figure 4.3A-C). We observed that NK cells also upregulated the expression of CD11c, and a subpopulation of NK cells upregulated the expression of Ly6C (Figure 4.3A-C).

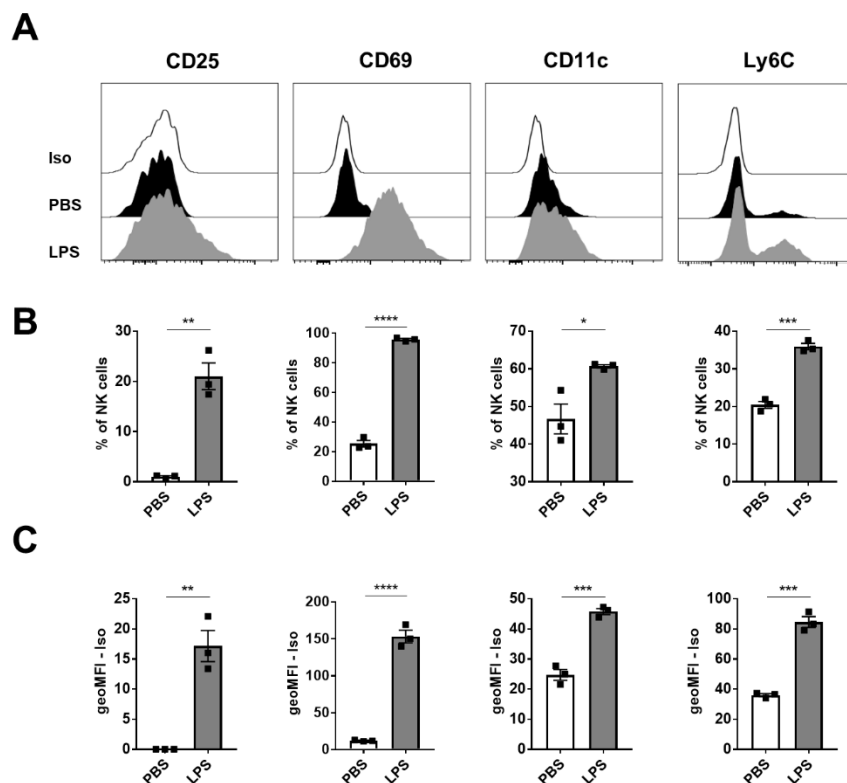


**Figure 4.3 NK cells show an activated phenotype after LPS injection.** (A-C) Representative flow-cytometry histograms (A), graphs showing frequencies of expressing cells (B), and expression (C) of CD25, CD69, CD11c and Ly6C by NK cells in the livers of PBS- or LPS-injected mice 16 h post-injection. Data represent one experiment with 3 mice/group. Iso, Isotype; geoMFI, geometric mean fluorescent intensity. (B-C) Data are shown as mean  $\pm$  SEM, analyzed by unpaired Student's *t*-Test. \*,  $p < 0.05$ ; \*\*,  $p < 0.01$ ; \*\*\*,  $p < 0.001$ ; \*\*\*\*,  $p < 0.0001$ . Symbols represent individual mice.

LSECs (gated as shown in Figure 4.4A) isolated from LPS-injected mice upregulated the expression of the adhesion molecules ICAM-1 and VCAM-1 (Figure 4.4C-E). We also analyzed the expression of membrane proteins that were shown to interact with receptors expressed by NK cells, and observed that LSECs express major histocompatibility complex (MHC) class I and II, programmed death-ligand 1 (PD-L1), CD155 and HVEM in PBS-injected mice (Figure 4 C+D). The expression of PD-L1 was increased on LSECs after LPS injection, whereas the expression of the other molecules remained unchanged (Figure 4.4C+D).

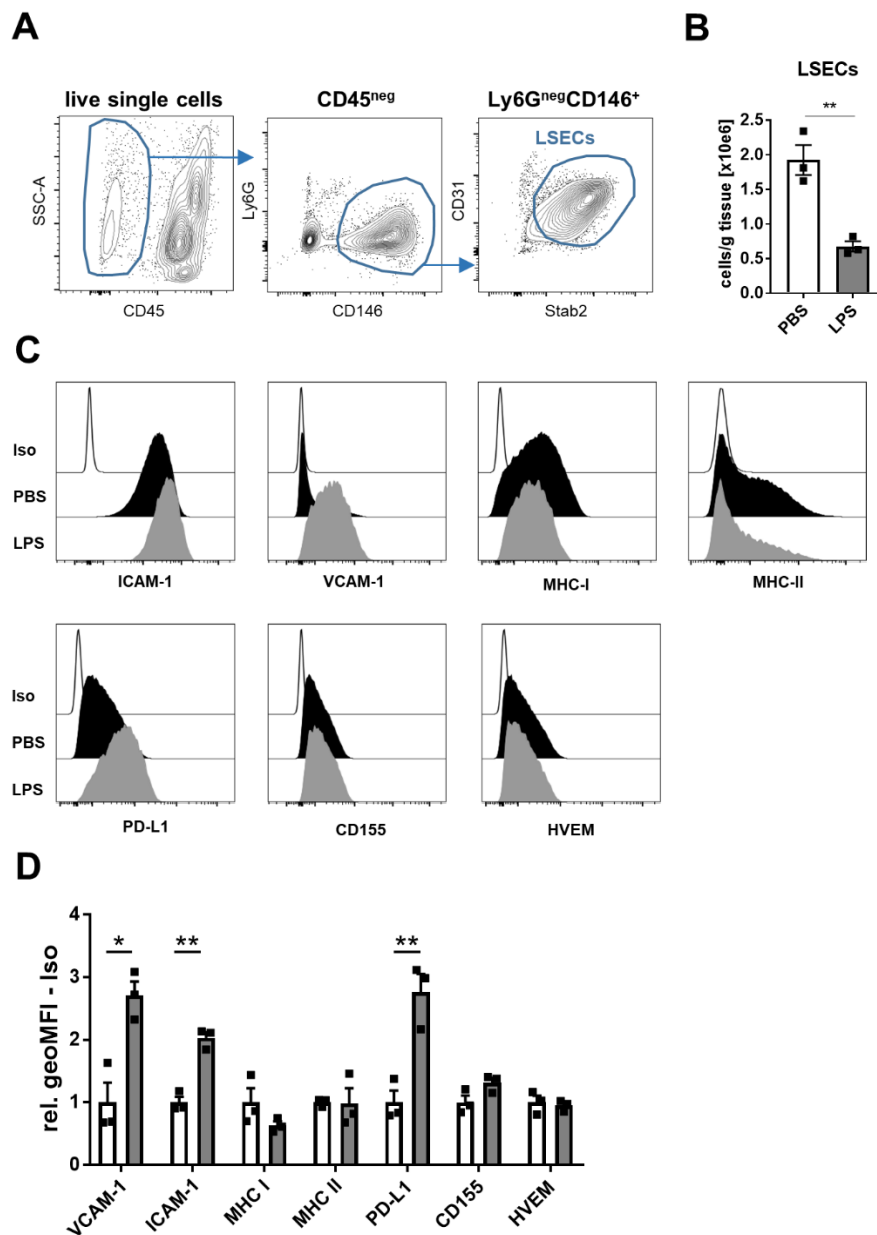


(Figure legend on the next page)

**Figure 4.4 LSECs upregulate endothelial activation markers after injection of LPS.** (A) LSECs were gated as live CD45<sup>neg</sup>Ly6G<sup>neg</sup>CD146<sup>+</sup>CD31<sup>+</sup>Stab2<sup>+</sup> cells. (B) Cell numbers of LSECs in PBS- or LPS-treated mice 16 h post-injection. (C-D) Representative histograms (C) and graph (D) showing the expression of selected molecules on LSECs in PBS- and LPS-injected mice. (D) Data are shown as mean  $\pm$  SEM, analyzed by unpaired Student's *t*-Test. \*,  $p < 0.05$ ; \*\*,  $p < 0.01$ . Symbols represent individual mice,  $n = 3$  mice/group from one performed experiment. Iso, Isotype, rel. geoMFI, relative geometric mean fluorescence intensity.

### 4.1.3 LSECs secrete leukocyte-attracting chemokines

As we observed the increased numbers of immune cells in the liver tissue after LPS injection, we hypothesized that increased concentration of chemoattractants might play a role. We analyzed the blood of PBS- and LPS-injected mice and could show that the chemokines CCL2, CCL3, CCL5 and CCL7, which were shown to attract Monocytes (Tsou et al., 2007; Weber et al., 2001), and CXCL10, which was shown to attract T cells and NK cells (Dufour et al., 2002; Wendel et al., 2008), were significantly elevated in the serum of LPS-injected animals (Figure 4.5A). *Cxcl10* transcripts were also significantly increased in homogenates of whole liver tissue (Figure 4.5B).

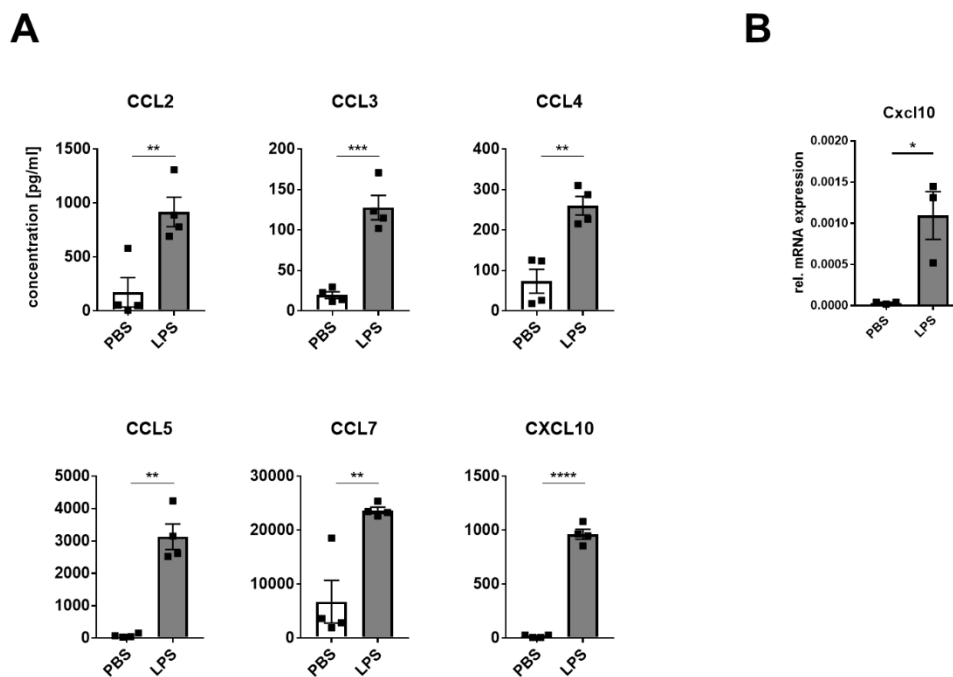


**Figure 4.5 Chemokines are increased in the serum and liver of LPS injected mice.** (A) Concentration of depicted chemokines in the serum of PBS- and LPS-injected mice 16 h post-injection, assessed by bead-based flow cytometry analysis.  $n = 4$  mice/group from a single experiment. (B) Relative mRNA expression of *Cxcl10* in homogenates of liver tissue from PBS or LPS injected mice.  $n = 3$  mice/group from a single experiment. (A+B) Data are shown as mean  $\pm$  SEM, analyzed by unpaired Student's *t*-Test. \*,  $p < 0.05$ ; \*\*,  $p < 0.01$ ; \*\*\*,  $p < 0.001$ ; \*\*\*\*,  $p < 0.0001$ . Symbols represent individual mice.



To evaluate chemokine-secreting cells in the inflamed liver, we sorted LSECs, Monocyte/Kupffer cells, T cells and NK+ILC1 (gated as shown in Figure 4.6A), and analyzed their chemokine profile by qPCR. We observed that NK cells and ILC1s, and T cells expressed mRNA transcripts for *Cx3cl1*, *Ccl1* and *Ccl5*, whereas Monocytes and Kupffer cells expressed transcripts for *Ccl2* and *Ccl7* (Figure 4.6B). In comparison to the sorted immune cells, LSECs showed the highest relative transcript amounts of *Ccl2*, *Cxcl9*, *Cxcl10* and *Cxcl11* (Figure 4.6B+C).

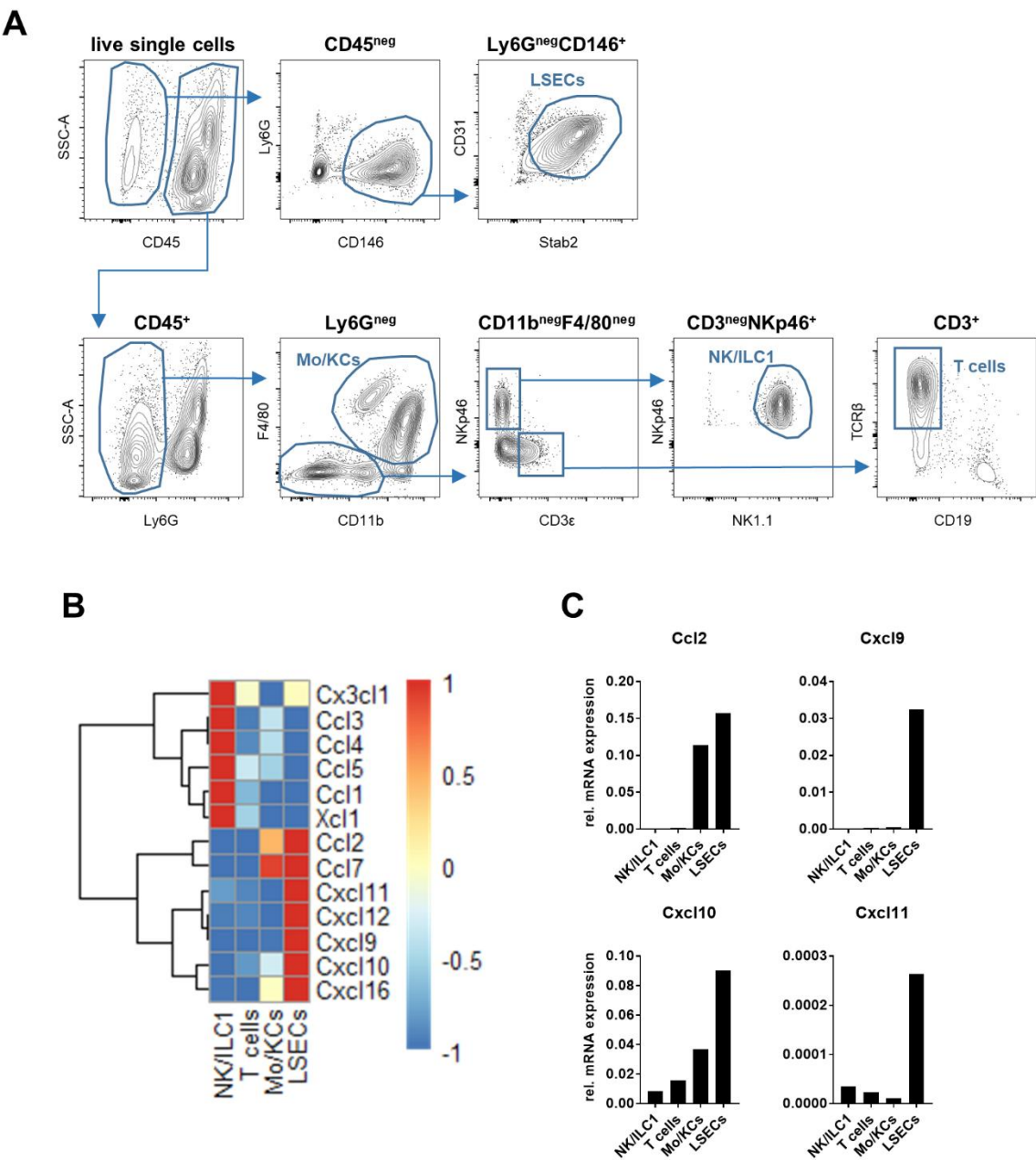


(Figure legend on the next page)

**Figure 4.6 LSECs are the major cellular source of transcripts encoding for CXCR3-ligands.** (A) Mice were challenged with LPS, and 16 h later, single-cell suspensions were prepared from pooled liver tissue of four mice, and indicated cell populations were purified by flow-cytometric sort. All subsets were pre-gated as single and live cells. LSECs were sorted as  $CD45^{neg}Ly6G^{neg}CD146^{+}CD31^{+}Stab2^{+}$ . Among  $CD45$ -expressing cells, Monocytes and Kupffer cells (MoKCs) were sorted as  $Ly6G^{neg}F4/80^{+}CD11b^{+}$ . Among  $Ly6G^{neg}F4/80^{neg}CD11b^{neg/dim}$  lymphocytes, NK cells and ILC1s (NK/ILC1) were purified as  $CD3\epsilon^{neg}NKp46^{+}NK1.1^{+}$ , and T cells as  $CD3\epsilon^{+}TCR\beta^{+}CD19^{neg}$ . (B) Heatmap displaying relative (to b2m) mRNA expression of depicted chemokines in the sorted cell populations, analyzed by qPCR. Data are scaled per row. (C) Relative mRNA expression of *Ccl2*, *Cxcl9*, *Cxcl10* and *Cxcl11* by NK/ILC1, T cells, Mo/KCs and LSECs.

To dissect LPS-induced changes in the transcriptome of LSECs, we compared the expression of gene transcripts of selected chemokines in LSECs sorted from PBS- and LPS-injected mice. We observed that the transcripts *Ccl2*, *Ccl3*, *Ccl4*, *Ccl5* and *Ccl7* were increased after LPS injection (Figure 4.7 top). Furthermore, LSECs upregulated the mRNA transcripts *Cxcl9*, *Cxcl10* and *Cxcl11* (Figure 6B bottom), which encode for the ligands to the chemokine receptor CXCR3. The transcripts for *Cxcl16* were decreased and there was no change in the mRNA expression of *Cx3cl1* in LSECs sorted from LPS injected mice (Figure 4.7 bottom).

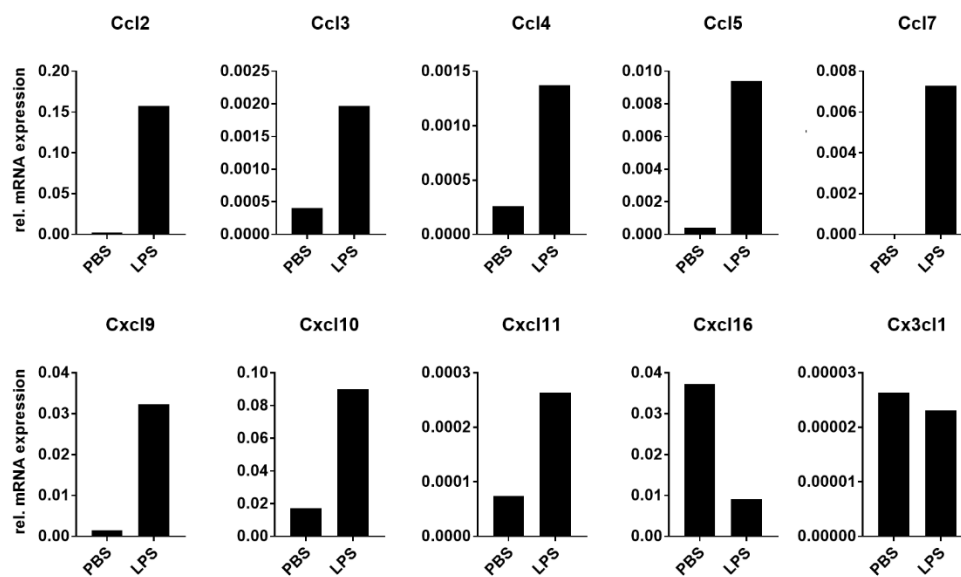


**Figure 4.7 LSECs upregulate chemokine transcript expression after LPS injection.** Relative mRNA expression of selected chemokines in LSECs sorted from PBS or LPS injected mice.

LPS binds to TLR4, which is constitutively expressed by LSECs, and its triggering was demonstrated to initiate the secretion of pro-inflammatory cytokines and the upregulation of adhesion molecules (Cabral et al., 2021; Uhrig et al., 2005). Previous reports show that the transcription of *Cxcl10* is mediated by the activation of the IFN- $\gamma$  receptor (Luster and Ravetch, 1987). To find out which stimuli in the microenvironment of the inflamed liver tissue are able to induce the transcription of chemokines by LSECs, we stimulated cultured LSECs with LPS or IFN- $\gamma$  for 24 h, and analyzed their chemokine transcript profile by qPCR.

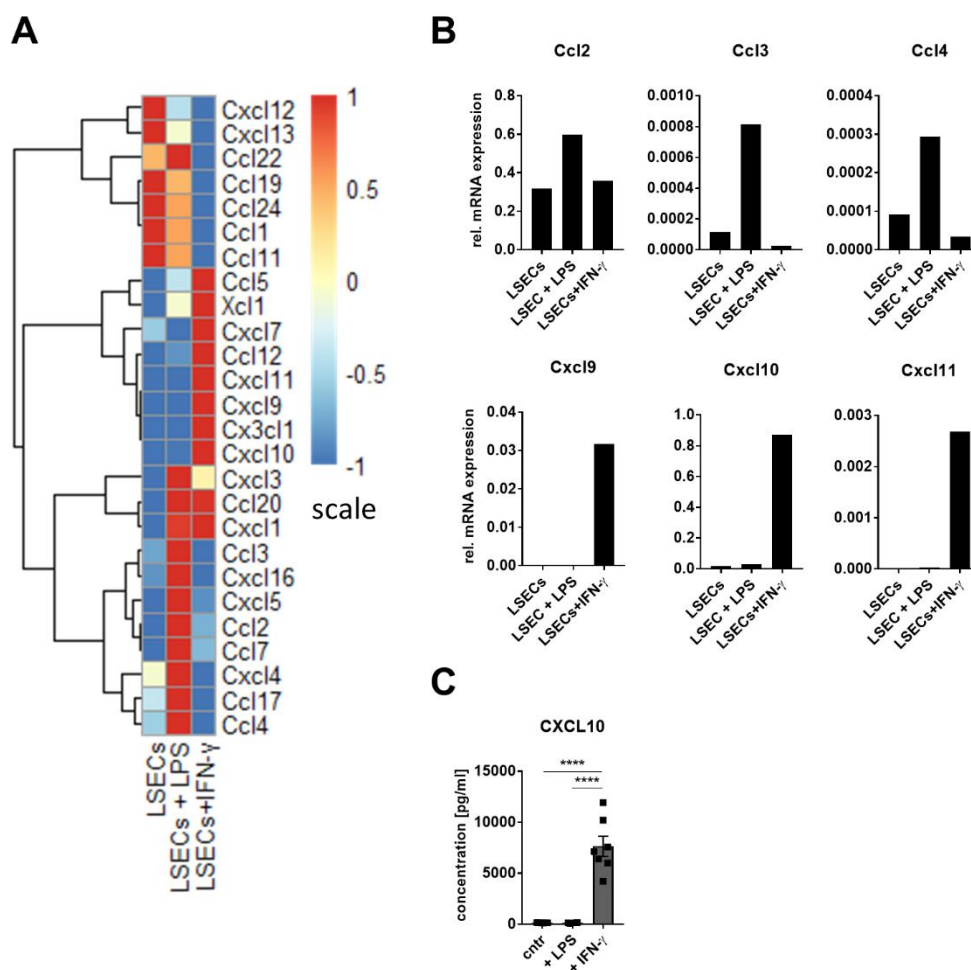


**Figure 4.8 The chemokine transcriptome of LSECs is differentially regulated by LPS and IFN- $\gamma$ .** LSECs purified from murine livers were treated with LPS or IFN- $\gamma$  for 24 h. (A) Heatmap displaying scaled relative (to Actin) mRNA expression of depicted chemokines, analyzed by qPCR. Data are scaled per row. (B) Relative mRNA expression of selected chemokines. (C) Concentration of CXCL10 protein in the supernatant of cultured LSECs measured by ELISA. Data are shown as mean  $\pm$  SEM, analyzed by ordinary one-way ANOVA. \*\*\*\*,  $p < 0.0001$ . Symbols represent biological replicates,  $n=7$  from four independent experiments. LSECs, not-stimulated; cntr, control.

We observed that the stimulation of LSECs with LPS was leading to an increase of transcripts for several chemokines important for the recruitment of monocytes, such as *Ccl2*, *Ccl3* and *Ccl4* (Figure 8A+B, top) (Tsou et al., 2007; Weber et al., 2001). After the stimulation of LSECs with IFN- $\gamma$  we observed increased transcripts of *Cxcl9*, *Cxcl10* and *Cxcl11* (Figure 4.8A+B, bottom). We then measured the concentration of CXCL10 protein in the supernatant of LSECs stimulated with LPS or IFN- $\gamma$  for 24 h. We observed that LSECs stimulated with LPS did not produce CXCL10, whereas the stimulation of LSECs with IFN- $\gamma$  induced the secretion of CXCL10 (Figure 4.8C). These findings suggest that LPS and IFN- $\gamma$  have distinct roles in shaping the LSEC chemokine production.

#### **4.1.4 NK cells are the major source of IFN- $\gamma$ in the liver**

We showed that LSECs produce CXCL10 in response to IFN- $\gamma$ , which plays an important role in the immune responses and was shown to drive LPS-induced mortality of mice (Chan et al., 2014; Emoto et al., 2002; Heremans et al., 1994). Certain types of immune cells, including TCR $\beta^+$  T cells, NKT cells, NK cells and ILC1s, can produce IFN- $\gamma$  upon activation. To determine the cellular sources of IFN- $\gamma$  in the liver of LPS-injected mice, we sorted LSECs, Monocyte and Kupffer cell compartment, T cells and NK1.1<sup>+</sup>NKp46<sup>+</sup> innate immune cells (sorted as shown in Figure 4.6A), and analyzed their cytokine profile by qPCR (Figure 4.9A). Among the analyzed cell populations, *Ifng* transcripts were most abundant in the compartment of NK1.1<sup>+</sup>NKp46<sup>+</sup> cells, followed by T cells (Figure 4.9A+B). We observed that in the inflamed liver tissue, Monocyte and Kupffer cell compartment showed expression of *Il12a* and *Il18*, whereas LSECs expressed transcripts for *Il15* (Figure 4.9A+B). These cytokines were shown to induce IFN- $\gamma$  production by NK cells (Fehniger et al., 1999; Lusty et al., 2017).

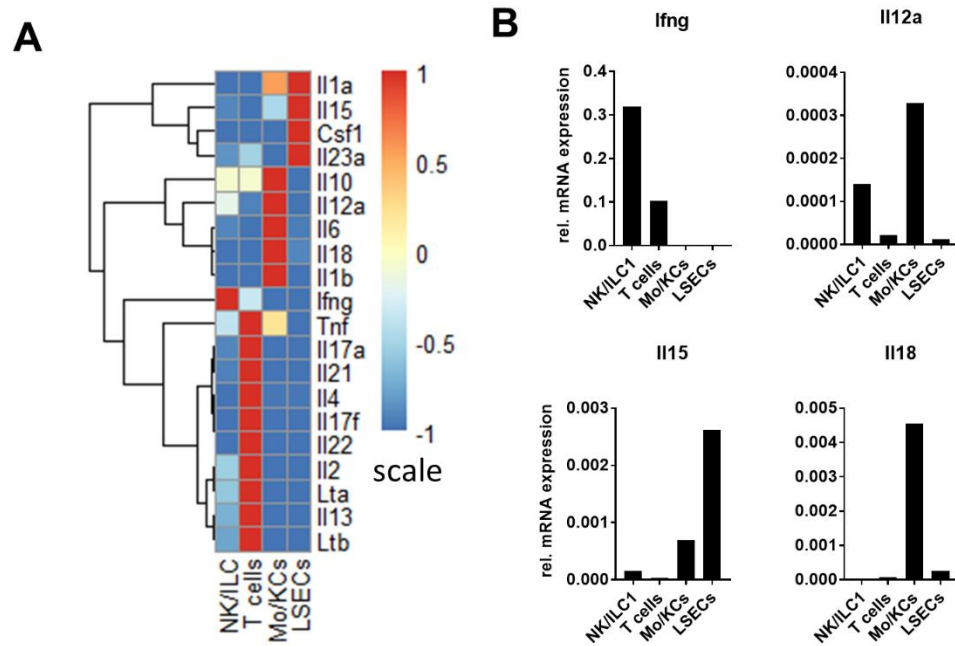


**Figure 4.9 Cytokine profile of innate lymphocytes, T cells, Monocytes/Kupffer cells and LSECs in inflamed liver tissue.** Mice were challenged with LPS, and 16 h later LSECs, NK1.1<sup>+</sup>NKp46<sup>+</sup> cells (NK/ILC), T cells and CD11b<sup>+</sup>F4/80<sup>+</sup> cells (Mo/KCs) were sorted from 4 pooled liver tissue samples (gated as in Figure 6A). (A) Heatmap displaying scaled relative (to b2m) mRNA expression of depicted cytokines, analyzed by qPCR. Data are scaled per row. (B) Graphs showing relative mRNA expression of *Ifng*, *Il12a*, *Il15* and *Il18* among the sorted cell populations.

Next, we injected mice with LPS and stained IFN- $\gamma$  intracellularly 6 h and 16 h after injection to analyze IFN- $\gamma$  production in liver, spleen and blood. We observed that NK cells significantly upregulated IFN- $\gamma$  production in the liver, spleen and blood already 6 h after LPS injection (Figure 4.10A-C). IFN- $\gamma$  expression by NK cells was sustained in the analyzed organs over a time of 6 – 16 h post-treatment with LPS. In comparison to ILC1s, TCR $\beta$ <sup>+</sup> T cells and other CD45<sup>+</sup>Lin<sup>neg</sup> cells, NK cells were the major source of IFN- $\gamma$  in liver, spleen and blood 16 h after LPS injection (Figure 4.10D).

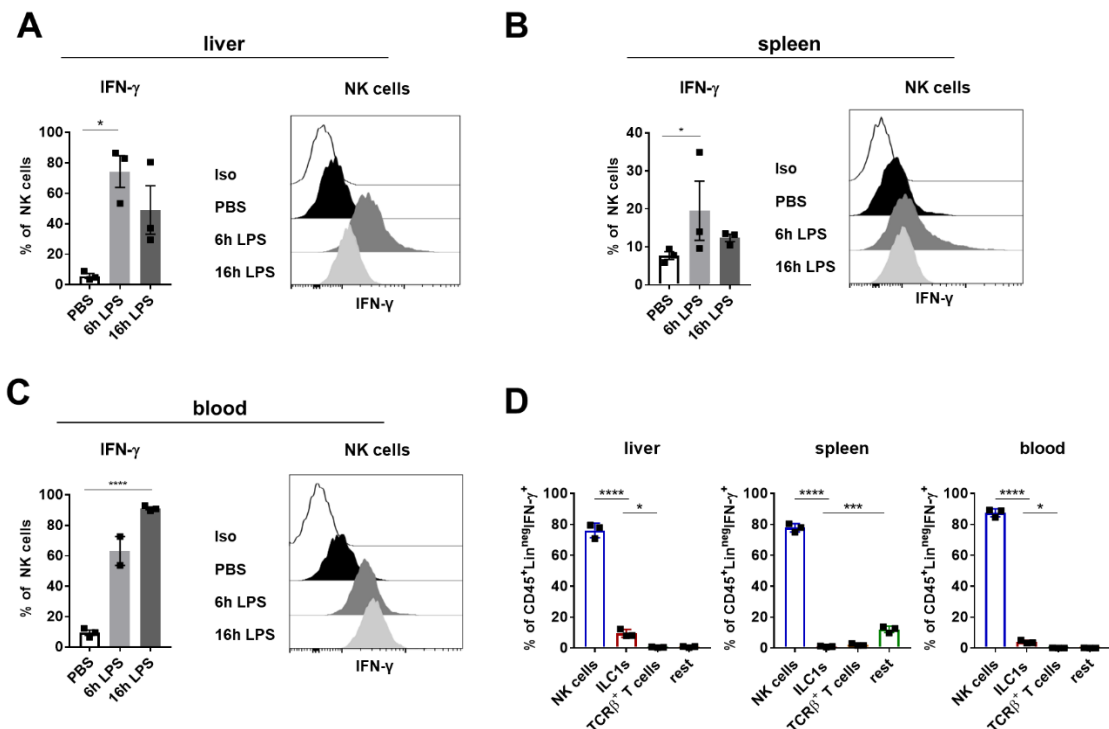


**Figure 4.10 NK cells are the major cellular source of IFN- $\gamma$  after LPS injection.** (A-C) Graphs showing frequencies (left) and representative flow-cytometry histograms (right) of IFN- $\gamma$ <sup>+</sup> NK cells in the liver (A), spleen (B) or blood (C) 6 h or 16 h post-injection of PBS or LPS. Iso, Isotype. (D) Frequencies of depicted immune cell subsets among: CD45<sup>+</sup>Lin<sup>neg</sup>IFN- $\gamma$ <sup>+</sup> cells 16 h after LPS injection in the liver (left), spleen (middle) or blood (right). (A-D) Data are shown as mean  $\pm$  SEM, analyzed by ordinary one-way ANOVA (B-C). \*,  $p < 0.05$ ; \*\*,  $p < 0.01$ ; \*\*\*,  $p < 0.001$ ; \*\*\*\*,  $p < 0.0001$ .  $n = 2-3$  mice/group from one experiment. Symbols represent individual mice.

#### 4.1.5 NK cells express the chemokine receptor CXCR3

We observed that the concentration of the chemokine CXCL10 was elevated in the serum and transcripts of *Cxcl10* were increased in the liver tissue of LPS injected mice. Moreover, LSECs expressed the highest transcript amounts of *Cxcl10* among the analyzed cellular compartments of the inflamed liver, and were secreting CXCL10 protein in response to IFN- $\gamma$ . Next, we analyzed the expression of CXCR3, the respective chemokine receptor for CXCL10, on NK cells and ILC1s and observed that a subset of NK cells expressed CXCR3 in the liver, spleen and blood of control mice (Figure 4.11A-C).

After LPS injection, the frequency of CXCR3<sup>+</sup> NK cells in liver, spleen and blood was significantly reduced. Hepatic ILC1s expressed the chemokine receptors CXCR3 and CXCR6 in PBS injected control mice (Figure 4.11D). The proportion of CXCR3<sup>+</sup> ILC1s was significantly reduced after LPS injection, whereas the expression of CXCR6 on ILC1s remained unchanged (Figure 4.11D).

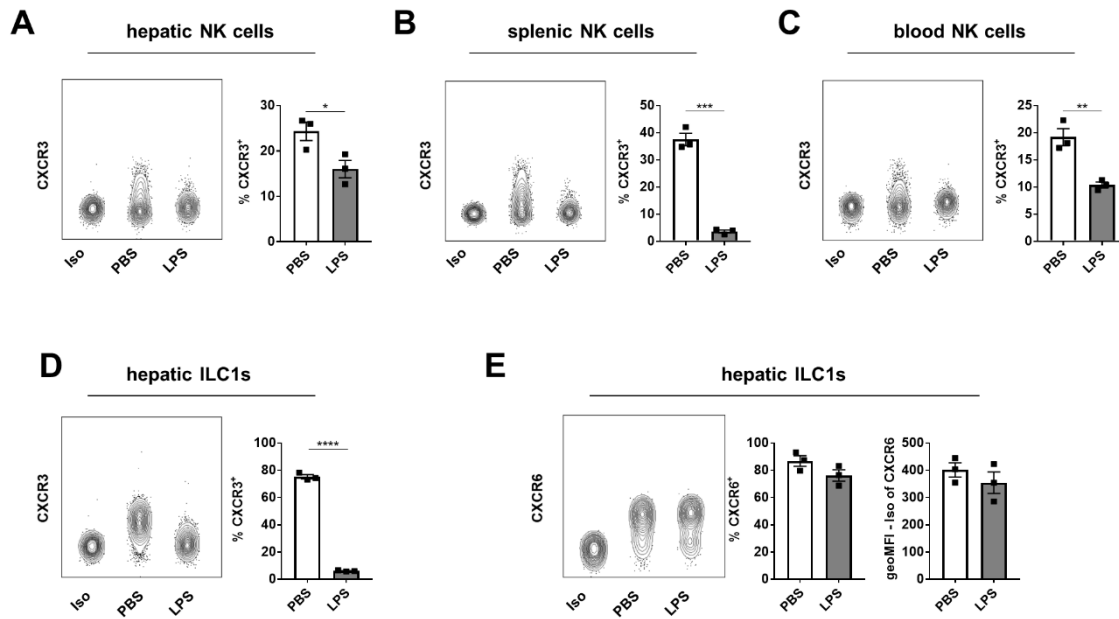


**Figure 4.11 NK cells and ILC1s express CXCR3 and downregulate its expression after LPS injection.** (A-C) Representative flow-cytometric plots and graphs showing the frequency of CXCR3<sup>+</sup> NK cells (gated as in Figure 4.2A) in the liver (A), spleen (B) and blood (C) of PBS- and LPS-injected mice 16 h post-injection. (D-E) Representative flow-cytometric plots and graphs showing the frequency of (D) CXCR3- and (E) CXCR6-expressing ILC1s (gated as in Figure 4.2A) in the liver. geoMFI, geometric mean fluorescent intensity. (A-E) Data are shown as mean  $\pm$  SEM, analyzed by unpaired Student's *t*-Test. \*, *p*<0.05; \*\*, *p*<0.01; \*\*\*, *p*<0.001; \*\*\*\*, *p*<0.0001. Data represent one experiment with 3 mice/group. Iso, Isotype. Symbols represent individual mice.

#### **4.1.6 LSECs attract NK cells by engaging CXCR3**

To investigate whether LSEC-secreted chemokines could attract NK cells and ILC1s, we cultured LSECs, and performed a migration assay with sorted innate lymphocytes (Figure 4.12A). Sorted NK1.1<sup>+</sup>NKp46<sup>+</sup> cells (sorted as shown in Figure 4.12B), comprising NK cells and ILC1s, were added into a Transwell insert placed on top of an LSEC layer, and were allowed to migrate through a 5 µm pore size membrane for 4 h. Afterwards, we counted the migrated NK cells or ILC1s using counting beads and flow cytometry.

We observed that, in comparison to medium control, unstimulated LSECs induced the migration of NK cells (Figure 4.12C). The migration of NK cells towards the LSEC layer was further increased if LSECs were pre-stimulated with IFN-γ for 24 h before the assay. Upon blockage of CXCR3 on NK cells, NK cell migration towards IFN-γ-stimulated LSECs was abrogated, which indicates that LSECs are attracting NK cells mainly via CXCR3. Likewise, LSECs were also able to attract ILC1s (Figure 4.12D). When comparing the frequency of NK cells and ILC1s among all migrated NK1.1<sup>+</sup>NKp46<sup>+</sup> cells, we observed that the migratory behavior of ILC1s towards the LSEC layer was increased in all conditions in comparison to NK cells (Figure 4.12E). The blockage of CXCR3 on ILC1 reduced but did not completely abrogate ILC1 migration, which suggests that ILC1s are not solely attracted in a CXCR3-dependent manner by LSECs.



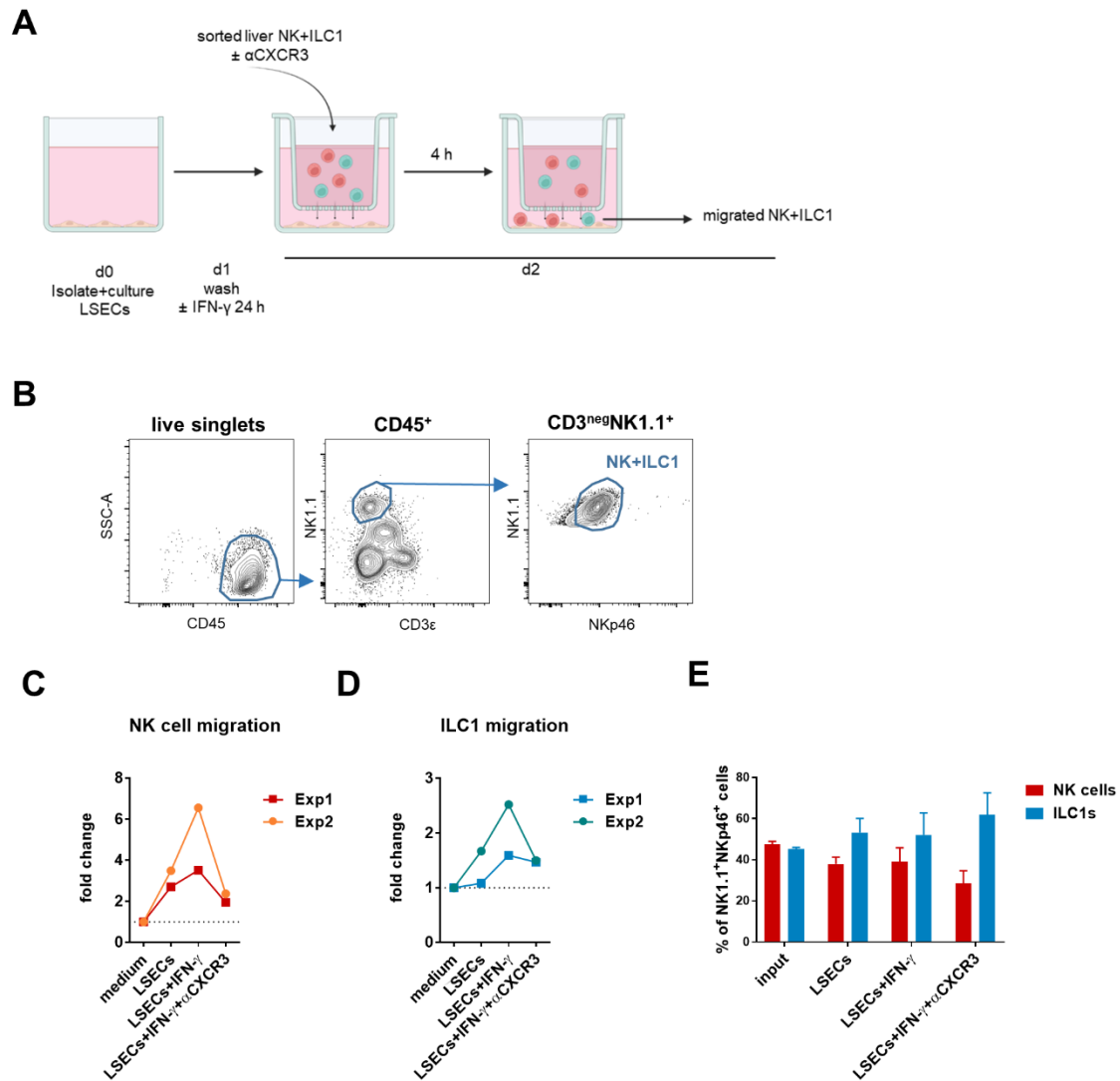


**Figure 4.12 NK cells are attracted by LSECs in a CXCR3-dependent manner.** (A) Schematic illustration depicting the migration assay towards an LSEC layer. (B) Single-cell suspensions of liver non-parenchymal cells were prepared from pooled livers of C57BL/6 mice. Hepatic NK cells and ILC1 (NK+ILC1) were sorted as live CD45<sup>+</sup>CD3ε<sup>neg</sup>NK1.1<sup>+</sup>NKp46<sup>+</sup> cells. (C-E) Sorted liver NK cells and ILC1s, treated with αCXCR3 antibody when indicated, were placed in an insert with 5 μm pore-size membrane, and incubated with LSECs for 4 h. Relative numbers of (C) NK cells (CD3ε<sup>neg</sup>NK1.1<sup>+</sup>NKp46<sup>+</sup>CD49a<sup>neg</sup>CD200R<sup>neg</sup>) and (D) ILC1 (CD3ε<sup>neg</sup>NK1.1<sup>+</sup>NKp46<sup>+</sup>CD49a<sup>+</sup>CD200R<sup>+</sup>) that migrated towards endothelial layer were determined by flow cytometry using counting-beads, and normalized to medium control. Each symbol represents an individual experiment (n=2) in which cells were derived from pooled tissue samples. (E) Frequencies of NK cells and ILC1 among migrated NK1.1<sup>+</sup>NKp46<sup>+</sup> cells.

#### **4.1.7 The effect of CXCR3 and VCAM-1 on NK cell recruitment to the liver of LPS-treated animals**

Leukocyte trafficking to the site of infection involves not only chemokine-supported migration via the blood stream, but as well adhesion to endothelium and subsequent extravasation from the blood vessels into the tissue. We observed the upregulation of the adhesion molecule VCAM-1 on LSECs after LPS injection (Figure 4.4C). It was reported that splenic NK cells express VLA-4, the ligand of VCAM-1, and that hepatic NK cells, but not ILC1s, express transcripts of *Itga4*, encoding for VLA-4 (Friedrich et al., 2021; Gan et al., 2012). Therefore, we investigated whether the accumulation of NK cells in the liver tissue after LPS injection depends on adhesion or migration. Therefore, we either blocked CXCR3-dependent migration, VCAM-1-dependent adhesion to the vasculature, or both with monoclonal antibodies (mAbs) (Figure 4.13A). As before, we observed an increase of NK cells in the livers 16 h post-injection of LPS in comparison to PBS-injected mice (Figure 4.13B). Neither the blocking of CXCR3, nor the blocking of VCAM-1 changed NK cell numbers in the inflamed liver tissue after LPS injection. Comparing the frequencies of different lymphocyte populations, we observed that the injection of  $\alpha$ CXCR3 mAbs depleted ILC1s and NKT cells in the liver (Figure 4.13C). Moreover, we observed reduced numbers of hepatic T cells and B cells after LPS injection. The injection of  $\alpha$ VCAM-1 mAbs did not change the distribution of the analyzed lymphocyte populations in the liver of LPS-injected mice.

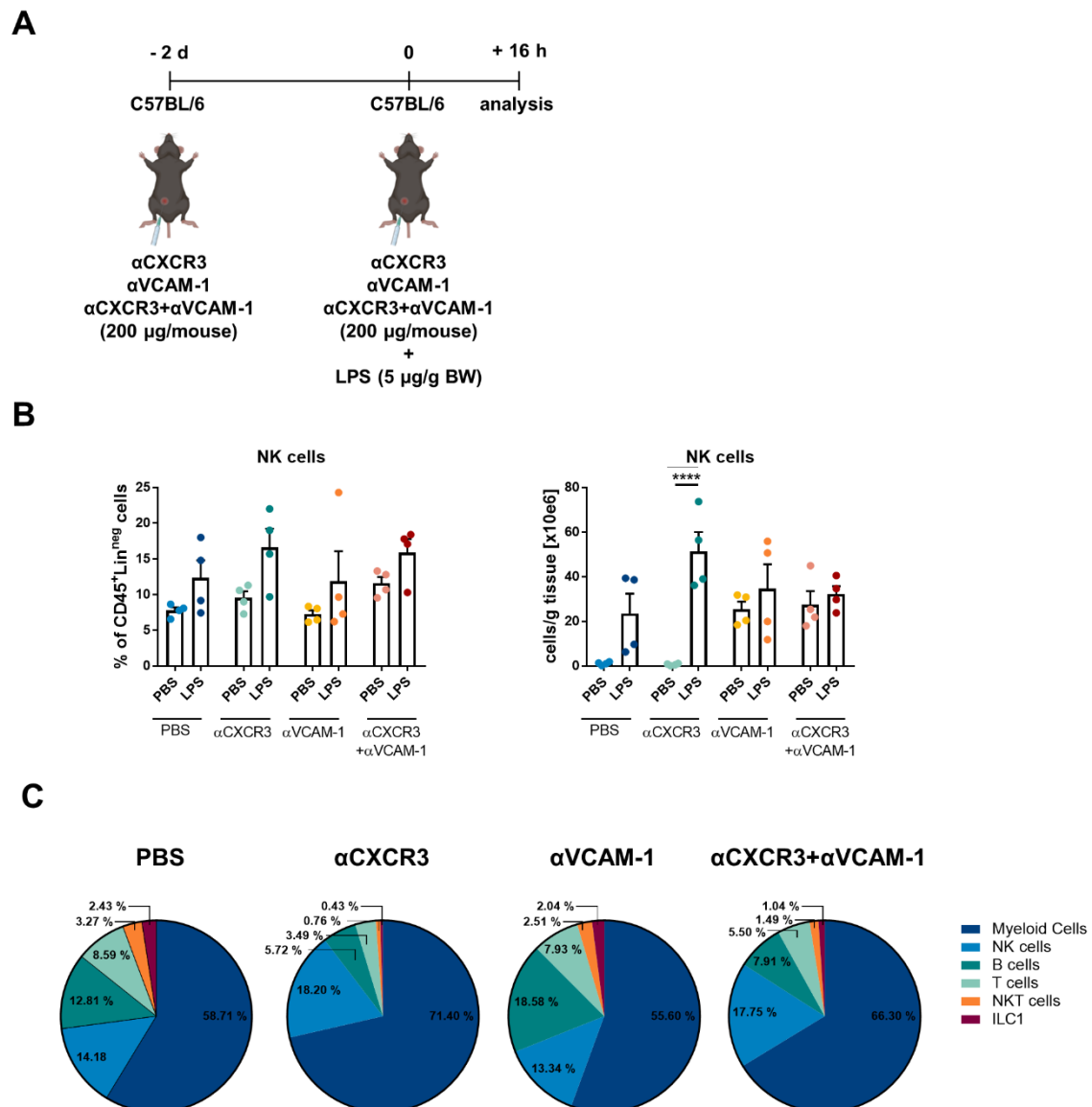


**Figure 4.13 The role of CXCR3 and VCAM-1 in lymphocyte accumulation in the inflamed liver tissue.** (A) Schematic illustration depicting the experimental setup. C57BL/6 mice were injected with LPS and monoclonal antibodies (mAbs) against CXCR3 or/and VCAM-1. (B) Proportion and cell numbers of NK cells (gated as in Figure 2A) in the liver of LPS- or PBS-injected mice  $\pm$  mAbs. Data are shown as mean  $\pm$  SEM, analyzed by regular two-way ANOVA. \*\*\*\*,  $p < 0.0001$ . Symbols represent individual mice. (C) Proportion of selected lymphocyte populations among CD45<sup>+</sup> cells in LPS-injected mice  $\pm$  mAbs presented as pie charts. Frequencies are shown as mean  $\pm$  SEM. (B+C) Data represent one experiment with 4 mice/group.

#### 4.1.8 Endothelium-derived CXCL10 supports NK cell recruitment to the inflamed liver

We showed that LSECs are able to secrete CXCL10 upon stimulation with IFN- $\gamma$  and that NK cells are attracted by LSECs in a CXCR3-dependent manner *in vitro*. We hypothesized that LSEC-secreted CXCL10 can recruit NK cells to the inflamed liver tissue. To investigate our hypothesis, we used mice with an endothelial cell (EC)-restricted deletion of *Cxcl10* (*Cdh5<sup>Cre</sup>Cxcl10<sup>fl/fl</sup>*) and littermate controls (*Cxcl10<sup>fl/fl</sup>*) in the LPS-induced inflammation model.

To confirm the successful deletion of *Cxcl10* from ECs, we isolated LSECs from healthy *Cxcl10<sup>fl/fl</sup>* and *Cdh5<sup>Cre</sup>Cxcl10<sup>fl/fl</sup>* mice, cultured them *in vitro* and stimulated the cells with IFN- $\gamma$  to induce CXCL10 secretion. We measured the amount of CXCL10 protein in the supernatant by ELISA 24 h after the stimulation. Indeed, LSECs isolated from *Cdh5<sup>Cre</sup>Cxcl10<sup>fl/fl</sup>* mice were unable to produce CXCL10 after IFN- $\gamma$  stimulation in comparison to LSECs isolated from *Cxcl10<sup>fl/fl</sup>* mice (Figure 4.14).

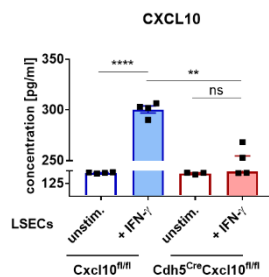


**Figure 4.14 LSECs from *Cdh5<sup>Cre</sup>Cxcl10<sup>fl/fl</sup>* mice do not upregulate CXCL10 in response to IFN- $\gamma$ .** LSECs were purified from livers of *Cxcl10<sup>fl/fl</sup>* mice and *Cdh5<sup>Cre</sup>Cxcl10<sup>fl/fl</sup>* mice and stimulated with IFN- $\gamma$  for 24 h *in vitro*. Concentration of CXCL10 protein in the cell culture supernatants was quantified by ELISA. Symbols represent LSECs derived from individual animals,  $n=3-4$ . unstim., unstimulated. Data are shown as mean  $\pm$  SEM, analyzed by ordinary one-way ANOVA. \*\*,  $p<0.01$ ; \*\*\*\*,  $p<0.0001$ ; ns, not significant.

Next, we examined the mice under steady state conditions to exclude an effect of the deletion of *Cxcl10* from ECs under homeostatic conditions. *Cxcl10<sup>fl/fl</sup>* and *Cdh5<sup>Cre</sup>Cxcl10<sup>fl/fl</sup>* mice showed no differences in BW, liver weight and liver-to-BW ratio (Figure 4.15A). We analyzed LSECs and the hepatic immune cell composition of the mice. The cells were gated as previously described (Figure 4.1C+D and Figure 4.2A). *Cxcl10* deletion did not affect the number of LSECs in the livers (Figure 4.15B). We also did not observe a change in the numbers of Kupffer cells, Monocytes, CD4<sup>+</sup> or CD8<sup>+</sup> T cells, nor ILC1s in the liver (Figure 4.15C). *Cdh5<sup>Cre</sup>Cxcl10<sup>fl/fl</sup>* mice did not show altered percentage or numbers of NK cells in the liver, spleen or blood (Figure 4.15D). This suggests that the deletion of *Cxcl10* from ECs has no impact on the immune cell

composition of the liver, and does not affect the abundance of NK cells in the liver, spleen and blood under homeostatic conditions.

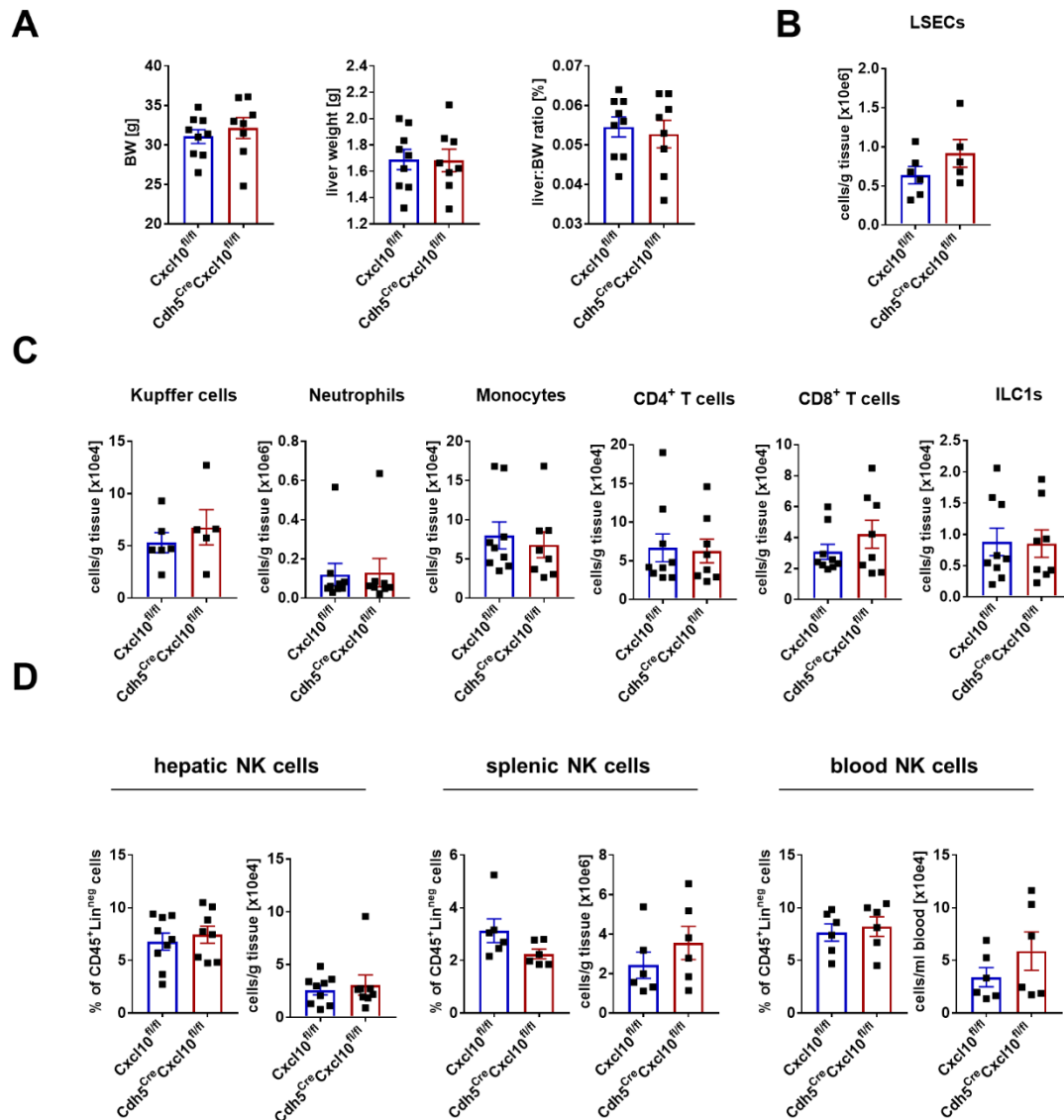


**Figure 4.15 LSECs and hepatic immune cell numbers in Cxcl10<sup>fl/fl</sup> mice and Cdh5<sup>Cre</sup>Cxcl10<sup>fl/fl</sup> mice.** Livers, spleens and blood were collected from Cxcl10<sup>fl/fl</sup> mice and Cdh5<sup>Cre</sup>Cxcl10<sup>fl/fl</sup> mice. Single cell suspensions were prepared and analyzed by flow cytometry. (A) Body weight (BW) (left), liver weight (middle) and liver-to-BW ratio (right) of Cxcl10<sup>fl/fl</sup> mice and Cdh5<sup>Cre</sup>Cxcl10<sup>fl/fl</sup> mice. *n*=8-9 mice/group from three individual experiments. (B) Quantification of LSECs (gated as shown in Figure 4A), *n*=6 mice/group from two individual experiments. (C) Cell numbers of indicated immune cell populations (gated as shown in Figure 4.1C+D and Figure 4.2A) in the livers of Cxcl10<sup>fl/fl</sup> mice and Cdh5<sup>Cre</sup>Cxcl10<sup>fl/fl</sup> mice. *n*=5-6 mice/group from two independent experiments (Kupffer cells, Neutrophils, Monocytes) and *n*=8-9 mice/group from 3 independent experiments (T cells and ILC1s). (D) Proportion and numbers of NK cells (gated as shown in Figure 2A) in the liver, spleen and blood of Cxcl10<sup>fl/fl</sup> mice and Cdh5<sup>Cre</sup>Cxcl10<sup>fl/fl</sup> mice. *n*=6 mice/group from two independent experiments (spleen and blood), and *n*=8-9 mice/group from 3 independent experiments (liver). (A-D) Data are shown as mean ± SEM, analyzed by unpaired Student's t-Test. Symbols represent individual mice.



**Figure 4.16 Effect of LPS on immune cell composition in the livers of *Cxcl10<sup>fl/fl</sup>* mice and *Cdh5<sup>Cre</sup>Cxcl10<sup>fl/fl</sup>* mice.** (A) Schematic illustration of the experimental procedure. (B) Body weight (BW) change relative to initial body weight (left), liver weight (middle) and liver-to-BW ratio (right) after treatment with LPS. *n*= 8-9 mice/group from three independent experiments. (C) Cell numbers of indicated immune cell subsets (gated as shown in Figure 4.1C+D) 16 h post-injection of PBS or LPS. *n*=5-6 mice/group from two independent experiments (Neutrophils, Monocytes) and *n*=8-9 mice/group from 3 independent experiments (T cells). (D) Expression of ICAM-1 and VCAM-1 on LSECs isolated from PBS- and LPS-injected *Cxcl10<sup>fl/fl</sup>* mice and *Cdh5<sup>Cre</sup>Cxcl10<sup>fl/fl</sup>* mice 16 h post-treatment; *n*=3 mice/group from one experiment. (B-D) Data are shown as mean  $\pm$  SEM, analyzed by ordinary one-way ANOVA. \*, *p*<0.05; \*\*, *p*<0.01; \*\*\*, *p*<0.001; \*\*\*\*, *p*<0.0001. Symbols represent individual mice. geoMFI, geometric mean fluorescent intensity; Iso, Isotype.

Lastly, we analyzed the cell numbers of innate NK1.1<sup>+</sup>NKp46<sup>+</sup> cell compartment in the livers of *Cxcl10<sup>fl/fl</sup>* and *Cdh5<sup>Cre</sup>Cxcl10<sup>fl/fl</sup>* mice. We could observe a significant increase in numbers of hepatic NK1.1<sup>+</sup>NKp46<sup>+</sup> cells in *Cxcl10<sup>fl/fl</sup>* mice after LPS injection, but in *Cdh5<sup>Cre</sup>Cxcl10<sup>fl/fl</sup>* the accumulation of NK1.1<sup>+</sup>NKp46<sup>+</sup> cells was abolished (Figure 4.17A). The numbers of ILC1s in the livers was not altered after LPS injection, neither in *Cxcl10<sup>fl/fl</sup>* nor in *Cdh5<sup>Cre</sup>Cxcl10<sup>fl/fl</sup>* mice. While hepatic NK cell numbers in *Cxcl10<sup>fl/fl</sup>* mice were significantly increased after LPS injection, the deletion of *Cxcl10* in *Cdh5<sup>Cre</sup>Cxcl10<sup>fl/fl</sup>* mice resulted in a diminished accumulation of NK cells in the liver tissue. We observed the upregulation of the activation markers CD25 and CD69 on hepatic NK cells from both, *Cxcl10<sup>fl/fl</sup>* and *Cdh5<sup>Cre</sup>Cxcl10<sup>fl/fl</sup>* mice after the injection of LPS (Figure 4.17B). Moreover, the ability of NK cells to produce IFN- $\gamma$  was not impaired. These data suggest that LSEC-derived CXCL10 supports NK cell recruitment to the liver tissue after LPS injection, but does not affect NK cell activation or function.

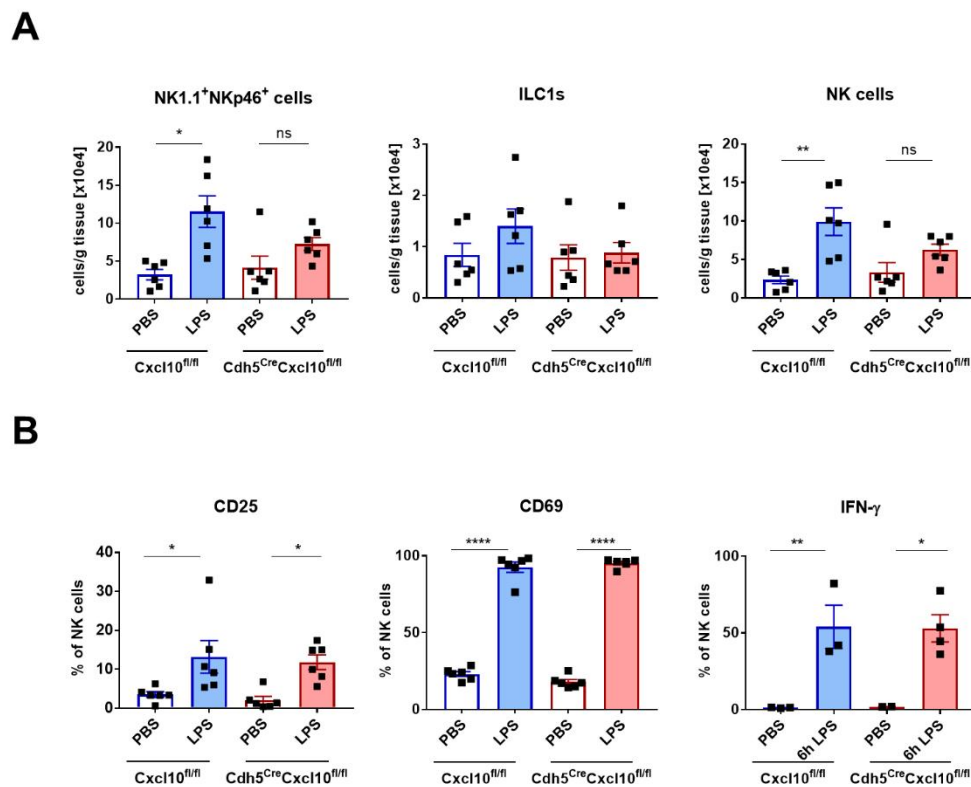


**Figure 4.17 Deletion of *Cxcl10* in ECs impairs NK cell recruitment to the liver after LPS injection.** (A) Cell numbers of NK1.1<sup>+</sup>NKp46<sup>+</sup> cells, ILC1s and NK cells (gated as shown in Figure 4.2A) in livers of *Cxcl10*<sup>fl/fl</sup> mice or *Cdh5*<sup>Cre</sup>*Cxcl10*<sup>fl/fl</sup> mice treated with LPS or PBS. (B) Frequency of CD25-, CD69- and IFN- $\gamma$ -expressing NK cells in the livers 16 h post-injection. (A+B) Data are shown as mean  $\pm$  SEM with each symbol representing an individual mouse. Data are analyzed by unpaired ordinary one-way ANOVA. ns, not significant; \*,  $p < 0.05$ ; \*\*,  $p < 0.01$ ; \*\*\*\*,  $p < 0.0001$ .  $n = 6$  mice/group from two independent experiments, or  $n = 3-4$  mice/group from one performed experiment (IFN- $\gamma$ <sup>+</sup> NK cells).



## 4.2 Interaction of LSECs and innate lymphocytes in hepatic metastasis

LSECs form the inner lining of the liver sinusoids, and therefore have a unique position, which allows them to interact with circulating cancer cells, as well as with tissue-infiltrating and -resident immune cells. The liver provides a unique microenvironment for metastatic cancer cells, which is regulated in part by LSECs. Understanding how LSECs facilitate or inhibit metastatic cancer cell adhesion, arrest, and invasion, and their role in modulating the immune cell response to metastatic cells might be a strategy to prevent or treat liver metastasis more effectively.

### 4.2.1 Effect of tumor cells on LSEC phenotype

LSECs have been demonstrated to influence the functions of T cells by expressing a variety of cell surface membrane proteins that participate in immune responses (Knolle and Wöhlleber, 2016). To analyze their potential to influence the activation and inhibition of innate lymphocytes, we first examined the expression of receptors and ligands shown to regulate NK cell and ILC1 function and how the expression of these molecules can be influenced by cancer cells. We isolated and cultured primary LSECs, co-cultured them together with the colorectal cancer cell line MC38 or the melanoma cell line B16, or stimulated the LSECs with tumor cell-derived supernatants for 24 h.

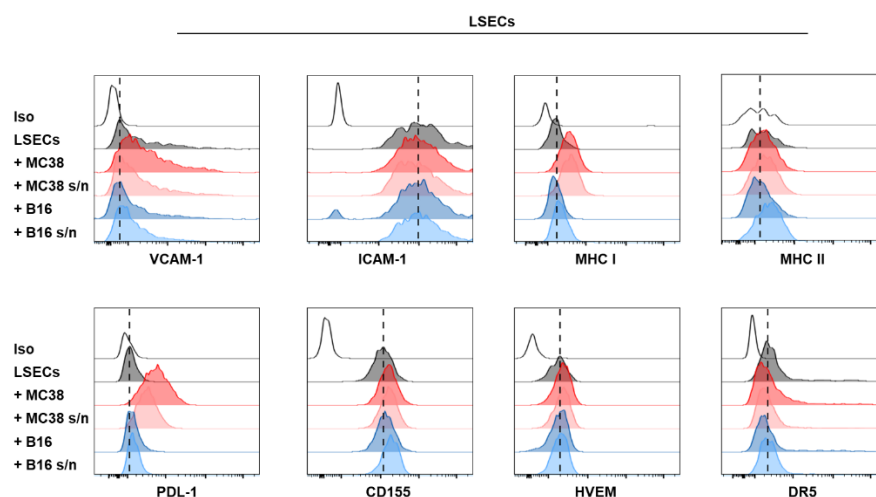


**Figure 4.18 LSEC phenotype after co-culture with tumor cells or treatment with tumor cell-derived supernatant.** LSECs were isolated from livers of C57BL/6 mice and treated with MC38, B16 or respective supernatants (s/n). LSECs were detached and expression of selected surface molecules was analyzed. Histograms show expression of VCAM-1, ICAM-1, MHC I and MHC II (top), and PD-L1, CD155, HVEM and DR5 (bottom) on LSECs (gated as shown in Figure 4A).

As described above, we observed the *ex vivo* expression of ICAM-1, VCAM-1, MHC I and MHC II, as well as PD-L1, CD155 and HVEM on LSECs from PBS-injected control C57BL/6 mice (Figure 4.4). After culture, LSECs expressed both adhesion molecules, VCAM-1 and ICAM-1, as well as MHC I, CD155, HVEM and DR5 (Figure 4.18). It was shown that LSECs constitutively express MHC II and regulate CD4<sup>+</sup> T cell polarization (Knolle et al., 1999; Lohse et al., 1996; Wiegard et al., 2005), which was in line with our data. However, after culture, LSECs did not express MHC II, and the expression remained absent after co-culture with tumor cells or stimulation with tumor cell-derived supernatants. We did not detect PD-L1 expression on LSECs after culture, but observed PD-L1 expression on LSECs after the co-culture with MC38 tumor cells. The expression of VCAM-1 was upregulated after co-culture with both tumor cell lines, MC38 and B16. The expression of other molecules was not affected by the co-culture of LSECs with B16 tumor cells or the stimulation with their supernatant. The treatment with MC38-derived supernatant increased the expression of MHC I and VCAM-1 on LSECs. The expression of PD-L1 on LSECs could be induced by MC38-derived supernatant, although less than the co-culture with MC38 tumor cells.

Our data suggests that the upregulation of MHC I, VCAM-1 and PD-L1 is contact-independent, although for PD-L1 only partially. In summary, we observed that LSECs express molecules that are important for the activation and function of innate lymphocyte cells.

#### **4.2.2 LSECs change their cytokine and chemokine profile in response to tumor cell secreted factors**

To uncover molecules that could be secreted by LSECs in culture and influenced by tumor cells, we analyzed their cytokine and chemokine transcriptome. LSECs were cultured in the presence of supernatants derived from MC38, B16, LL2 (lung carcinoma) or RMA-S (T-leukemia) tumor cell lines for 24 h and selected transcript sets were analyzed by qPCR (Figure 4.19A-E). We observed that the stimulation with tumor cell-derived supernatants reduced the expression of transcripts for *Il16*, *Ccl20*, *Bmp6*, *Ltb* and *Hc* (Figure 4.19A-E). Contrary, LSECs upregulated the mRNA expression of interferons and interleukins, including *Il15*, *Il22*, *Il27*, *Il2* and *Il12a/b*, in response to tumor cell-derived supernatants (Figure 4.19A). In response to RMA-S-derived supernatants, LSECs also upregulated the expression of *Il4* and *Il23a*.

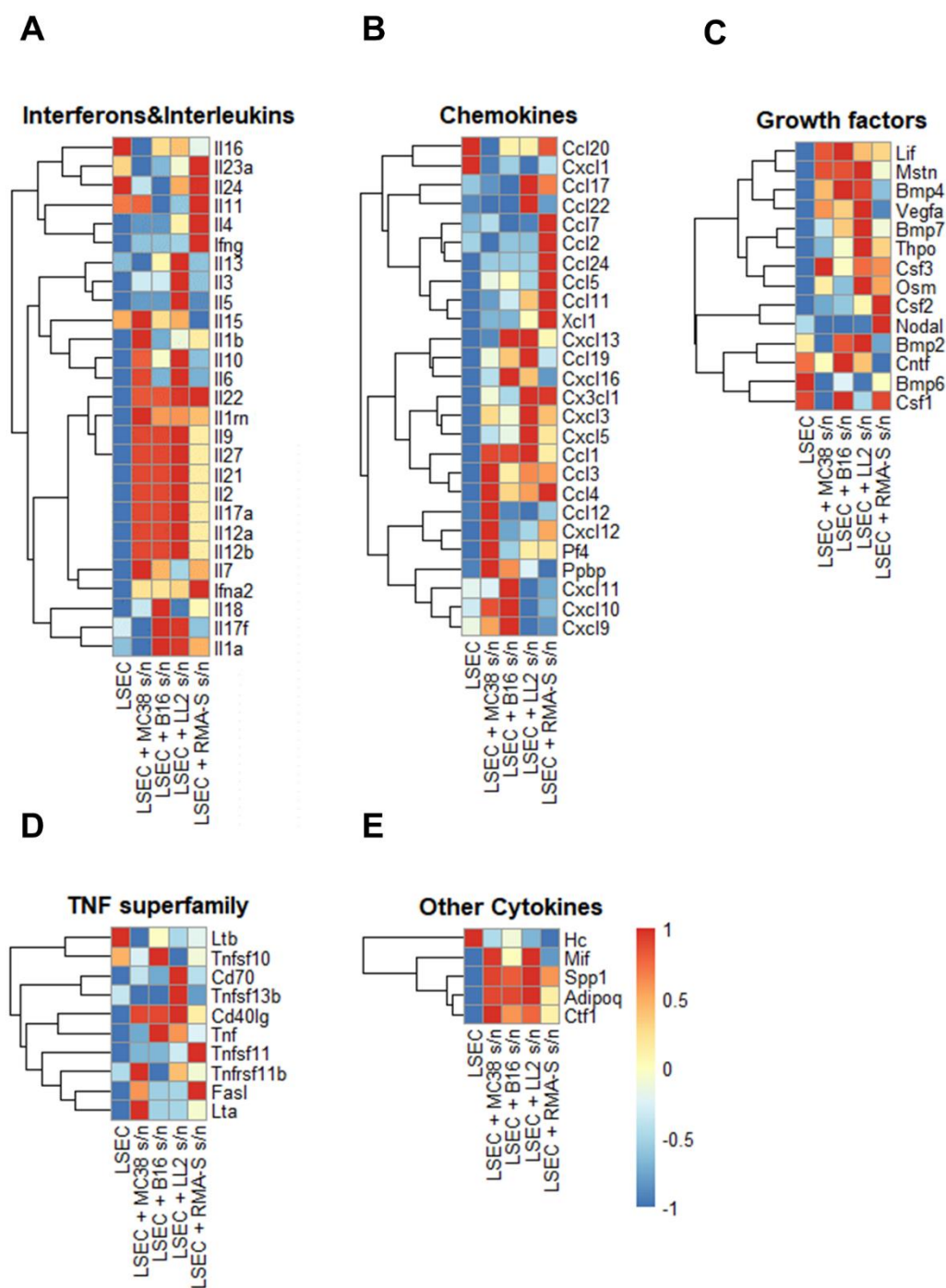


**Figure 4.19 LSEC transcriptome of selected cytokines and chemokines after stimulation with tumor cell supernatants.** LSECs were cultured and stimulated with supernatants (s/n) derived from MC38, B16, LL2 or RMA-S tumor cells for 24 h. RNA was isolated and gene sets of cytokines and chemokines were analyzed by qPCR. (A-E) Heatmaps displaying scaled relative (to Actin) mRNA expression of interferons and interleukins (A), chemokines (B), growth factors (C), TNF superfamily members (D) and other cytokines (E) analyzed by qPCR. Data are scaled per row.

Transcripts for the chemokines CCL1, CCL3 and CCL4, were increased by the stimulation of LSECs with all tested supernatants, whereas the upregulation of transcripts for *Cxcl9*, *Cxcl10* and *Cxcl11*, was restricted to the stimulation of LSECs with MC38- and B16-derived supernatants (Figure 4.19B). We observed that stimulated LSECs also showed increased transcripts for the growth factors *Vegfa*, *Csf3*, *Bmp4* and *Bmp7*, independent of tumor cell entity (Figure 4.19C). Transcripts encoding for TNF superfamily members, *Cd40l*, *Tnfrsf11b* and *Fasl*, were increased by the treatment of LSECs with tumor cell-derived supernatant (Figure 4.19D), as well as transcripts for other cytokines like *Spp1* and *Ctf1* (Figure 4.19E).

#### **4.2.3 LSECs reduce NK cell-mediated killing of target cells in a contact-dependent manner**

As we observed that LSECs express activating and inhibitory ligands for NK cell and ILC1 receptors, and change their phenotype and transcriptome of soluble factors after encounter of tumor cells, we wanted to elucidate their impact on innate lymphocyte-mediated killing against target cells. We co-cultured sorted hepatic NK cells or ILC1s together with LSECs, tumor supernatant pre-exposed LSECs (tLSECs), or stimulated them with LSEC-derived supernatant for 24 h. Subsequently, we performed a cytotoxicity assay against MC38 colorectal cancer cells (Figure 4.20A, sorting strategy in Figure 4.20B). NK cells that were co-cultured with LSECs showed a delayed and reduced cytotoxicity against MC38 target cells (Figure 4.20C+D). When stimulated with LSEC-derived supernatant, this inhibitory effect was not observed. Likewise, if LSECs were pre-exposed to tumor cell-derived supernatant before the co-culture with NK cells, NK cell cytotoxicity was not reduced or delayed. ILC1-mediated cytotoxicity against MC38 was also reduced after co-culture with LSECs (Figure 4.20E+F). In addition, the effect was dependent on cell-to-cell contact, as stimulation of ILC1s with LSEC supernatant did not reduce ILC1 cytotoxicity. Contrary to the results observed for NK cells, tLSECs also reduced ILC1-mediated killing. These data indicate that under homeostatic conditions, cell-to-cell contact to LSECs has an immunoregulatory effect on hepatic NK cells and ILC1s. In the presence of tumor cells, LSECs permit NK cell-, but not ILC1-mediated killing against tumor cells.

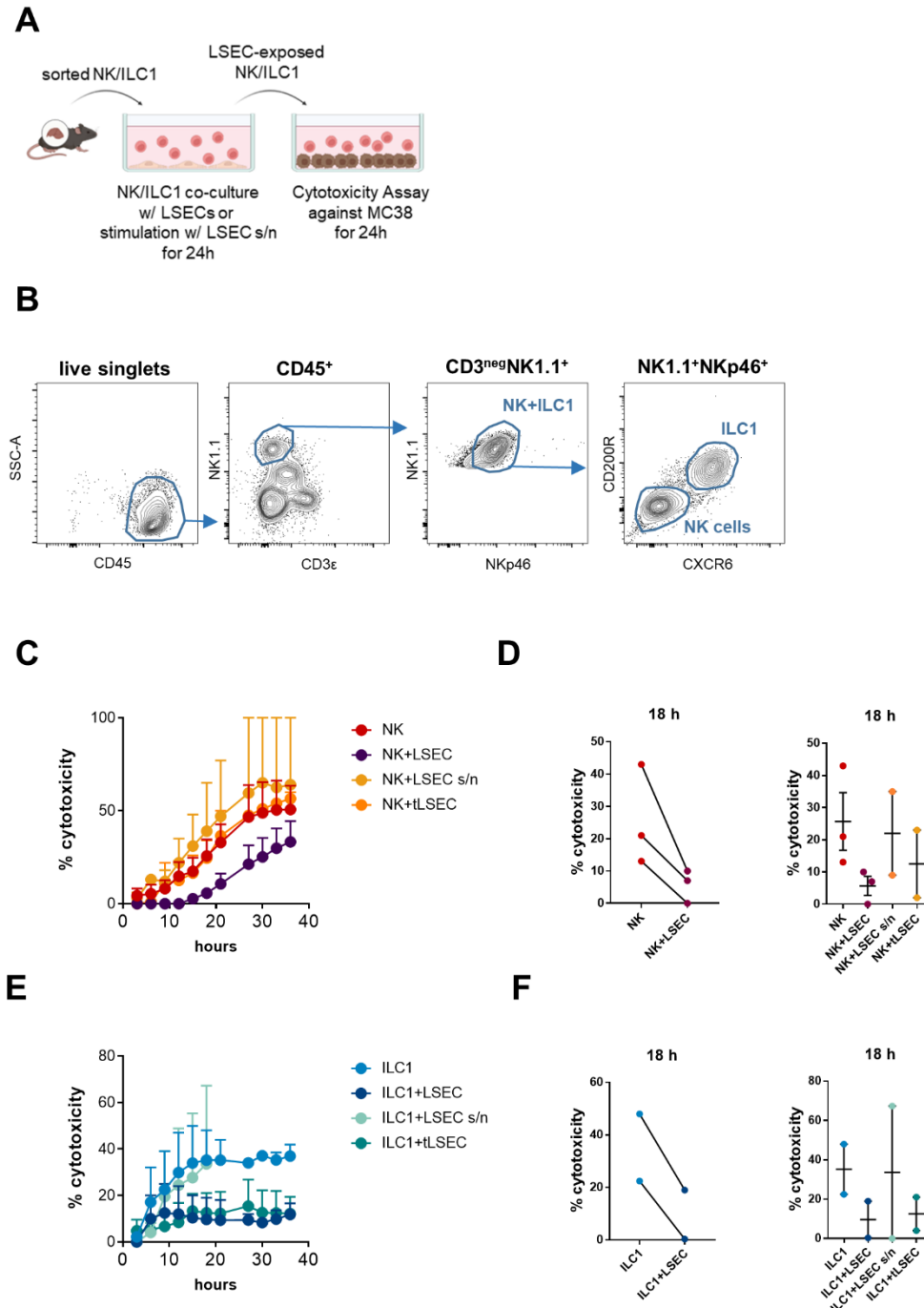


**Figure 4.20 NK cell and ILC1 cytotoxicity is affected by LSECs.** (A) Schematic illustration depicting the setup for cytotoxicity assay of LSEC-exposed NK cells and ILC1 against MC38 target cells. (B) Single-cell suspensions of liver non-parenchymal cells were prepared from pooled livers of C57BL/6 mice. NK cells and ILC1s were gated as CD45<sup>+</sup>CD3 $\epsilon$ <sup>neg</sup>NK1.1<sup>+</sup>NKp46<sup>+</sup> cells. NK cells were sorted as CD200R<sup>neg</sup>CXCR6<sup>neg</sup>, and ILC1s were sorted as CD200R<sup>+</sup>CXCR6<sup>+</sup> cells. (C) Sorted cells were pre-exposed to LSECs, LSEC supernatant (s/n) or tumor cell supernatant-stimulated LSECs (tLSECs) for 24 h. NK cell cytotoxicity against MC38 was measured for 36 h in a 3 h intervals.  $n=2-3$  independent experiments. (D) NK cell cytotoxicity against MC38 at 18 h time point. (E) Sorted ILC1s were pre-exposed to LSECs, LSEC supernatant (s/n) or tumor cell supernatant-stimulated LSECs (tLSECs) for 24 h. ILC1 cytotoxicity against MC38 was measured for 36 h in a 3 h intervals.  $n=2$  independent experiments. (F) ILC1 cytotoxicity against MC38 at 18 h time point. (C-F) Data are shown as (C+E) mean + SEM and (D+F) mean  $\pm$  SEM.

#### 4.2.4 Effect of LSECs on NK cell phenotype

To elucidate the reduced killing ability of LSEC-exposed NK cells, we examined the expression of molecules, including NK cell activating and inhibitory receptors, maturation markers and death-receptor ligands on NK cells after the exposure to LSECs or LSEC-derived supernatant (Figure 4.21A).

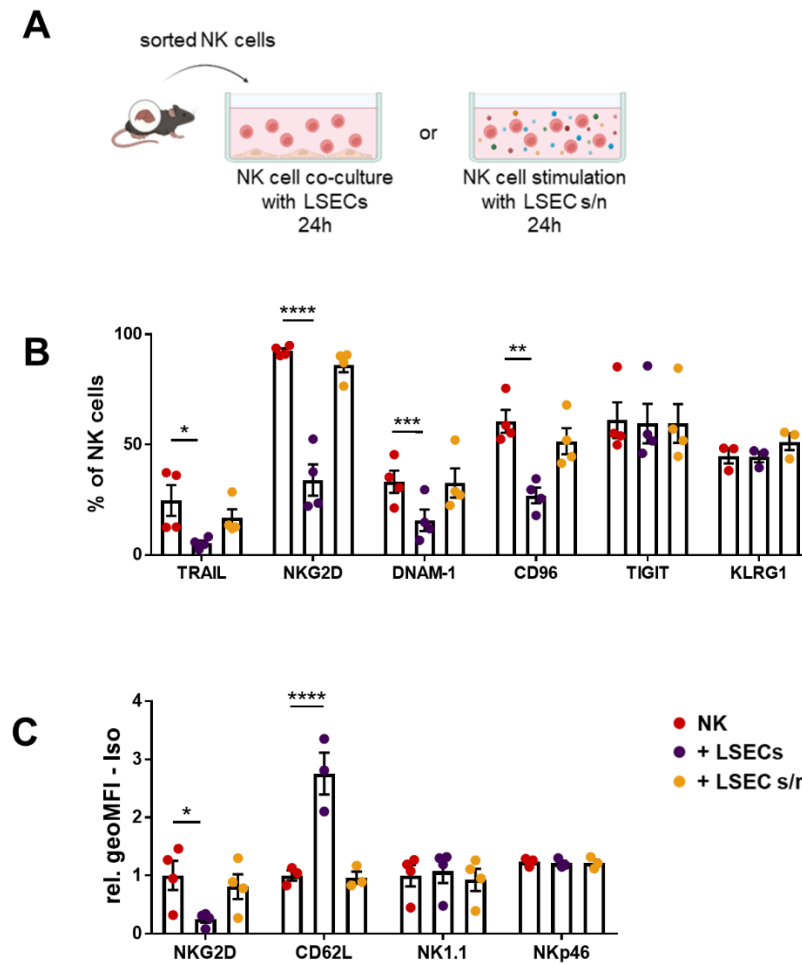


**Figure 4.21 LSECs induce phenotypic changes of NK cells.** (A) Schematic illustration depicting the co-culture of sorted hepatic NK cells with LSECs, or their stimulation with LSEC-derived supernatant (s/n). (B) Single cell suspensions of liver non-parenchymal cells were prepared from pooled livers of C57BL/6 mice. NK cells were sorted as  $CD45^+CD3\epsilon^{neg}NK1.1^+NKp46^+CD200R^{neg}CXCR6^{neg}$  cells (as shown in Figure 4.20B). Sorted NK cells were co-cultured with LSECs or stimulated with LSEC-derived supernatant (s/n) for 24 h. Bar graphs show frequencies of NK cells expressing TRAIL, NKG2D, DNAM-1, CD96, TIGIT and KLRG1, analyzed by flow cytometry. (D) Quantification of NKG2D, CD62L, NK1.1 and NKp46 expression by NK cells upon co-culture with LSECs or exposure to LSEC s/n. (B+C) Data are shown as mean  $\pm$  SEM,  $n=3-4$  independent experiments. Data are analyzed by unpaired ordinary one-way ANOVA. \*,  $p<0.05$ ; \*\*,  $p<0.01$ ; \*\*\*,  $p<0.001$ ; \*\*\*\*,  $p<0.0001$ . rel. geoMFI, relative geometric mean fluorescent intensity.

Upon co-culture, the proportion of NK cells expressing TRAIL, DNAM-1 and CD96 was reduced (Figure 4.21B). TIGIT and KLRG1 expression remained unchanged. The expression of the activating receptor NKG2D was significantly downregulated after co-culture with LSECs, whereas the expression of NK1.1 and NKp46 was unchanged (Figure 4.21B+C). Upon exposure to LSECs, NK cells significantly upregulated the expression of CD62L (Figure 4.21C). The stimulation of NK cells with LSEC-derived supernatant did not change the expression of the examined molecules, indicating that the ability of LSECs to change NK cell phenotype is contact dependent.

#### **4.2.5 Effect of distant, subcutaneous tumors on LSEC phenotype**

As we observed that tumor cell-derived supernatant could change LSEC phenotype and transcriptome, we wanted to investigate if LSECs play a role in metastatic niche formation and immune cell regulation prior to tumor cell invasion of the liver. Therefore, we injected MC38 colorectal cancer cells subcutaneously to the right flank of C57BL/6 mice to unravel if distant, subcutaneous tumors can have an impact on LSECs in the liver. We monitored the tumor growth for 17 days, or until the tumor reached a diameter of 1.5 cm (Figure 4.22A). We neither observed a change in liver or spleen weight in tumor-bearing mice in comparison to PBS-injected controls (Figure 4.22B), nor differences in LSEC numbers (Figure 4.22C). The expression of MHC II was increased on LSECs isolated from all three tumor-bearing mice (Figure 4.22D+E). We observed increased expression of VCAM-1 and PD-L1, as well as decreased expression of MHC I on LSECs from one MC38 tumor-bearing mouse (No. 1) with a tumor volume of 800 mm<sup>3</sup>, but no change in the expression of these molecules on LSECs isolated from the other mice bearing much smaller tumors. ICAM-1, CD155, HVEM and CD31 expression remained unaffected. These data suggest that the effect of distant tumors on LSECs might be dependent on size or state of progression of the tumor.

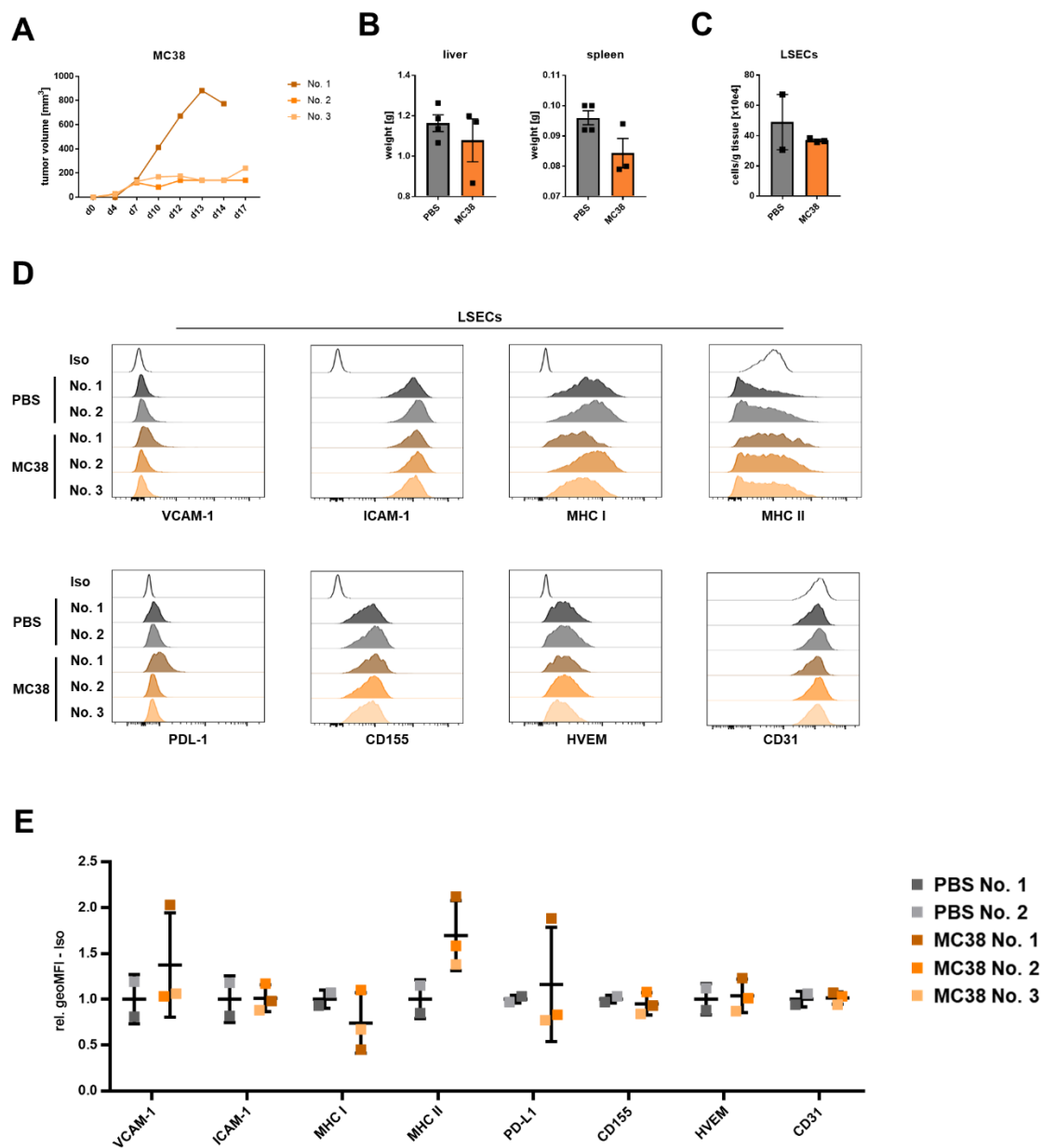


**Figure 4.22 Phenotype of LSECs in MC38 tumor-bearing mice.** MC38 tumor cells ( $1 \times 10^6$  cells/mouse) or PBS were injected subcutaneously to C57BL/6 mice. (A) Tumor growth of three individual animals over time. (B) Liver and spleen weight of PBS- or MC38-injected mice. (C) Quantification of LSECs isolated from PBS- or MC38-injected mice. (D) Histograms of selected surface molecules expressed by LSECs (gated as shown in Figure 4.4A). Iso, Isotype (E) Quantification of selected surface molecules expressed by LSECs. Data are shown as mean  $\pm$  SEM with symbols representing individual mice,  $n=2-3$ . rel. geoMFI, relative geometric mean fluorescent intensity; Iso, Isotype.



Next, we analyzed NK cells and ILC1s in liver, tumor tissue and spleen (gated as shown in Figure 4.2A). We did not observe a difference in frequencies or cell numbers of NK cells or ILC1s in the liver between tumor cell-injected mice or control mice (Figure 4.23A+B), while the frequencies and cell numbers of NK cells in the spleen of MC38-injected mice was decreased (Figure 4.23C). In tumor tissue, mouse No. 1, which displayed the biggest tumor, showed the highest number of NK cells (Figure 4.23D). Contrary to that, ILC1 numbers in the tumor tissue of mouse No. 1 were the lowest in comparison to the tumors of the other tumor-bearing mice.

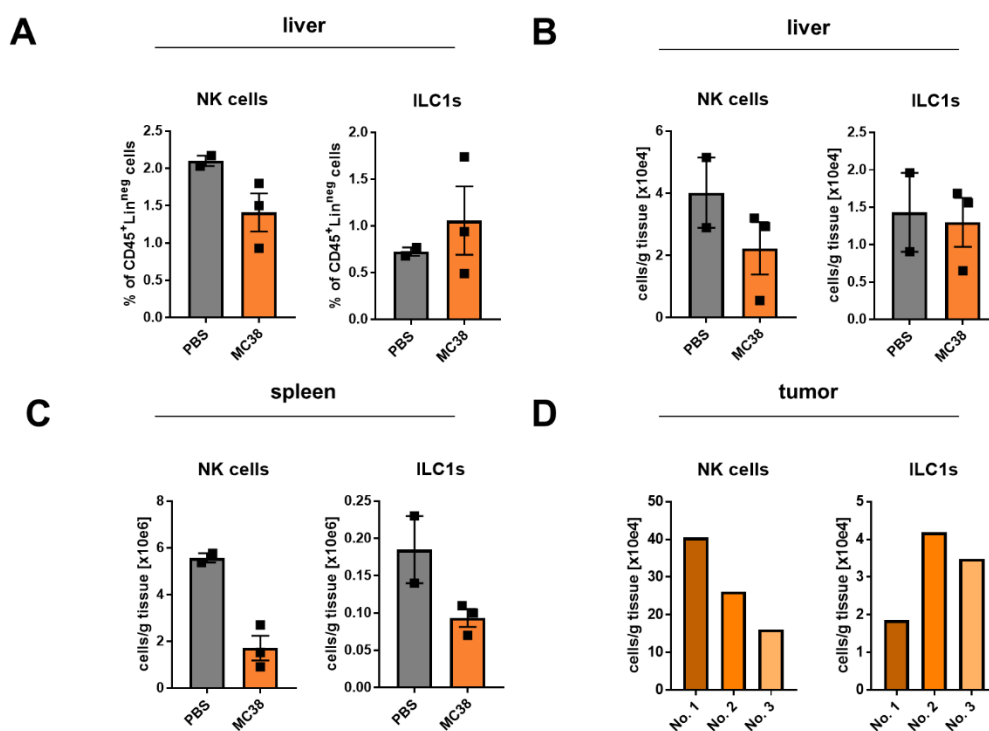


**Figure 4.23 Quantification of NK cells and ILC1s in MC38 tumor-bearing mice.** MC38 tumor cells ( $1 \times 10^6$  cells/mouse) or PBS were injected subcutaneously to C57BL/6 mice. Mice were sacrificed and single-cell suspensions of lymphocytes isolated from liver, spleen and tumor were analyzed by flow cytometry. (A+B) NK cell and ILC1 (gated as shown in Figure 2A) frequencies (A) and cell numbers (B) in the liver of PBS- or MC38-injected mice. (C) Cell numbers of NK cells and ILC1s in the spleen. (D) NK cell and ILC1 cell numbers in the tumor tissue of individual mice. (A-C) Data are shown as mean  $\pm$  SEM with symbols representing individual mice,  $n=2-3$ .

#### 4.2.6 Cytokine and chemokine expression by different tumor cell lines

To find out which tumor-secreted factors could influence the LSEC phenotype, we analyzed the mRNA expression of selected cytokines and chemokines by different tumor cell lines: T-leukemia cell line RMA-S, lung carcinoma cell line LL2, colorectal cancer cell line MC38 and the melanoma cell line B16 (Figure 4.24). We observed that the different tumor cell lines are expressing distinct, but also overlapping mRNA transcript profiles. The epithelial-derived tumor cell lines LL2, MC38 and B16 show many common transcripts, whereas the leukemia cell line RMA-S pre-dominantly expresses transcripts for cytokines, for example *Tnf*, *Lta*, *Il16*, *Il17f*. Transcripts for genes like *Vegfa*, *Mif*, *Tgfb2*, *Csf1* and *Sppi* are pre-dominantly expressed by the epithelial-derived cancer cell lines. In comparison to the other cell lines, LL2 expressed more *Bmp6*, *Cxcl3*, and *Il4* mRNA. MC38 and B16 pre-dominantly expressed transcripts for several chemokine genes, like *Ccl20*, *Cxcl10*, *Cxcl11* and *Cx3cl1*. Relative mRNA expression for *Trail*, *Il6* and *C5a* where highly expressed by MC38.

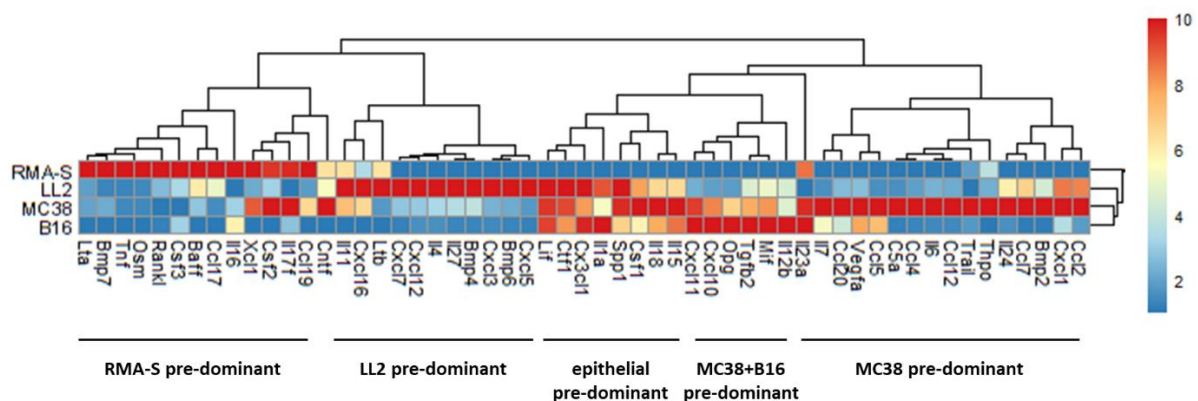


**Figure 4.24 Tumor cell transcriptomes of selected cytokines and chemokines.** RNA was isolated from cultured RMA-S, LL2, MC38 or B16 tumor cells, and gene transcripts of selected cytokines and chemokines were analyzed by qPCR. Heatmap displaying relative (to Actin) mRNA expression of selected genes. Data are scaled per row.

#### 4.2.7 LSECs and NK cells in hepatic metastases

To study LSECs and NK cells in the context of hepatic metastases, we injected MC38 tumor cells via the portal vein to induce metastatic-like tumor growth in the liver. We used a luciferase-expressing MC38 colorectal cancer cell line to track the tumor growth over 14 days. We observed metastasis growth via bioluminescent imaging. Tumors selectively grew in the liver, whereas other organs remained tumor free (Figure 4.25A+B). Upon dissection, a few macroscopically visible nodules were detected on the surface of the organ (Figure 4.25C). Measured body weight (BW), liver weight, liver-to-BW ratio and spleen weight were comparable to the PBS-injected control animal (Figure 4.25D).

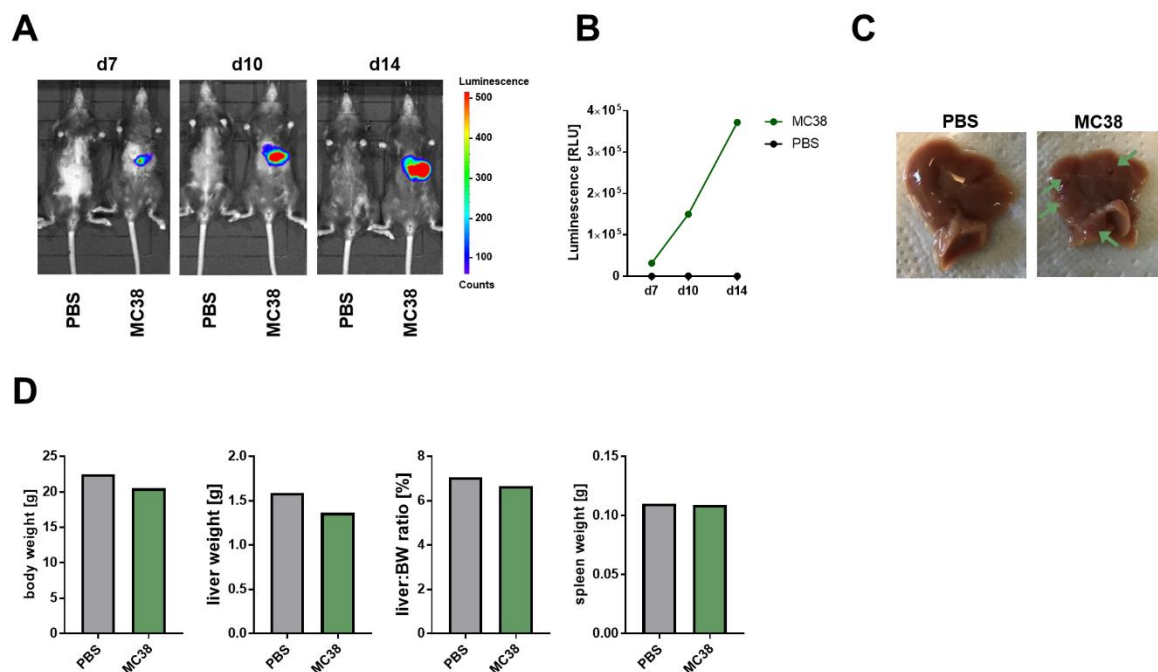


**Figure 4.25 Establishment of a hepatic metastasis model by portal vein injection of tumor cells.** MC38 tumor cells ( $1 \times 10^6$  cells/mouse) or PBS were injected via the portal vein to C57BL/6 mice. (A) Bioluminescence measured by in vivo imaging system (IVIS) on day 7, 10 and 14 after tumor cell injection. (B) Quantification of Luminescence per region of interest. RLU, relative light unit. (C) Images of livers from PBS- or MC38-injected mice at endpoint. Arrows indicate macroscopic metastatic nodules. (D) Body weight (BW), liver weight, liver-to-BW ratio and spleen weight of PBS- or MC38-injected mice. (B+D) Data represent one experiment with  $n =$  one test animal per group.

Next, we compared the expression of selected surface molecules on LSECs isolated from PBS-injected control or MC38-injected mice (gated as shown in Figure 4.4A). The numbers of LSECs in the metastases-bearing mouse were comparable to the control animal (Figure 4.26A). Flow-cytometric data indicated changes in MHC II expression on LSECs. (Figure 4.26B). The expression of Lyve-1, CD31, ICAM-1, VCAM-1, MHC I, PD-L1 and HVEM was unaffected.

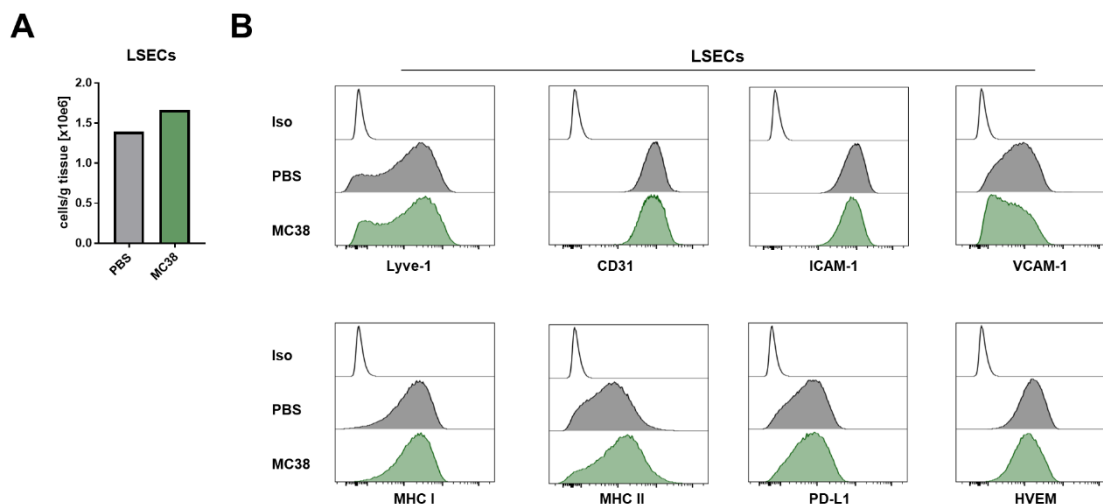


**Figure 4.26 Phenotype of LSECs in metastatic liver.** LSECs were isolated from the liver of PBS- or MC38-injected mice and analyzed by flow cytometry. (A) Cell numbers of LSECs. (B) Histograms of selected surface molecules expressed by LSECs (gated as shown in Figure 4A). Data represent one experiment with  $n =$  one test animal per group. Iso, Isotype.

Contrarily to LSECs, in the liver of the MC38-injected animal, we detected increased numbers of NK cells and ILC1s (Figure 4.27A), while NK cell and ILC1 numbers in the spleen were decreased (Figure 4.27B).

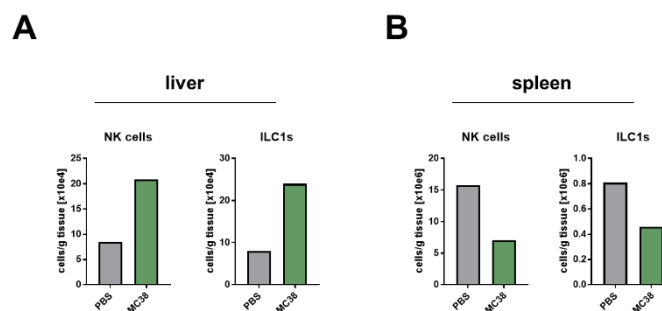


**Figure 4.27 Quantification of NK cells and ILC1s in the tumor-bearing liver.** Single-cell suspensions were prepared from livers and spleens. NK cells and ILC1s (gates as shown in Figure 4.2A) were analyzed by flow cytometry. (A) Quantification of NK cells and ILC1s in the livers of PBS- or MC38-injected mice. (B) Number of NK cells and ILC1s in the spleen. (A+B) Data represent one experiment with  $n =$  one test animal per group.

## 5 DISCUSSION

### 5.1 Alterations of LSECs in inflammation and metastasis

The liver harbors a unique microenvironment with tolerogenic immune functions to limit hypersensitivity to food-antigens and bacterial products. LSECs comprise about 20 % of the hepatic cells and line the liver sinusoids (Sorensen et al., 2015). In comparison to other endothelial cells, they lack a basement membrane but harbor fenestrations, enabling a controlled transport of macromolecules from the bloodstream to the liver parenchyma (Szafranska et al., 2021). LSECs act as regulators of lymphocyte adhesion and migration across the sinusoidal endothelium into the inflamed tissue by expressing adhesion molecules and chemokines (Geraud et al., 2017; Geraud et al., 2013; Harjunpaa et al., 2019). Due to low blood pressure and velocity in the liver sinusoids, circulating immune cells slow down and crawl along the sinusoidal capillaries to extravasate from the blood stream into the tissue. This prolongs their interaction with LSECs, which could enable phenotypic and functional modulation of immune cells. Here we characterized the phenotypic changes and the cytokine/chemokine profile of LSECs in response to LPS, IFN- $\gamma$ , and tumor cells or tumor cell-secreted factors.

#### 5.1.1 The response of LSECs to inflammatory mediators

LSECs are the first contact partners for circulating immune cells in the liver, and therefore, play a crucial role in shaping the local immune microenvironment in homeostasis and disease (Amersfoort et al., 2022). Acute and chronic hepatitis, resulting from viral infections, autoimmune disorders, or exposure to toxins, is marked by significant infiltration of activated lymphocytes, in both the liver parenchyma and perivascular tissue. During hepatitis and in response to LPS, LSECs were shown to lose fenestrations, become activated, and form a basement membrane (Cheluvappa et al., 2010; Ni et al., 2017; Szafranska et al., 2021). LPS is the major ligand for TLR4, which was reported to be expressed by LSECs (Nakamoto and Kanai, 2014; Uhrig et al., 2005). LSECs efficiently clear LPS from the blood stream during bacterial infections, and in response, secrete pro-inflammatory cytokines and increase the expression of adhesion molecules (Cabral et al., 2021; Uhrig et al., 2005). Moreover,

it has been demonstrated that LSECs isolated from fibrotic livers produce the pro-inflammatory cytokine TNF $\alpha$ , and the chemokines CCL2, CCL3, CCL4, CCL5 and CXCL1 (Connolly et al., 2010). In line with this, we observed that LSECs increased the expression of the adhesion molecules VCAM-1 and ICAM-1 after the injection of LPS, and show a distinct chemokine profile in response to the inflammatory mediators LPS and IFN- $\gamma$ , or tumor cell-derived supernatant. We show that the stimulation of cultured LSECs with LPS leads to the increased expression of genes encoding for the chemokines CCL2, CCL3, CCL4 and CCL7. Concurrently, we observed that LSECs displayed transcripts for these chemokines in LPS-injected mice, but not in PBS-injected control mice. CCL2 has been demonstrated to play a role in attracting inflammatory monocytes to the liver (Baeck et al., 2012) and the deletion of *Ccr2* resulted in a decreased presence of inflammatory monocytes in a liver fibrosis model induced by carbon tetrachloride (CCl<sub>4</sub>), leading to reduced inflammatory liver damage (Mitchell et al., 2009). Furthermore, mice lacking *Ccr2* exhibited diminished liver damage in models of acetaminophen-induced acute liver injury (Mossanen et al., 2016) and non-alcoholic steatohepatitis (Miura et al., 2012). Moreover, we observed the transcription of *Cxcl1* by LSECs in response to both LPS and IFN- $\gamma$ . Neutrophils are recruited to the liver and undergo activation by binding of CXCL1 to its chemokine receptor CXCR2 (Capucetti et al., 2020; Liu et al., 2022). Moreover, LSECs were shown to secrete CXCL1 and attract neutrophils in a model of liver fibrosis (Hilscher et al., 2019). Notably, *in vitro* stimulation with LPS and examination of murine liver sections have demonstrated that LSECs, together with hepatic stellate cells, are a significant source of CXCL1 (Bigorgne et al., 2016). Together with our findings, LSECs can be identified as secretors of key chemokines to enable a hepatic immune response to inflammatory stimuli.

### 5.1.2 LSECs in hepatic cancer and metastasis

The liver is a common site for metastasis from colorectal, pancreatic or breast adenocarcinomas (de Ridder et al., 2016). Due to nutrient rich blood supply from the gut and the immunosuppressive environment of the liver, it is a favorable environment for circulating cancer cells. LSECs contribute to the tolerogenic environment by expression of inhibitory ligands, lack of co-stimulatory molecule expression, and the secretion of TGF- $\beta$ , IL-10 and PGE2 (Carambia et al., 2013; Carambia et al., 2014; Diehl et al., 2008; Rieder et al., 1990). We as well demonstrate here, that in response to tumor cell-derived supernatant, LSECs express higher transcripts for *Il10* in comparison to unstimulated LSECs. It was also shown that CXCL12 is recruiting CXCR4-expressing tumor cells and enables transendothelial migration into the tissue (Zabel et al., 2009). In our *in vitro* studies, we observed that LSECs express relative mRNA expression of *Cx12* in response to MC38-derived supernatant. Therefore, LSECs respond to MC38-secreted factors by increasing the expression of tumor cell-attracting chemokines, which could support metastatic spreading of tumors to the liver.

Angiogenic factors, like VEGF, angiopoietins, PDGFs, and migration inhibitory factor (MIF), contribute to the promotion of angiogenesis in metastasis and are important targets for cancer therapies (Ferrara and Kerbel, 2005; Ogawa et al., 2000). Moreover, studies show a correlation of the angiogenic activity with a high risk of vascular invasion, metastasis, and poor prognosis (Poon et al., 2002; Sun et al., 1999). Whereas paracrine VEGF signaling from tumor cells or stromal cells was demonstrated to support vessel growth, proliferation, permeability and differentiation, autocrine VEGF signaling was indispensable for endothelial survival (Lee et al., 2007; Shibuya and Claesson-Welsh, 2006). Moreover, constitutive VEGF signaling is required for the maintenance of endothelial fenestrations in pancreatic islets (Kamba et al., 2006). Concordantly, we observed *Vegfa* mRNA expression in tumor cells, but also upregulation of *Vegfa* in LSECs after the treatment with tumor cell-derived supernatant. This indicates that tumor cell-secreted factors can induce angiogenic programs in LSECs, which could support a pro-metastatic environment in the liver.

In a metastasis model, endothelial cells were shown to support myeloid cell mobilization and the recruitment of CCR2<sup>+</sup>Tie2<sup>-</sup> metastasis-associated macrophages via the secretion of G-CSF and CCL2 (Srivastava et al., 2014). The secretion of CCL2 was triggered by autocrine signaling of Angiopoietin 2 (Ang2) by activated endothelial cells, and antiangiogenic therapy with  $\alpha$ Ang2 antibody, in combination with  $\alpha$ VEGFA and chemotherapy, reduced the accumulation of pro-tumorigenic myeloid cells and metastatic burden. We also observed increased relative mRNA expression of *Csf3*, encoding for G-CSF, and *Ccl2* in response to tumor cell-derived supernatant in LSECs, postulating that LSECs could be involved in the recruitment of metastasis-associated macrophages to the liver to create a pro-tumorigenic environment.

Next to its angiogenic effect, MIF is involved in the upregulation of ICAM-1 and VCAM-1 on endothelial cells (Amin et al., 2006). Moreover, exosomes secreted by pancreatic ductal adenocarcinomas were shown to carry MIF, which led to a pre-metastatic niche formation and increased liver metastatic burden in mice (Costa-Silva et al., 2015). We observed an upregulation of VCAM-1 on LSECs in response to MC38 in a contact-independent manner *in vitro*, as well as in response to progressing distant tumor *in vivo*, underlining that tumor cells can influence LSECs via soluble factors. *Mif* transcripts were pre-dominantly expressed by the epithelial tumor cell lines LL2, B16 and MC38, and upregulated in LSECs after the stimulation with tumor-cell derived supernatant. Thus, tumor cell-secreted factors induce transcriptional and phenotypic changes in LSECs, which could enhance the attraction and adhesion of circulating metastatic cells by the secretion of chemokines and increased expression of adhesion molecules on sinusoidal endothelium, supporting the formation of metastatic nodules in the liver.

The vascular network within the liver comprises a dual system, consisting of the arterial/venous and the sinusoidal endothelium. It is thought that both components play a role in the development of hepatocellular carcinoma (HCC) by undergoing a transition from a venous to a capillary endothelial cell-like phenotype, characterized by the expression of markers typical of continuous, non-fenestrated endothelial cells (Nakamura et al., 1997). Tumor-associated ECs from human HCC samples were shown to express TNF receptor p75 and the integrins  $\alpha$ v $\beta$ 3 and  $\alpha$ v $\beta$ 5, which increased tumor cell adhesion to endothelium (Wu et al., 2008). Moreover, ECs isolated from



human HCC samples did not express the LSEC marker Clec4g but were shown to upregulate markers of macrovascular ECs, like PECAM, CD34, and PLVAP. These vessels showed reduced permeability and could limit lymphocyte recruitment to the tumor (Aizarani et al., 2019). Another study showed, that LSECs in murine and human HCC lose the expression of Lyve-1, Stab1/2 and CD32b (Geraud et al., 2013). It was shown, that tumor cells in growing nodules coopted and remodeled preexisting sinusoidal vessels, showing enlarged, CD31<sup>hi</sup> expressing intratumoral microvessels with a basement membrane (Im et al., 2013; Runge et al., 2014). In our model, we did not observe changes in the expression of Lyve-1 or CD31 on LSECs after portal vein tumor cell delivery and node formation. However, the number of study animals was low, and ECs within macroscopic nodules were not investigated and compared to ECs from adjacent tissue. The phenotypic changes and remodeling of sinusoidal endothelium during liver metastasis requires further inquiry.

Metastasizing tumor cells tend to settle in close proximity to the endothelium of the secondary tumor site. It was shown that primary tumors induce a systemic reprogramming of the endothelium and foster a pro-metastatic niche via the expansion of NG2<sup>+</sup> perivascular cells in the lung (Singhal et al., 2021). Moreover, another study revealed that lung ECs promote stem cell properties and survival of disseminated tumor cells, after endothelial reprogramming by metastasis-associated macrophages, and an induction of a pro-metastatic vascular niche (Hongu et al., 2022). Recently, it has been published that lung endothelium-derived homeostatic Wnt signaling drives the induction of latency in metastasizing tumor cells, promoting a tumor-suppressive environment (Jakab et al., 2024). However, metastasizing-proliferative tumor cells could induce gene sets in niche-specific ECs resembling the primary tumor site, supporting tumor cell proliferation and outgrowth. We showed here that LSECs react to distant, subcutaneous primary tumors by phenotypic changes, including upregulation of VCAM-1, MHC II and PD-L1, which seemed to be dependent on the progressive state of the primary tumor. In our liver metastasis model, induced by the injection of MC38 tumor cells via the portal vein, we also observed the upregulation of MHC II on LSECs 14 days after tumor cell injection.

Together, our data support the hypothesis that distant tumors could promote a metastatic niche formation in the liver by modulating the sinusoidal endothelium via soluble factors or exosomes, leading to enhanced transcription of immunosuppressive cytokines and increased expression of tolerogenic surface molecules by LSECs.

## **5.2 NK cells and ILC1s in inflammation and metastasis**

While NK cells primarily exert cytotoxic functions against infected or transformed cells, tissue-resident ILC1s contribute to tissue homeostasis and immune surveillance in barrier tissues, such as the liver. Investigating how these cell populations interact and collaborate with the liver microenvironment during inflammation and metastasis can provide strategies for therapies to enhance the cytotoxic activity of NK cells or promoting the tissue-protective functions of ILC1s.

### **5.2.1 NK cells are the major producers of IFN- $\gamma$ in LPS-induced endotoxemia**

NK cells contribute to LPS-induced inflammation and mortality of mice by the secretion of IFN- $\gamma$  and TNF- $\alpha$  (Chan et al., 2014; Emoto et al., 2002; Heremans et al., 1994). It has also been shown that ILC1s protect against CCl<sub>4</sub>- and acetaminophen-induced acute liver injury via the production of IFN- $\gamma$ , which induced Bcl-xL expression in hepatocytes, and this protected from hepatocyte apoptosis (Nabekura et al., 2020). The neutralization of IFN- $\gamma$  or the depletion of innate lymphocytes with monoclonal antibodies were effective to reduce mortality of mice in response to LPS injection, whereas the depletion of CD4<sup>+</sup> or CD8<sup>+</sup> T cells did not affect the disease course (Heremans et al., 1994; Heremans et al., 1990). NK cells show a fast reactivity to LPS *in vivo*, shown by the upregulation of CD25 and CD69 at 3 – 6 h post injection, especially in the spleen (Rasid et al., 2016). The re-analysis of deposited single cell RNA sequencing data showed that NK cells upregulated *Ifng* in a sepsis model, induced by poly:IC/LPS injections, and showed highest transcript amounts when compared to other cellular compartments, like NKT cells and T cells (Papaioannou et al., 2023; Sun et al., 2022). Moreover, it has been demonstrated that murine NK cells from spleen, lung and peritoneum are substantial sources of IFN- $\gamma$  and granzyme B in response to LPS in mice (Rasid et al., 2016).

In our study, NK cells, but not ILC1s or T cells, accumulated in the livers 16 h post-injection of LPS. In line with the literature, we observed the upregulation of the CD69 and CD25, as well as increased expression of CD11c and Ly6C on hepatic NK cells after LPS injection, indicative of NK cell activation. Additionally, the frequency of IFN- $\gamma$ -producing NK cells in liver, spleen and blood increased 6 h after, and was maintained until at least 16 h after the injection of LPS. In comparison to other lymphocytes, we identified NK cells to be the major producers of IFN- $\gamma$ , followed by ILC1s. It was shown that memory CD8<sup>+</sup> T cells in the spleen and lymph nodes also serve as an early source of IFN- $\gamma$  in LPS-injected mice, but to a lower extent than NKT cells and NK cells (Kambayashi et al., 2003). It is possible that the minor contribution of T cells to the pool of IFN- $\gamma$ -producing cells in liver, spleen and blood in our study might be associated with the early time points of investigation, the route or dose of LPS administration.

IFN- $\gamma$  production by NK cells is synergistically induced by IL-12 and IL-18, among others (Fehniger et al., 1999; Lusty et al., 2017). We observed that hepatic monocyte and KCs expressed mRNA for *Il12a* and *Il18*, and KCs were already reported to secrete IL-12 and IL-18 in response to LPS *in vitro* (Seki et al., 2001). Therefore, KCs could provide these cytokines in the liver microenvironment and induce the production of IFN- $\gamma$  by tissue-resident ILC1s and accumulating NK cells. IFN- $\gamma$  neutralization was shown to limit lymphocyte infiltration, Fas-induced apoptosis of hepatocytes, and production of pro-inflammatory cytokines, and was protective against acetaminophen-induced acute liver injury and lethality (Ishida et al., 2002). Moreover, NK cell derived IFN- $\gamma$  was reported to contribute to Concanavalin A-induced liver injury (Kusters et al., 1996) and to dampen liver regeneration after partial hepatectomy (Sun and Gao, 2004). Given its role in LPS-induced mortality (Chan et al., 2014), limiting the recruitment of NK cells to the liver might be beneficial to reduce liver damage during endotoxemia or liver injury. On the other hand, IFN- $\gamma$  is important to increase antigen presentation by APCs to bridge innate and adaptive immunity during anti-viral and anti-tumor responses in the liver, and to activate KCs (Crispe, 2009). Therefore, therapeutic strategies aimed at modulating NK cell recruitment should consider maintaining the beneficial effects of IFN- $\gamma$  in hepatic immune responses.

Overall, we could show that during LPS-induced endotoxemia, activated NK cells accumulate in the liver and secrete IFN- $\gamma$ , which might be supported by activated KCs providing the pro-inflammatory cytokines IL-12 and IL-18.

### **5.2.2 NK cells and ILC1s in the liver tumor microenvironment**

The importance of circulating and tissue-resident innate lymphocytes to protect against metastasis was demonstrated by a study in which the genetic deletion of *Mcl-1* from Ncr1-expressing cells resulted in the complete absence of NK1.1<sup>+</sup>NKp46<sup>+</sup> innate lymphocytes and the development of multiorgan metastasis after the injection of B16F10 melanoma cells (Sathe et al., 2014). Moreover, innate lymphocyte depletion by antibodies ( $\alpha$ NK1.1 and  $\alpha$ -asialo-GM1) increased metastatic burden in lung, liver and brain (Diefenbach et al., 2001; Malladi et al., 2016; Spiegel et al., 2016). The susceptibility of Rag2<sup>-/-</sup>Il2rg<sup>-/-</sup> mice (which lack T cells, B cells and NK cells) to lung and liver metastasis, could be rescued by the adoptive transfer of NK cells (Chan et al., 2014; Martinet et al., 2015). In the liver, NK cells have been shown to contribute to the control of CRC liver metastasis, which was supported by KC-secreted IL-18 (Dupaul-Chicoine et al., 2015). IL-18 production by KCs was induced by the activation of the inflammasome by tumor-derived agonists. IL-18 mediated NK cell maturation and anti-tumor activity, which was independent of IFN- $\gamma$ , but rather mediated by FasL-mediated killing. In another study, activated hepatic stellate cells (HSCs) limited NK cell anti-metastatic functions through the secretion of CXCL12 in response to liver injury (Correia et al., 2021). NK cell activity could be restored via IL-15, resulting in disseminated cancer cells quiescence, subsequently reducing metastatic burden in the liver. A recent study investigated the synergy of liver-resident ILC1s and circulating NK cells in controlling liver metastasis (Ducimetiere et al., 2021). It was shown that hepatic ILC1s impeded the seeding of metastasizing tumor cells, whereas circulating NK cells controlled metastasis progression. Moreover, it was observed that, depending on the tumor entity, nodule-infiltrating NK cells showed distinct transcriptomic profiles, phenotypes and functions. A subset of CD49a<sup>+</sup>Eomes<sup>+</sup> NK cells was observed to infiltrate MC38- and CT26-derived metastases and retained key features of differentiation and functionality, represented by the expression of IFN- $\gamma$  and granzyme B. Cells with this phenotype were not detected in LLC-derived metastases. The authors postulated that the CD49a<sup>+</sup>Eomes<sup>+</sup> intranodular NK cell population was shaped by TGF- $\beta$  signaling, supported by the

observation that metastatic nodules were enriched in *Tgfb1* expression. Accordingly, the deletion of the *Tgfb2* gene from NKp46<sup>+</sup> cells effectively enhanced control of MC38 metastasis in the liver (Ducimetiere et al., 2021). Similar phenotype of tumor-infiltrating NK cells, characterized by the upregulation of CD49a on Eomes<sup>+</sup> NK cells and loss of anti-tumor activity, was induced by TGF- $\beta$  in the tumor microenvironment of MCA-induced fibrosarcomas and B16F10 lung metastasis (Gao et al., 2017). These previous studies demonstrate the importance of NK cells in limiting tumor growth and metastasis formation and highlight the need to modulate the tumor microenvironment to preserve NK cell-mediated anti-tumor functions.

We used a model whereby tumor cell-derived nodules grew in the liver upon the injection of MC38 tumor cells via the portal vein, and observed an increase of NK cell and ILC1 numbers in the livers of the tumor injected mouse, concomitant with decreased numbers of NK cells and ILC1s in the spleen. We also observed decreased numbers of NK cells in the spleen after LPS injection and subcutaneous injection of tumor cells, rising the hypothesis that NK cells might be recruited from the periphery to the tumor or metastatic sites. *In vitro*, we observed that both NK cells and ILC1s exerted cytotoxicity against MC38 tumor cells. Here, ILC1s showed a fast onset of target killing. In comparison, NK cells displayed a later onset, but a prolonged and higher cytotoxicity against MC38 tumor cells.

To assess soluble factors that could affect a metastatic niche and the tumor microenvironment in favor of the tumor cells, and dampen immune cell-mediated anti-tumor responses, we analyzed the cytokine and chemokine profiles of different tumor cell lines. Hereby, MC38 and B16 expressed *Tgfb2* and *Il23*. *Tgfb2* gene deletion from NKp46<sup>+</sup> cells was shown to reduce MC38-derived metastasis in the liver and prevented the emergence of a nodule-specific CD49a<sup>+</sup> NK cell subset with reduced effector functions (Ducimetiere et al., 2021). Endogenous IL-23 in the tumor microenvironment was revealed to suppress NK cell-mediated tumor control by reducing perforin and IFN- $\gamma$  production by NK cells (Teng et al., 2010). Neutralization and deficiency of IL-23p19 reduced the number of B16F10 lung metastases in an NK cell dependent manner, and seemed to be mediated by a greater availability of IL12, promoting NK cell effector functions.

In summary we showed that NK cells and ILC1s accumulate in the metastasis-bearing liver and are cytotoxic against colorectal cancer cells *in vitro*. Promoting NK cell attraction to the liver, and preventing the loss of innate lymphocyte anti-tumor capacities due to the tolerogenic environment in the liver or tumor-secreted factors, may enhance the efficacy of immunotherapeutic strategies against liver metastasis.

### **5.3 The crosstalk of LSECs and innate lymphocytes**

NKp46<sup>+</sup> immune cells, which include NK cells and ILC1s, were shown to reside on the luminal side of the sinusoids in healthy liver tissue (Ducimetiere et al., 2021), and are therefore continuously interacting with LSECs. Due to their close proximity, we hypothesized that LSECs and innate lymphocytes might regulate each other's function in liver inflammation and hepatic metastasis.

#### **5.3.1 LSECs regulate NK cell and ILC1 phenotype and function**

LSECs express MHC II and have the potential to act as APCs (Limmer et al., 2000; Racanelli and Rehermann, 2006). However, due to their low expression of the costimulatory molecules CD80/86 (Diehl et al., 2008) and the production of IL-10 and prostaglandin E<sub>2</sub> (Knolle et al., 1998), LSECs do not function as other professional APCs, and do not drive CD4<sup>+</sup> T cell differentiation to Th1 cells under homeostatic conditions (Carambia et al., 2013). Rather, they are involved in the development of regulatory T cells (Knolle et al., 1999; Kruse et al., 2009). Additionally, LSECs were shown to express B7-H1, along with a low expression of co-stimulatory molecules, which results in a balanced of stimulatory versus inhibitory signaling, that supports the induction of CD8<sup>+</sup> T cell tolerance (Diehl et al., 2008; Hochst et al., 2012). LSECs also indirectly regulate CD4<sup>+</sup> and CD8<sup>+</sup> T cell function by reducing the expression of CD80/86 and IL-12 by dendritic cells in a contact-dependent manner (Schildberg et al., 2008). However, LSECs were also demonstrated to prime CD8<sup>+</sup> T cells and initiate their effector functions in the presence of CD4<sup>+</sup> T cell help via co-presentation of antigens (Wittlich et al., 2017). As LSECs were shown to regulate the function of T cells, we wanted to assess their potential role in controlling phenotype and function of NK cells. We observed that *in vitro* co-culture of LSECs and NK cells decreased expression of CD96 and TRAIL, and the activating receptors NKG2D and DNAM-1 on

NK cells, which is in line with transcriptomic data (Papaioannou et al., 2023). Concordantly, NK cell and ILC1 cytotoxicity against the MC38 tumor cells was reduced upon co-culture with LSECs. This initial interaction required cell-to-cell contact, as the stimulation of NK cells or ILC1s with LSEC-derived supernatant did not alter their cytotoxicity. NK cell cytotoxic activity against MC38 target cells was not limited after co-culture with LSECs that have been treated with MC38-derived supernatant (tLSECs). This effect was restricted to NK cells, as killing of target cells by ILC1s was reduced by both LSECs and tLSECs. We observed that LSECs express CD155, the ligand of CD96, DNAM-1 and TIGIT. It was reported that binding of NK cells to plate-bound CD155 reduced CD96 and DNAM-1 surface expression, suggesting that CD155 can induce ligand-mediated internalization or capping of the receptor from NK cells (Chan et al., 2014). Also, NK cells isolated from DNAM-1-deficient mice were less cytotoxic against CD155-expressing target cells *in vitro*, and DNAM-1-deficient mice showed increased MCA-induced fibrosarcomas (Iguchi-Manaka et al., 2008). In another study, DNAM-1- and DNAM-1/CD96-deficient mice bared more B16F10-induced lung metastasis in comparison to WT control animals (Chan et al., 2014). Thus, CD155-expressing LSECs could mediate the downregulation of CD96 and DNAM-1 on NK cells during co-culture, and reduce their ability to kill target cells *in vitro*.

We also observed that LSECs express PD-L1 under homeostatic conditions and upregulate PD-L1 expression after LPS injection, and in response to MC38 tumor cells *in vitro*. It was previously shown that LSECs suppressed the secretion of IFN- $\gamma$  by Th1, and IL-17 by Th17 cells *in vitro* via PD-L1 and limited expression of co-stimulatory molecules (Carambia et al., 2013). Moreover, it was reported that lymphatic ECs and tumor-associated ECs express Rae-1, the ligand for the activating receptor NKG2D, which caused the internalization of NKG2D from the cell surface of NK cells and resulted in reduced NK cell antitumor response (Thompson et al., 2017). If any of these mechanisms result in the reduction of NK cell effector functions against target cells, and how tumor cell-imprinted LSECs authorize NK cell cytotoxicity needs to be further investigated.

### 5.3.2 Feedback regulation of innate lymphocytes and LSECs mediated by IFN- $\gamma$

It was shown that IFN- $\gamma$  supports chemokine production, including CXCL9, CXCL10, and CXCL11 (Cole et al., 1998; Farber, 1990; Luster et al., 1985), and the expression of adhesion molecules, such as ICAM-1 and VCAM-1 (Ren et al., 2010). CXCL9/10/11 are ligands for CXCR3 that contribute to an accumulation of activated lymphocytes, such as NK cells and effector T cells, in inflamed and transformed tissues (Bugide et al., 2021; Dufour et al., 2002; Wendel et al., 2008). We observed that LSECs from LPS-injected mice increased *Cxcl9/10/11* mRNA expression, and displayed the highest relative amounts of these transcripts in comparison to other analyzed cellular compartments. We have also recently analyzed deposited single cell RNA sequencing data by Sun et al., and showed that, in the context of endotoxemia (polyI:C+LPS), LSECs upregulated *Cxcl10* comparable to the myeloid cell compartment (Papaioannou et al., 2023; Sun et al., 2022). Our *in vitro* experiments showed, that LPS could not enhance *Cxcl9/10/11* transcripts, but rather required exposure of LSECs to IFN- $\gamma$ . IFN- $\gamma$  exposure resulted in both transcription and protein secretion of CXCL10 by LSECs. We observed that NK cells were the major producers of IFN- $\gamma$  in the liver after LPS injections, and could therefore support CXCL10 secretion by LSECs. Moreover, we showed that LSECs increased IL-12/18-induced production of IFN- $\gamma$  by NK cells in a contact-dependent manner (Papaioannou et al., 2023), and could be mediated by the expression of activating ligands or trans-presentation of soluble factors by LSECs. We observed that LSECs express CD155 and HVEM, the ligands to the activating receptors DNAM-1 and CD160, respectively. Additionally, NK cells downregulated the expression of DNAM-1 during co-cultures with LSECs, indicating receptor-ligand engagement. We also show that LSECs express transcripts for *Il15* in LPS-injected mice, which has also been reported previously in other models (Cabral et al., 2021; Guilliams et al., 2022). Therefore, it is possible that LSECs produce and trans-present IL-15 to NK cells, in turn priming for enhanced IFN- $\gamma$  production.

In conclusion, we identified LSECs and NK cells as interacting partners during LPS-induced endotoxemia. LSECs provide stimulatory signals to enhance IFN- $\gamma$  production of NK cells in the presence of pro-inflammatory cytokines, which in turn supports chemokine production by LSECs.



### 5.3.3 LSECs support the chemotaxis of NK cells and ILC1s

LSECs have been reported to support the retention, attraction and entry of immune cells in the liver. For example, they produce CXCL16, and recruit sinusoid-patrolling CXCR6<sup>+</sup> NKT cells (Geissmann et al., 2005; Heydtmann et al., 2005; Mossanen et al., 2019). LSEC-secreted CXCL16 promoted the accumulation of NKT cells in the liver, which were important for anti-tumor surveillance in primary and metastatic liver cancer (Ma et al., 2018). We observed that hepatic ILC1s expressed CXCR3 and CXCR6, the chemokine receptors for CXCL10 and CXCL16, respectively. Both unstimulated and IFN- $\gamma$ -treated LSECs were able to attract ILC1s *in vitro*. The migration of ILC1s towards IFN- $\gamma$ -stimulated LSECs was only partially dependent on CXCR3, which hints that IFN- $\gamma$  also induced other chemokines, which could attract ILC1s under inflammatory conditions. Our data show that endothelial specific deletion of *Cxcl10* did not have an impact on ILC1 retention under homeostatic condition in the liver, and did not influence their numbers in LPS-induced liver inflammation. As we observed that LSECs showed the highest relative transcript amounts for *Cxcl16* in comparison to other analyzed cellular compartments, CXCL16 could play a prominent role in LSEC-mediated retention of ILC1s.

NK cells were shown to be recruited from the BM to the liver via the CXCR3-CXCL10 axis during non-alcoholic steatohepatitis (NASH) and to play a protective role against the progression of fibrosis (Bourayou et al., 2024; Fan et al., 2020). We observed increased numbers of NK cells in the liver after the injection of LPS to mice. This correlated with the downregulation of CXCR3 expression on NK cells, indicating receptor-ligand engagement (Meiser et al., 2008). Moreover, the accumulation of NK cells in the liver coincided with an increase of CXCL10 concentration in serum and with the increased mRNA expression of *Cxcl10* in the liver tissue, and by sorted LSECs. We revealed that the transcription of *Cxcl10* and the secretion of CXCL10 by LSECs are not induced by LPS itself, but rather required exposure to IFN- $\gamma$ , which was mainly secreted by NK cells in the inflamed liver tissue. We showed that NK cells can be recruited by IFN- $\gamma$ -stimulated LSECs in a CXCR3-dependent manner *in vitro*. Moreover, endothelial-specific deletion of *Cxcl10* reduced NK cell accumulation in the liver of LPS-injected mice. Therefore our data reveal a positive feedback loop between LSECs and innate lymphocytes to support NK cell migration to the liver via endothelial-derived CXCL10 during LPS-induced endotoxemia.

CXCR3 ligands were also reported attract immune cells to tumor tissue (Bugide et al., 2021; Chheda et al., 2016; Reynders et al., 2019; Wendel et al., 2008). Moreover, CXCR3-mediated trafficking at the tumor vasculature enabled the extravasation of cytotoxic T lymphocytes to the tumor bed (Mikucki et al., 2015). A recent study also showed that capillary ECs in lung metastasis upregulated the angiokine genes *Cxcl10*, *Ccl5*, *Slit3*, *Lrg1* and *Angpt2* (Hongu et al., 2022; Jakab et al., 2024; Singhal et al., 2021). Tumor-associated high-endothelial venules were shown to express mRNAs encoding for the inflammatory chemokines CXCL9 and CXCL10, as well as mRNAs encoding the adhesion molecules ICAM-1 and VCAM-1 (Asrir et al., 2022). During our study, we also observed increased expression of *Cxcl9* and *Cxcl10* mRNA transcripts by LSECs, as well as the upregulation of VCAM-1 expression on LSECs in response to tumor cell-derived supernatants and distant, subcutaneous tumors. Although the role of the chemokines CXCL9 and CXCL10 has been demonstrated, the molecular and functional characteristics of tumor blood vessels mediating lymphocyte attraction into tumors remain poorly defined. We demonstrated that LSECs were able to attract NK cells in a CXCR3-dependent manner *in vitro*, and that endothelial cell-derived CXCL10 supports the recruitment of NK cells to the inflamed liver after LPS-induced endotoxemia. Moreover, we observed that LSECs upregulate mRNAs encoding for CXCL9/10/11 in response to tumor cell-derived supernatant. We therefore postulate that LSEC-derived CXCL10 is not only supporting NK cell attraction during liver inflammation, but could also play a fundamental role in the recruitment of NK cells to hepatic tumor tissue in context of metastatic growth in the liver.

## 6 SUMMARY

The liver is enriched in innate lymphocytes, mainly comprising circulating Natural Killer (NK) cells and liver-resident type 1 innate lymphoid cells (ILC1s), which continuously interact with Liver Sinusoidal Endothelial Cells (LSECs). LSECs line the liver sinusoids and have high endocytic capacities, clearing endo- and exogenous macromolecules from the blood. Innate lymphocytes provide the early defense against infections and malignancies by exerting cytotoxicity and by secreting pro-inflammatory cytokines. However, the local tissue microenvironment that supports NK cell and ILC1 functions in the liver remains not fully explored.

Here, we show that LSECs exposed to inflammatory or tumor cell-derived stimuli, displayed changes in their phenotype and cytokine/chemokine expression profile. LSECs exposed to tumor cells or tumor-conditioned media upregulated the surface expression of PD-L1 and MHC I, the ligands of inhibitory receptors expressed by innate lymphocytes. Co-culture of NK cells and ILC1s with healthy purified LSECs altered their phenotype and reduced their cytotoxicity against the colon carcinoma cell line MC38. In contrast, NK cell cytotoxicity was not reduced after encountering tumor cell supernatant pre-exposed LSECs. Thus, LSECs are able to regulate NK cell and ILC1 cytotoxic function against target cells in dependency of received exogenous signals.

During inflammation, LSECs supported NK cell migration via the production of immune cell-attracting chemokines. In livers of LPS-injected mice, accumulating NK cells were the major source of IFN- $\gamma$ , whereas activated LSECs produced CXCL10. IFN- $\gamma$  promoted the production of CXCL10 by LSECs, and NK cells migrated towards LSECs in a CXCR3-dependent manner. We show that conditional *Cxcl10* gene-deletion in endothelial cells curtailed NK cell accumulation in the liver after LPS treatment *in vivo*.

In conclusion, our findings unveil that LSECs responded to microbial antigens, immune-derived inflammatory signals, and tumor cell-secreted factors, leading to LSEC activation and chemokine production. We identified LSECs as an important player in NK cell recruitment and anti-tumor functions. Acting as central regulators, LSECs fuel a positive feedback loop of NK cell attraction and activation within the inflamed liver tissue.



## 7 REFERENCES

- Adams, N.M. und Sun, J.C. (2018). Spatial and temporal coordination of antiviral responses by group 1 ILCs. *Immunol Rev* 286, 23-36. <https://doi.org/10.1111/imr.12710>
- Aizarani, N., Saviano, A., Sagar, Mailly, L., Durand, S., Herman, J.S., Pessaux, P., Baumert, T.F. und Grun, D. (2019). A human liver cell atlas reveals heterogeneity and epithelial progenitors. *Nature* 572, 199-204. <https://doi.org/10.1038/s41586-019-1373-2>
- Amersfoort, J., Eelen, G. und Carmeliet, P. (2022). Immunomodulation by endothelial cells - partnering up with the immune system? *Nat Rev Immunol*. <https://doi.org/10.1038/s41577-022-00694-4>
- Amin, M.A., Haas, C.S., Zhu, K., Mansfield, P.J., Kim, M.J., Lackowski, N.P. und Koch, A.E. (2006). Migration inhibitory factor up-regulates vascular cell adhesion molecule-1 and intercellular adhesion molecule-1 via Src, PI3 kinase, and NFkappaB. *Blood* 107, 2252-2261. <https://doi.org/10.1182/blood-2005-05-2011>
- Anton, O.M., Peterson, M.E., Hollander, M.J., Dorward, D.W., Arora, G., Traba, J., Rajagopalan, S., Snapp, E.L., Garcia, K.C., Waldmann, T.A., *et al.* (2020). Trans-endocytosis of intact IL-15/alpha-IL-15 complex from presenting cells into NK cells favors signaling for proliferation. *Proc Natl Acad Sci U S A* 117, 522-531. <https://doi.org/10.1073/pnas.1911678117>
- Asrir, A., Tardiveau, C., Coudert, J., Laffont, R., Blanchard, L., Bellard, E., Veerman, K., Bettini, S., Lafouresse, F., Vina, E., *et al.* (2022). Tumor-associated high endothelial venules mediate lymphocyte entry into tumors and predict response to PD-1 plus CTLA-4 combination immunotherapy. *Cancer Cell* 40, 318-334 e319. <https://doi.org/10.1016/j.ccell.2022.01.002>
- Baeck, C., Wehr, A., Karlmark, K.R., Heymann, F., Vucur, M., Gassler, N., Huss, S., Klussmann, S., Eulberg, D., Luedde, T., *et al.* (2012). Pharmacological inhibition of the chemokine CCL2 (MCP-1) diminishes liver macrophage infiltration and steatohepatitis in chronic hepatic injury. *Gut* 61, 416-426. <https://doi.org/10.1136/gutjnl-2011-300304>
- Baiocchi, A., Del Nonno, F., Taibi, C., Visco-Comandini, U., D'Offizi, G., Piacentini, M. und Falasca, L. (2019). Liver sinusoidal endothelial cells (LSECs) modifications in patients with chronic hepatitis C. *Sci Rep* 9, 8760. <https://doi.org/10.1038/s41598-019-45114-1>
- Bernardini, G., Sciume, G., Bosisio, D., Morrone, S., Sozzani, S. und Santoni, A. (2008). CCL3 and CXCL12 regulate trafficking of mouse bone marrow NK cell subsets. *Blood* 111, 3626-3634. <https://doi.org/10.1182/blood-2007-08-106203>
- Bernardini, G., Sciume, G. und Santoni, A. (2013). Differential chemotactic receptor requirements for NK cell subset trafficking into bone marrow. *Front Immunol* 4, 12. <https://doi.org/10.3389/fimmu.2013.00012>
- Bezman, N.A., Jhatakia, A., Kearney, A.Y., Brender, T., Maurer, M., Henning, K., Jenkins, M.R., Rogers, A.J., Neeson, P.J., Korman, A.J., *et al.* (2017). PD-1 blockade enhances elotuzumab efficacy in mouse tumor models. *Blood Adv* 1, 753-765. <https://doi.org/10.1182/bloodadvances.2017004382>
- Bhandari, S., Larsen, A.K., McCourt, P., Smedsrod, B. und Sorensen, K.K. (2021). The Scavenger Function of Liver Sinusoidal Endothelial Cells in Health and Disease. *Front Physiol* 12, 757469. <https://doi.org/10.3389/fphys.2021.757469>
- Bigorgne, A.E., John, B., Ebrahimkhani, M.R., Shimizu-Albergine, M., Campbell, J.S. und Crispe, I.N. (2016). TLR4-Dependent Secretion by Hepatic Stellate Cells of

- the Neutrophil-Chemoattractant CXCL1 Mediates Liver Response to Gut Microbiota. *PLoS One* 11, e0151063. <https://doi.org/10.1371/journal.pone.0151063>
- Blum, J.S., Wearsch, P.A. und Cresswell, P. (2013). Pathways of antigen processing. *Annu Rev Immunol* 31, 443-473. <https://doi.org/10.1146/annurev-immunol-032712-095910>
- Bonilla, F.A. und Oettgen, H.C. (2010). Adaptive immunity. *J Allergy Clin Immunol* 125, S33-40. <https://doi.org/10.1016/j.jaci.2009.09.017>
- Borrego, F., Robertson, M.J., Ritz, J., Pena, J. und Solana, R. (1999). CD69 is a stimulatory receptor for natural killer cell and its cytotoxic effect is blocked by CD94 inhibitory receptor. *Immunology* 97, 159-165. <https://doi.org/10.1046/j.1365-2567.1999.00738.x>
- Bourayou, E., Perchet, T., Meunier, S., Bouvier, H., Mailhe, M.P., Melanitou, E., Cumano, A. und Golub, R. (2024). Bone marrow monocytes sustain NK cell-poiesis during non-alcoholic steatohepatitis. *Cell Rep* 43, 113676. <https://doi.org/10.1016/j.celrep.2024.113676>
- Bradfield, P.F., Scheiermann, C., Nourshargh, S., Ody, C., Luscinskas, F.W., Rainger, G.E., Nash, G.B., Miljkovic-Licina, M., Aurrand-Lions, M. und Imhof, B.A. (2007). JAM-C regulates unidirectional monocyte transendothelial migration in inflammation. *Blood* 110, 2545-2555. <https://doi.org/10.1182/blood-2007-03-078733>
- Braet, F. und Wisse, E. (2002). Structural and functional aspects of liver sinusoidal endothelial cell fenestrae: a review. *Comp Hepatol* 1, 1. <https://doi.org/10.1186/1476-5926-1-1>
- Bugide, S., Gupta, R., Green, M.R. und Wajapeyee, N. (2021). EZH2 inhibits NK cell-mediated antitumor immunity by suppressing CXCL10 expression in an HDAC10-dependent manner. *Proc Natl Acad Sci U S A* 118. <https://doi.org/10.1073/pnas.2102718118>
- Burt, B.M., Plitas, G., Stableford, J.A., Nguyen, H.M., Bamboat, Z.M., Pillarisetty, V.G. und DeMatteo, R.P. (2008). CD11c identifies a subset of murine liver natural killer cells that responds to adenoviral hepatitis. *J Leukoc Biol* 84, 1039-1046. <https://doi.org/10.1189/jlb.0408256>
- Cabral, F., Al-Rahem, M., Skaggs, J., Thomas, T.A., Kumar, N., Wu, Q., Fadda, P., Yu, L., Robinson, J.M., Kim, J., *et al.* (2021). Stabilin receptors clear LPS and control systemic inflammation. *iScience* 24, 103337. <https://doi.org/10.1016/j.isci.2021.103337>
- Capucetti, A., Albano, F. und Bonecchi, R. (2020). Multiple Roles for Chemokines in Neutrophil Biology. *Front Immunol* 11, 1259. <https://doi.org/10.3389/fimmu.2020.01259>
- Carambia, A., Frenzel, C., Bruns, O.T., Schwinge, D., Reimer, R., Hohenberg, H., Huber, S., Tiegs, G., Schramm, C., Lohse, A.W., *et al.* (2013). Inhibition of inflammatory CD4 T cell activity by murine liver sinusoidal endothelial cells. *J Hepatol* 58, 112-118. <https://doi.org/10.1016/j.jhep.2012.09.008>
- Carambia, A., Freund, B., Schwinge, D., Heine, M., Laschtowitz, A., Huber, S., Wraith, D.C., Korn, T., Schramm, C., Lohse, A.W., *et al.* (2014). TGF-beta-dependent induction of CD4(+)CD25(+)Foxp3(+) Tregs by liver sinusoidal endothelial cells. *J Hepatol* 61, 594-599. <https://doi.org/10.1016/j.jhep.2014.04.027>
- Carayannopoulos, L.N., Naidenko, O.V., Fremont, D.H. und Yokoyama, W.M. (2002). Cutting edge: murine UL16-binding protein-like transcript 1: a newly described transcript encoding a high-affinity ligand for murine NKG2D. *J Immunol* 169, 4079-4083. <https://doi.org/10.4049/jimmunol.169.8.4079>

- Cerwenka, A., Baron, J.L. und Lanier, L.L. (2001). Ectopic expression of retinoic acid early inducible-1 gene (RAE-1) permits natural killer cell-mediated rejection of a MHC class I-bearing tumor in vivo. *Proc Natl Acad Sci U S A* 98, 11521-11526. <https://doi.org/10.1073/pnas.201238598>
- Chaix, J., Tessmer, M.S., Hoebe, K., Fuseri, N., Ryffel, B., Dalod, M., Alexopoulou, L., Beutler, B., Brossay, L., Vivier, E., *et al.* (2008). Cutting edge: Priming of NK cells by IL-18. *J Immunol* 181, 1627-1631. <https://doi.org/10.4049/jimmunol.181.3.1627>
- Chan, C.J., Martinet, L., Gilfillan, S., Souza-Fonseca-Guimaraes, F., Chow, M.T., Town, L., Ritchie, D.S., Colonna, M., Andrews, D.M. und Smyth, M.J. (2014). The receptors CD96 and CD226 oppose each other in the regulation of natural killer cell functions. *Nat Immunol* 15, 431-438. <https://doi.org/10.1038/ni.2850>
- Cheluvappa, R., Denning, G.M., Lau, G.W., Grimm, M.C., Hilmer, S.N. und Le Couteur, D.G. (2010). Pathogenesis of the hyperlipidemia of Gram-negative bacterial sepsis may involve pathomorphological changes in liver sinusoidal endothelial cells. *Int J Infect Dis* 14, e857-867. <https://doi.org/10.1016/j.ijid.2010.02.2263>
- Chheda, Z.S., Sharma, R.K., Jala, V.R., Luster, A.D. und Haribabu, B. (2016). Chemoattractant Receptors BLT1 and CXCR3 Regulate Antitumor Immunity by Facilitating CD8+ T Cell Migration into Tumors. *J Immunol* 197, 2016-2026. <https://doi.org/10.4049/jimmunol.1502376>
- Chiossone, L., Dumas, P.Y., Vienne, M. und Vivier, E. (2018). Natural killer cells and other innate lymphoid cells in cancer. *Nat Rev Immunol* 18, 671-688. <https://doi.org/10.1038/s41577-018-0061-z>
- Clausen, J., Vergeiner, B., Enk, M., Petzer, A.L., Gastl, G. und Gunsilius, E. (2003). Functional significance of the activation-associated receptors CD25 and CD69 on human NK-cells and NK-like T-cells. *Immunobiology* 207, 85-93. <https://doi.org/10.1078/0171-2985-00219>
- Cogger, V.C., Warren, A., Fraser, R., Ngu, M., McLean, A.J. und Le Couteur, D.G. (2003). Hepatic sinusoidal pseudocapillarization with aging in the non-human primate. *Exp Gerontol* 38, 1101-1107. <https://doi.org/10.1016/j.exger.2003.07.002>
- Cole, K.E., Strick, C.A., Paradis, T.J., Ogborne, K.T., Loetscher, M., Gladue, R.P., Lin, W., Boyd, J.G., Moser, B., Wood, D.E., *et al.* (1998). Interferon-inducible T cell alpha chemoattractant (I-TAC): a novel non-ELR CXC chemokine with potent activity on activated T cells through selective high affinity binding to CXCR3. *J Exp Med* 187, 2009-2021. <https://doi.org/10.1084/jem.187.12.2009>
- Connolly, M.K., Bedrosian, A.S., Malhotra, A., Henning, J.R., Ibrahim, J., Vera, V., Cieza-Rubio, N.E., Hassan, B.U., Pachter, H.L., Cohen, S., *et al.* (2010). In hepatic fibrosis, liver sinusoidal endothelial cells acquire enhanced immunogenicity. *J Immunol* 185, 2200-2208. <https://doi.org/10.4049/jimmunol.1000332>
- Cooper, M.A., Elliott, J.M., Keyel, P.A., Yang, L., Carrero, J.A. und Yokoyama, W.M. (2009). Cytokine-induced memory-like natural killer cells. *Proc Natl Acad Sci U S A* 106, 1915-1919. <https://doi.org/10.1073/pnas.0813192106>
- Correia, A.L., Guimaraes, J.C., Auf der Maur, P., De Silva, D., Trefny, M.P., Okamoto, R., Bruno, S., Schmidt, A., Mertz, K., Volkmann, K., *et al.* (2021). Hepatic stellate cells suppress NK cell-sustained breast cancer dormancy. *Nature* 594, 566-571. <https://doi.org/10.1038/s41586-021-03614-z>
- Costa-Silva, B., Aiello, N.M., Ocean, A.J., Singh, S., Zhang, H., Thakur, B.K., Becker, A., Hoshino, A., Mark, M.T., Molina, H., *et al.* (2015). Pancreatic cancer exosomes initiate pre-metastatic niche formation in the liver. *Nat Cell Biol* 17, 816-826. <https://doi.org/10.1038/ncb3169>
- Crispe, I.N. (2009). The liver as a lymphoid organ. *Annu Rev Immunol* 27, 147-163. <https://doi.org/10.1146/annurev.immunol.021908.132629>

- Daussy, C., Faure, F., Mayol, K., Viel, S., Gasteiger, G., Charrier, E., Bienvenu, J., Henry, T., Debien, E., Hasan, U.A., *et al.* (2014). T-bet and Eomes instruct the development of two distinct natural killer cell lineages in the liver and in the bone marrow. *J Exp Med* 211, 563-577. <https://doi.org/10.1084/jem.20131560>
- De Creus, A., Abe, M., Lau, A.H., Hackstein, H., Raimondi, G. und Thomson, A.W. (2005). Low TLR4 expression by liver dendritic cells correlates with reduced capacity to activate allogeneic T cells in response to endotoxin. *J Immunol* 174, 2037-2045. <https://doi.org/10.4049/jimmunol.174.4.2037>
- de Ridder, J., de Wilt, J.H., Simmer, F., Overbeek, L., Lemmens, V. und Nagtegaal, I. (2016). Incidence and origin of histologically confirmed liver metastases: an explorative case-study of 23,154 patients. *Oncotarget* 7, 55368-55376. <https://doi.org/10.18632/oncotarget.10552>
- den Haan, J.M., Arens, R. und van Zelm, M.C. (2014). The activation of the adaptive immune system: cross-talk between antigen-presenting cells, T cells and B cells. *Immunol Lett* 162, 103-112. <https://doi.org/10.1016/j.imlet.2014.10.011>
- Diefenbach, A., Colonna, M. und Koyasu, S. (2014). Development, differentiation, and diversity of innate lymphoid cells. *Immunity* 41, 354-365. <https://doi.org/10.1016/j.immuni.2014.09.005>
- Diefenbach, A., Jamieson, A.M., Liu, S.D., Shastri, N. und Raulet, D.H. (2000). Ligands for the murine NKG2D receptor: expression by tumor cells and activation of NK cells and macrophages. *Nat Immunol* 1, 119-126. <https://doi.org/10.1038/77793>
- Diefenbach, A., Jensen, E.R., Jamieson, A.M. und Raulet, D.H. (2001). Rae1 and H60 ligands of the NKG2D receptor stimulate tumour immunity. *Nature* 413, 165-171. <https://doi.org/10.1038/35093109>
- Diehl, L., Schurich, A., Grochtmann, R., Hegenbarth, S., Chen, L. und Knolle, P.A. (2008). Tolerogenic maturation of liver sinusoidal endothelial cells promotes B7-homolog 1-dependent CD8+ T cell tolerance. *Hepatology* 47, 296-305. <https://doi.org/10.1002/hep.21965>
- DiSanto, J.P., Muller, W., Guy-Grand, D., Fischer, A. und Rajewsky, K. (1995). Lymphoid development in mice with a targeted deletion of the interleukin 2 receptor gamma chain. *Proc Natl Acad Sci U S A* 92, 377-381. <https://doi.org/10.1073/pnas.92.2.377>
- Dokun, A.O., Kim, S., Smith, H.R., Kang, H.S., Chu, D.T. und Yokoyama, W.M. (2001). Specific and nonspecific NK cell activation during virus infection. *Nat Immunol* 2, 951-956. <https://doi.org/10.1038/ni714>
- Dostert, C., Grusdat, M., Letellier, E. und Brenner, D. (2019). The TNF Family of Ligands and Receptors: Communication Modules in the Immune System and Beyond. *Physiol Rev* 99, 115-160. <https://doi.org/10.1152/physrev.00045.2017>
- Dubois, S., Mariner, J., Waldmann, T.A. und Tagaya, Y. (2002). IL-15Ralpha recycles and presents IL-15 in trans to neighboring cells. *Immunity* 17, 537-547. [https://doi.org/10.1016/s1074-7613\(02\)00429-6](https://doi.org/10.1016/s1074-7613(02)00429-6)
- Ducimetiere, L., Lucchiari, G., Litscher, G., Nater, M., Heeb, L., Nunez, N.G., Wyss, L., Burri, D., Vermeer, M., Gschwend, J., *et al.* (2021). Conventional NK cells and tissue-resident ILC1s join forces to control liver metastasis. *Proc Natl Acad Sci U S A* 118. <https://doi.org/10.1073/pnas.2026271118>
- Dufour, J.H., Dziejman, M., Liu, M.T., Leung, J.H., Lane, T.E. und Luster, A.D. (2002). IFN-gamma-inducible protein 10 (IP-10; CXCL10)-deficient mice reveal a role for IP-10 in effector T cell generation and trafficking. *J Immunol* 168, 3195-3204. <https://doi.org/10.4049/jimmunol.168.7.3195>
- Dupaul-Chicoine, J., Arabzadeh, A., Dagenais, M., Douglas, T., Champagne, C., Morizot, A., Rodrigue-Gervais, I.G., Breton, V., Colpitts, S.L., Beauchemin, N., *et*



- al.* (2015). The Nlrp3 Inflammasome Suppresses Colorectal Cancer Metastatic Growth in the Liver by Promoting Natural Killer Cell Tumoricidal Activity. *Immunity* 43, 751-763. <https://doi.org/10.1016/j.immuni.2015.08.013>
- Emoto, M., Miyamoto, M., Yoshizawa, I., Emoto, Y., Schaible, U.E., Kita, E. und Kaufmann, S.H. (2002). Critical role of NK cells rather than V alpha 14(+)NKT cells in lipopolysaccharide-induced lethal shock in mice. *J Immunol* 169, 1426-1432. <https://doi.org/10.4049/jimmunol.169.3.1426>
- Fan, Y., Zhang, W., Wei, H., Sun, R., Tian, Z. und Chen, Y. (2020). Hepatic NK cells attenuate fibrosis progression of non-alcoholic steatohepatitis in dependent of CXCL10-mediated recruitment. *Liver Int* 40, 598-608. <https://doi.org/10.1111/liv.14307>
- Farber, J.M. (1990). A macrophage mRNA selectively induced by gamma-interferon encodes a member of the platelet factor 4 family of cytokines. *Proc Natl Acad Sci U S A* 87, 5238-5242. <https://doi.org/10.1073/pnas.87.14.5238>
- Fehniger, T.A., Shah, M.H., Turner, M.J., VanDeusen, J.B., Whitman, S.P., Cooper, M.A., Suzuki, K., Wechser, M., Goodsaid, F. und Caligiuri, M.A. (1999). Differential cytokine and chemokine gene expression by human NK cells following activation with IL-18 or IL-15 in combination with IL-12: implications for the innate immune response. *J Immunol* 162, 4511-4520.
- Ferrara, N. und Kerbel, R.S. (2005). Angiogenesis as a therapeutic target. *Nature* 438, 967-974. <https://doi.org/10.1038/nature04483>
- Ficht, X. und Iannacone, M. (2020). Immune surveillance of the liver by T cells. *Sci Immunol* 5. <https://doi.org/10.1126/sciimmunol.aba2351>
- Friedrich, C., Taggenbrock, R., Doucet-Ladeveze, R., Golda, G., Moenius, R., Arampatzi, P., Kragten, N.A.M., Kreymborg, K., Gomez de Agüero, M., Kastenmüller, W., *et al.* (2021). Effector differentiation downstream of lineage commitment in ILC1s is driven by Hobit across tissues. *Nat Immunol* 22, 1256-1267. <https://doi.org/10.1038/s41590-021-01013-0>
- Fukuda, Y., Nagura, H., Imoto, M. und Koyama, Y. (1986). Immunohistochemical studies on structural changes of the hepatic lobules in chronic liver diseases. *Am J Gastroenterol* 81, 1149-1155.
- Gan, Y., Liu, R., Wu, W., Bompreszi, R. und Shi, F.D. (2012). Antibody to alpha4 integrin suppresses natural killer cells infiltration in central nervous system in experimental autoimmune encephalomyelitis. *J Neuroimmunol* 247, 9-15. <https://doi.org/10.1016/j.jneuroim.2012.03.011>
- Gao, Y., Souza-Fonseca-Guimaraes, F., Bald, T., Ng, S.S., Young, A., Ngiow, S.F., Rautela, J., Straube, J., Waddell, N., Blake, S.J., *et al.* (2017). Tumor immunoevasion by the conversion of effector NK cells into type 1 innate lymphoid cells. *Nat Immunol* 18, 1004-1015. <https://doi.org/10.1038/ni.3800>
- Gasteiger, G., Fan, X., Dikiy, S., Lee, S.Y. und Rudensky, A.Y. (2015). Tissue residency of innate lymphoid cells in lymphoid and nonlymphoid organs. *Science* 350, 981-985. <https://doi.org/10.1126/science.aac9593>
- Geissmann, F., Cameron, T.O., Sidobre, S., Manlongat, N., Kronenberg, M., Briskin, M.J., Dustin, M.L. und Littman, D.R. (2005). Intravascular immune surveillance by CXCR6+ NKT cells patrolling liver sinusoids. *PLoS Biol* 3, e113. <https://doi.org/10.1371/journal.pbio.0030113>
- Geraud, C., Koch, P.S., Zierow, J., Klapproth, K., Busch, K., Olsavszky, V., Leibing, T., Demory, A., Ulbrich, F., Diett, M., *et al.* (2017). GATA4-dependent organ-specific endothelial differentiation controls liver development and embryonic hematopoiesis. *J Clin Invest* 127, 1099-1114. <https://doi.org/10.1172/JCI90086>

- Geraud, C., Mogler, C., Runge, A., Evdokimov, K., Lu, S., Schledzewski, K., Arnold, B., Hammerling, G., Koch, P.S., Breuhahn, K., *et al.* (2013). Endothelial transdifferentiation in hepatocellular carcinoma: loss of Stabilin-2 expression in peri-tumourous liver correlates with increased survival. *Liver Int* 33, 1428-1440. <https://doi.org/10.1111/liv.12262>
- Gong, J., Tu, W., Liu, J. und Tian, D. (2022). Hepatocytes: A key role in liver inflammation. *Front Immunol* 13, 1083780. <https://doi.org/10.3389/fimmu.2022.1083780>
- Guilliams, M., Bonnardel, J., Haest, B., Vanderborght, B., Wagner, C., Remmerie, A., Bujko, A., Martens, L., Thone, T., Browaeys, R., *et al.* (2022). Spatial proteogenomics reveals distinct and evolutionarily conserved hepatic macrophage niches. *Cell* 185, 379-396 e338. <https://doi.org/10.1016/j.cell.2021.12.018>
- Hams, E., Bermingham, R. und Fallon, P.G. (2015). Macrophage and Innate Lymphoid Cell Interplay in the Genesis of Fibrosis. *Front Immunol* 6, 597. <https://doi.org/10.3389/fimmu.2015.00597>
- Hanke, T., Takizawa, H., McMahon, C.W., Busch, D.H., Pamer, E.G., Miller, J.D., Altman, J.D., Liu, Y., Cado, D., Lemonnier, F.A., *et al.* (1999). Direct assessment of MHC class I binding by seven Ly49 inhibitory NK cell receptors. *Immunity* 11, 67-77. [https://doi.org/10.1016/s1074-7613\(00\)80082-5](https://doi.org/10.1016/s1074-7613(00)80082-5)
- Harjunpaa, H., Llort Asens, M., Guenther, C. und Fagerholm, S.C. (2019). Cell Adhesion Molecules and Their Roles and Regulation in the Immune and Tumor Microenvironment. *Front Immunol* 10, 1078. <https://doi.org/10.3389/fimmu.2019.01078>
- Hayakawa, Y. und Smyth, M.J. (2006). CD27 dissects mature NK cells into two subsets with distinct responsiveness and migratory capacity. *J Immunol* 176, 1517-1524. <https://doi.org/10.4049/jimmunol.176.3.1517>
- Heremans, H., Dillen, C., van Damme, J. und Billiau, A. (1994). Essential role for natural killer cells in the lethal lipopolysaccharide-induced Schwartzman-like reaction in mice. *Eur J Immunol* 24, 1155-1160. <https://doi.org/10.1002/eji.1830240522>
- Heremans, H., Van Damme, J., Dillen, C., Dijkmans, R. und Billiau, A. (1990). Interferon gamma, a mediator of lethal lipopolysaccharide-induced Schwartzman-like shock reactions in mice. *J Exp Med* 171, 1853-1869. <https://doi.org/10.1084/jem.171.6.1853>
- Heydtmann, M., Lalor, P.F., Eksteen, J.A., Hubscher, S.G., Briskin, M. und Adams, D.H. (2005). CXC chemokine ligand 16 promotes integrin-mediated adhesion of liver-infiltrating lymphocytes to cholangiocytes and hepatocytes within the inflamed human liver. *J Immunol* 174, 1055-1062. <https://doi.org/10.4049/jimmunol.174.2.1055>
- Hilscher, M.B., Sehrawat, T., Arab, J.P., Zeng, Z., Gao, J., Liu, M., Kostallari, E., Gao, Y., Simonetto, D.A., Yaqoob, U., *et al.* (2019). Mechanical Stretch Increases Expression of CXCL1 in Liver Sinusoidal Endothelial Cells to Recruit Neutrophils, Generate Sinusoidal Microthrombi, and Promote Portal Hypertension. *Gastroenterology* 157, 193-209 e199. <https://doi.org/10.1053/j.gastro.2019.03.013>
- Hochst, B., Schildberg, F.A., Bottcher, J., Metzger, C., Huss, S., Turler, A., Overhaus, M., Knoblich, A., Schneider, B., Pantelis, D., *et al.* (2012). Liver sinusoidal endothelial cells contribute to CD8 T cell tolerance toward circulating carcinoembryonic antigen in mice. *Hepatology* 56, 1924-1933. <https://doi.org/10.1002/hep.25844>
- Hongu, T., Pein, M., Insua-Rodriguez, J., Gutjahr, E., Mattavelli, G., Meier, J., Decker, K., Descot, A., Bozza, M., Harbottle, R., *et al.* (2022). Perivascular tenascin C

- triggers sequential activation of macrophages and endothelial cells to generate a pro-metastatic vascular niche in the lungs. *Nat Cancer* 3, 486-504. <https://doi.org/10.1038/s43018-022-00353-6>
- Horst, A.K., Neumann, K., Diehl, L. und Tiegs, G. (2016). Modulation of liver tolerance by conventional and nonconventional antigen-presenting cells and regulatory immune cells. *Cell Mol Immunol* 13, 277-292. <https://doi.org/10.1038/cmi.2015.112>
- Hsu, J., Hodgins, J.J., Marathe, M., Nicolai, C.J., Bourgeois-Daigneault, M.C., Trevino, T.N., Azimi, C.S., Scheer, A.K., Randolph, H.E., Thompson, T.W., *et al.* (2018). Contribution of NK cells to immunotherapy mediated by PD-1/PD-L1 blockade. *J Clin Invest* 128, 4654-4668. <https://doi.org/10.1172/JCI99317>
- Iguchi-Manaka, A., Kai, H., Yamashita, Y., Shibata, K., Tahara-Hanaoka, S., Honda, S., Yasui, T., Kikutani, H., Shibuya, K. und Shibuya, A. (2008). Accelerated tumor growth in mice deficient in DNAM-1 receptor. *J Exp Med* 205, 2959-2964. <https://doi.org/10.1084/jem.20081611>
- Im, J.H., Tapmeier, T., Balathasan, L., Gal, A., Yameen, S., Hill, S., Smart, S., Noterdaeme, O., Kelly, M., Brady, M., *et al.* (2013). G-CSF rescues tumor growth and neo-angiogenesis during liver metastasis under host angiopoietin-2 deficiency. *Int J Cancer* 132, 315-326. <https://doi.org/10.1002/ijc.27677>
- Ishida, Y., Kondo, T., Ohshima, T., Fujiwara, H., Iwakura, Y. und Mukaida, N. (2002). A pivotal involvement of IFN-gamma in the pathogenesis of acetaminophen-induced acute liver injury. *FASEB J* 16, 1227-1236. <https://doi.org/10.1096/fj.02-0046com>
- Jakab, M., Lee, K.H., Uvarovskii, A., Ovchinnikova, S., Kulkarni, S.R., Jakab, S., Rostalski, T., Spegg, C., Anders, S. und Augustin, H.G. (2024). Lung endothelium exploits susceptible tumor cell states to instruct metastatic latency. *Nat Cancer*. <https://doi.org/10.1038/s43018-023-00716-7>
- Kamba, T., Tam, B.Y., Hashizume, H., Haskell, A., Sennino, B., Mancuso, M.R., Norberg, S.M., O'Brien, S.M., Davis, R.B., Gowen, L.C., *et al.* (2006). VEGF-dependent plasticity of fenestrated capillaries in the normal adult microvasculature. *Am J Physiol Heart Circ Physiol* 290, H560-576. <https://doi.org/10.1152/ajpheart.00133.2005>
- Kambayashi, T., Assarsson, E., Lukacher, A.E., Ljunggren, H.G. und Jensen, P.E. (2003). Memory CD8+ T cells provide an early source of IFN-gamma. *J Immunol* 170, 2399-2408. <https://doi.org/10.4049/jimmunol.170.5.2399>
- Karlhofer, F.M., Ribaldo, R.K. und Yokoyama, W.M. (1992). The interaction of Ly-49 with H-2Dd globally inactivates natural killer cell cytolytic activity. *Trans Assoc Am Physicians* 105, 72-85.
- Karlsson, S., Ruokonen, E., Varpula, T., Ala-Kokko, T.I., Pettila, V. und Finnsepsis Study, G. (2009). Long-term outcome and quality-adjusted life years after severe sepsis. *Crit Care Med* 37, 1268-1274. <https://doi.org/10.1097/CCM.0b013e31819c13ac>
- Kim, S., Poursine-Laurent, J., Truscott, S.M., Lybarger, L., Song, Y.J., Yang, L., French, A.R., Sunwoo, J.B., Lemieux, S., Hansen, T.H., *et al.* (2005). Licensing of natural killer cells by host major histocompatibility complex class I molecules. *Nature* 436, 709-713. <https://doi.org/10.1038/nature03847>
- Klose, C.S.N. und Artis, D. (2020). Innate lymphoid cells control signaling circuits to regulate tissue-specific immunity. *Cell Res* 30, 475-491. <https://doi.org/10.1038/s41422-020-0323-8>
- Klose, C.S.N., Flach, M., Mohle, L., Rogell, L., Hoyler, T., Ebert, K., Fabiunke, C., Pfeifer, D., Sexl, V., Fonseca-Pereira, D., *et al.* (2014). Differentiation of type 1

- ILCs from a common progenitor to all helper-like innate lymphoid cell lineages. *Cell* 157, 340-356. <https://doi.org/10.1016/j.cell.2014.03.030>
- Knolle, P.A., Schmitt, E., Jin, S., Germann, T., Duchmann, R., Hegenbarth, S., Gerken, G. und Lohse, A.W. (1999). Induction of cytokine production in naive CD4(+) T cells by antigen-presenting murine liver sinusoidal endothelial cells but failure to induce differentiation toward Th1 cells. *Gastroenterology* 116, 1428-1440. [https://doi.org/10.1016/s0016-5085\(99\)70508-1](https://doi.org/10.1016/s0016-5085(99)70508-1)
- Knolle, P.A., Uhrig, A., Hegenbarth, S., Loser, E., Schmitt, E., Gerken, G. und Lohse, A.W. (1998). IL-10 down-regulates T cell activation by antigen-presenting liver sinusoidal endothelial cells through decreased antigen uptake via the mannose receptor and lowered surface expression of accessory molecules. *Clin Exp Immunol* 114, 427-433. <https://doi.org/10.1046/j.1365-2249.1998.00713.x>
- Knolle, P.A. und Wohlleber, D. (2016). Immunological functions of liver sinusoidal endothelial cells. *Cell Mol Immunol* 13, 347-353. <https://doi.org/10.1038/cmi.2016.5>
- Kruse, N., Neumann, K., Schrage, A., Derkow, K., Schott, E., Erben, U., Kuhl, A., Loddenkemper, C., Zeitz, M., Hamann, A., *et al.* (2009). Priming of CD4+ T cells by liver sinusoidal endothelial cells induces CD25<sup>low</sup> forkhead box protein 3-regulatory T cells suppressing autoimmune hepatitis. *Hepatology* 50, 1904-1913. <https://doi.org/10.1002/hep.23191>
- Kudo, S., Matsuno, K., Ezaki, T. und Ogawa, M. (1997). A novel migration pathway for rat dendritic cells from the blood: hepatic sinusoids-lymph translocation. *J Exp Med* 185, 777-784. <https://doi.org/10.1084/jem.185.4.777>
- Kusters, S., Gantner, F., Kunstle, G. und Tiegs, G. (1996). Interferon gamma plays a critical role in T cell-dependent liver injury in mice initiated by concanavalin A. *Gastroenterology* 111, 462-471. <https://doi.org/10.1053/gast.1996.v111.pm8690213>
- Lanier, L.L. (2005). NK cell recognition. *Annu Rev Immunol* 23, 225-274. <https://doi.org/10.1146/annurev.immunol.23.021704.115526>
- Lee, H., Quek, C., Silva, I., Tasker, A., Batten, M., Rizos, H., Lim, S.Y., Nur Gide, T., Shang, P., Attrill, G.H., *et al.* (2019). Integrated molecular and immunophenotypic analysis of NK cells in anti-PD-1 treated metastatic melanoma patients. *Oncoimmunology* 8, e1537581. <https://doi.org/10.1080/2162402X.2018.1537581>
- Lee, S., Chen, T.T., Barber, C.L., Jordan, M.C., Murdock, J., Desai, S., Ferrara, N., Nagy, A., Roos, K.P. und Iruela-Arispe, M.L. (2007). Autocrine VEGF signaling is required for vascular homeostasis. *Cell* 130, 691-703. <https://doi.org/10.1016/j.cell.2007.06.054>
- Li, D. und Wu, M. (2021). Pattern recognition receptors in health and diseases. *Signal Transduct Target Ther* 6, 291. <https://doi.org/10.1038/s41392-021-00687-0>
- Lieberman, J. (2003). The ABCs of granule-mediated cytotoxicity: new weapons in the arsenal. *Nat Rev Immunol* 3, 361-370. <https://doi.org/10.1038/nri1083>
- Limmer, A., Ohl, J., Kurts, C., Ljunggren, H.G., Reiss, Y., Groettrup, M., Momburg, F., Arnold, B. und Knolle, P.A. (2000). Efficient presentation of exogenous antigen by liver endothelial cells to CD8+ T cells results in antigen-specific T-cell tolerance. *Nat Med* 6, 1348-1354. <https://doi.org/10.1038/82161>
- Liu, N., Bauer, M. und Press, A.T. (2022). The immunological function of CXCR2 in the liver during sepsis. *J Inflamm (Lond)* 19, 23. <https://doi.org/10.1186/s12950-022-00321-y>
- Liu, W., Tang, L., Zhang, G., Wei, H., Cui, Y., Guo, L., Gou, Z., Chen, X., Jiang, D., Zhu, Y., *et al.* (2004). Characterization of a novel C-type lectin-like gene, LSECtin: demonstration of carbohydrate binding and expression in sinusoidal endothelial

- cells of liver and lymph node. *J Biol Chem* 279, 18748-18758. <https://doi.org/10.1074/jbc.M311227200>
- Lohse, A.W., Knolle, P.A., Bilo, K., Uhrig, A., Waldmann, C., Ibe, M., Schmitt, E., Gerken, G. und Meyer Zum Buschenfelde, K.H. (1996). Antigen-presenting function and B7 expression of murine sinusoidal endothelial cells and Kupffer cells. *Gastroenterology* 110, 1175-1181. <https://doi.org/10.1053/gast.1996.v110.pm8613007>
- Lorente, S., Hautefeuille, M. und Sanchez-Cedillo, A. (2020). The liver, a functionalized vascular structure. *Sci Rep* 10, 16194. <https://doi.org/10.1038/s41598-020-73208-8>
- Lozano, E., Dominguez-Villar, M., Kuchroo, V. und Hafler, D.A. (2012). The TIGIT/CD226 axis regulates human T cell function. *J Immunol* 188, 3869-3875. <https://doi.org/10.4049/jimmunol.1103627>
- Luster, A.D. und Ravetch, J.V. (1987). Biochemical characterization of a gamma interferon-inducible cytokine (IP-10). *J Exp Med* 166, 1084-1097. <https://doi.org/10.1084/jem.166.4.1084>
- Luster, A.D., Unkeless, J.C. und Ravetch, J.V. (1985). Gamma-interferon transcriptionally regulates an early-response gene containing homology to platelet proteins. *Nature* 315, 672-676. <https://doi.org/10.1038/315672a0>
- Lusty, E., Poznanski, S.M., Kwofie, K., Mandur, T.S., Lee, D.A., Richards, C.D. und Ashkar, A.A. (2017). IL-18/IL-15/IL-12 synergy induces elevated and prolonged IFN-gamma production by ex vivo expanded NK cells which is not due to enhanced STAT4 activation. *Mol Immunol* 88, 138-147. <https://doi.org/10.1016/j.molimm.2017.06.025>
- Ma, C., Han, M., Heinrich, B., Fu, Q., Zhang, Q., Sandhu, M., Agdashian, D., Terabe, M., Berzofsky, J.A., Fako, V., et al. (2018). Gut microbiome-mediated bile acid metabolism regulates liver cancer via NKT cells. *Science* 360. <https://doi.org/10.1126/science.aan5931>
- Malladi, S., Macalinao, D.G., Jin, X., He, L., Basnet, H., Zou, Y., de Stanchina, E. und Massague, J. (2016). Metastatic Latency and Immune Evasion through Autocrine Inhibition of WNT. *Cell* 165, 45-60. <https://doi.org/10.1016/j.cell.2016.02.025>
- Mao, Y., van Hoef, V., Zhang, X., Wennerberg, E., Lorent, J., Witt, K., Masvidal, L., Liang, S., Murray, S., Larsson, O., et al. (2016). IL-15 activates mTOR and primes stress-activated gene expression leading to prolonged antitumor capacity of NK cells. *Blood* 128, 1475-1489. <https://doi.org/10.1182/blood-2016-02-698027>
- Marrone, G., Shah, V.H. und Gracia-Sancho, J. (2016). Sinusoidal communication in liver fibrosis and regeneration. *J Hepatol* 65, 608-617. <https://doi.org/10.1016/j.jhep.2016.04.018>
- Martinet, L., Ferrari De Andrade, L., Guilleroy, C., Lee, J.S., Liu, J., Souza-Fonseca-Guimaraes, F., Hutchinson, D.S., Kolesnik, T.B., Nicholson, S.E., Huntington, N.D., et al. (2015). DNAM-1 expression marks an alternative program of NK cell maturation. *Cell Rep* 11, 85-97. <https://doi.org/10.1016/j.celrep.2015.03.006>
- Matsuno, K., Ezaki, T., Kudo, S. und Uehara, Y. (1996). A life stage of particle-laden rat dendritic cells in vivo: their terminal division, active phagocytosis, and translocation from the liver to the draining lymph. *J Exp Med* 183, 1865-1878. <https://doi.org/10.1084/jem.183.4.1865>
- McDonald, B., Jenne, C.N., Zhuo, L., Kimata, K. und Kubes, P. (2013). Kupffer cells and activation of endothelial TLR4 coordinate neutrophil adhesion within liver sinusoids during endotoxemia. *Am J Physiol Gastrointest Liver Physiol* 305, G797-806. <https://doi.org/10.1152/ajpgi.00058.2013>

- McKenzie, A.N.J., Spits, H. und Eberl, G. (2014). Innate lymphoid cells in inflammation and immunity. *Immunity* 41, 366-374. <https://doi.org/10.1016/j.immuni.2014.09.006>
- McLean, A.J., Cogger, V.C., Chong, G.C., Warren, A., Markus, A.M., Dahlstrom, J.E. und Le Couteur, D.G. (2003). Age-related pseudocapillarization of the human liver. *J Pathol* 200, 112-117. <https://doi.org/10.1002/path.1328>
- Meiser, A., Mueller, A., Wise, E.L., McDonagh, E.M., Petit, S.J., Saran, N., Clark, P.C., Williams, T.J. und Pease, J.E. (2008). The chemokine receptor CXCR3 is degraded following internalization and is replenished at the cell surface by de novo synthesis of receptor. *J Immunol* 180, 6713-6724. <https://doi.org/10.4049/jimmunol.180.10.6713>
- Mikucki, M.E., Fisher, D.T., Matsuzaki, J., Skitzki, J.J., Gaulin, N.B., Muhitch, J.B., Ku, A.W., Frelinger, J.G., Odunsi, K., Gajewski, T.F., *et al.* (2015). Non-redundant requirement for CXCR3 signalling during tumoricidal T-cell trafficking across tumour vascular checkpoints. *Nat Commun* 6, 7458. <https://doi.org/10.1038/ncomms8458>
- Miller, M.C. und Mayo, K.H. (2017). Chemokines from a Structural Perspective. *Int J Mol Sci* 18. <https://doi.org/10.3390/ijms18102088>
- Mitchell, C., Couton, D., Couty, J.P., Anson, M., Crain, A.M., Bizet, V., Renia, L., Pol, S., Mallet, V. und Gilgenkrantz, H. (2009). Dual role of CCR2 in the constitution and the resolution of liver fibrosis in mice. *Am J Pathol* 174, 1766-1775. <https://doi.org/10.2353/ajpath.2009.080632>
- Miura, K., Yang, L., van Rooijen, N., Ohnishi, H. und Seki, E. (2012). Hepatic recruitment of macrophages promotes nonalcoholic steatohepatitis through CCR2. *Am J Physiol Gastrointest Liver Physiol* 302, G1310-1321. <https://doi.org/10.1152/ajpgi.00365.2011>
- Miyake, K. (2007). Innate immune sensing of pathogens and danger signals by cell surface Toll-like receptors. *Semin Immunol* 19, 3-10. <https://doi.org/10.1016/j.smim.2006.12.002>
- Mosmann, T.R., Cherwinski, H., Bond, M.W., Giedlin, M.A. und Coffman, R.L. (1986). Two types of murine helper T cell clone. I. Definition according to profiles of lymphokine activities and secreted proteins. *J Immunol* 136, 2348-2357.
- Mossanen, J.C., Kohlhepp, M., Wehr, A., Krenkel, O., Liepelt, A., Roeth, A.A., Mockel, D., Heymann, F., Lammers, T., Gassler, N., *et al.* (2019). CXCR6 Inhibits Hepatocarcinogenesis by Promoting Natural Killer T- and CD4(+) T-Cell-Dependent Control of Senescence. *Gastroenterology* 156, 1877-1889 e1874. <https://doi.org/10.1053/j.gastro.2019.01.247>
- Mossanen, J.C., Krenkel, O., Ergen, C., Govaere, O., Liepelt, A., Puengel, T., Heymann, F., Kalthoff, S., Lefebvre, E., Eulberg, D., *et al.* (2016). Chemokine (C-C motif) receptor 2-positive monocytes aggravate the early phase of acetaminophen-induced acute liver injury. *Hepatology* 64, 1667-1682. <https://doi.org/10.1002/hep.28682>
- Nabekura, T., Riggan, L., Hildreth, A.D., O'Sullivan, T.E. und Shibuya, A. (2020). Type 1 Innate Lymphoid Cells Protect Mice from Acute Liver Injury via Interferon-gamma Secretion for Upregulating Bcl-xL Expression in Hepatocytes. *Immunity* 52, 96-108 e109. <https://doi.org/10.1016/j.immuni.2019.11.004>
- Nakamoto, N. und Kanai, T. (2014). Role of toll-like receptors in immune activation and tolerance in the liver. *Front Immunol* 5, 221. <https://doi.org/10.3389/fimmu.2014.00221>
- Nakamura, S., Muro, H., Suzuki, S., Sakaguchi, T., Konno, H., Baba, S. und Syed, A.S. (1997). Immunohistochemical studies on endothelial cell phenotype in

- hepatocellular carcinoma. *Hepatology* 26, 407-415. <https://doi.org/10.1002/hep.510260222>
- Ni, J., Miller, M., Stojanovic, A., Garbi, N. und Cerwenka, A. (2012). Sustained effector function of IL-12/15/18-preactivated NK cells against established tumors. *J Exp Med* 209, 2351-2365. <https://doi.org/10.1084/jem.20120944>
- Ni, Y., Li, J.M., Liu, M.K., Zhang, T.T., Wang, D.P., Zhou, W.H., Hu, L.Z. und Lv, W.L. (2017). Pathological process of liver sinusoidal endothelial cells in liver diseases. *World J Gastroenterol* 23, 7666-7677. <https://doi.org/10.3748/wjg.v23.i43.7666>
- Nielsen, C.M., Wolf, A.S., Goodier, M.R. und Riley, E.M. (2016). Synergy between Common gamma Chain Family Cytokines and IL-18 Potentiates Innate and Adaptive Pathways of NK Cell Activation. *Front Immunol* 7, 101. <https://doi.org/10.3389/fimmu.2016.00101>
- Norris, S., Coleman, A., Kuri-Cervantes, L., Bower, M., Nelson, M. und Goodier, M.R. (2012). PD-1 expression on natural killer cells and CD8(+) T cells during chronic HIV-1 infection. *Viral Immunol* 25, 329-332. <https://doi.org/10.1089/vim.2011.0096>
- Norris, S., Collins, C., Doherty, D.G., Smith, F., McEntee, G., Traynor, O., Nolan, N., Hegarty, J. und O'Farrelly, C. (1998). Resident human hepatic lymphocytes are phenotypically different from circulating lymphocytes. *J Hepatol* 28, 84-90. [https://doi.org/10.1016/s0168-8278\(98\)80206-7](https://doi.org/10.1016/s0168-8278(98)80206-7)
- Ogawa, H., Nishihira, J., Sato, Y., Kondo, M., Takahashi, N., Oshima, T. und Todo, S. (2000). An antibody for macrophage migration inhibitory factor suppresses tumour growth and inhibits tumour-associated angiogenesis. *Cytokine* 12, 309-314. <https://doi.org/10.1006/cyto.1999.0562>
- Ohteki, T., Ho, S., Suzuki, H., Mak, T.W. und Ohashi, P.S. (1997). Role for IL-15/IL-15 receptor beta-chain in natural killer 1.1+ T cell receptor-alpha beta+ cell development. *J Immunol* 159, 5931-5935.
- Osna, N.A., Donohue, T.M., Jr. und Kharbanda, K.K. (2017). Alcoholic Liver Disease: Pathogenesis and Current Management. *Alcohol Res* 38, 147-161.
- Pandey, E., Nour, A.S. und Harris, E.N. (2020). Prominent Receptors of Liver Sinusoidal Endothelial Cells in Liver Homeostasis and Disease. *Front Physiol* 11, 873. <https://doi.org/10.3389/fphys.2020.00873>
- Panwar, A., Das, P. und Tan, L.P. (2021). 3D Hepatic Organoid-Based Advancements in LIVER Tissue Engineering. *Bioengineering (Basel)* 8. <https://doi.org/10.3390/bioengineering8110185>
- Papaioannou, S., See, J.X., Jeong, M., De La Torre, C., Ast, V., Reiners-Koch, P.S., Sati, A., Mogler, C., Platten, M., Cerwenka, A., *et al.* (2023). Liver sinusoidal endothelial cells orchestrate NK cell recruitment and activation in acute inflammatory liver injury. *Cell Rep* 42, 112836. <https://doi.org/10.1016/j.celrep.2023.112836>
- Pardo, J., Balkow, S., Anel, A. und Simon, M.M. (2002). Granzymes are essential for natural killer cell-mediated and perf-facilitated tumor control. *Eur J Immunol* 32, 2881-2887. [https://doi.org/10.1002/1521-4141\(200210\)32:10<2881::AID-IMMU2881>3.0.CO;2-K](https://doi.org/10.1002/1521-4141(200210)32:10<2881::AID-IMMU2881>3.0.CO;2-K)
- Pasarin, M., La Mura, V., Gracia-Sancho, J., Garcia-Caldero, H., Rodriguez-Vilarrupla, A., Garcia-Pagan, J.C., Bosch, J. und Abraldes, J.G. (2012). Sinusoidal endothelial dysfunction precedes inflammation and fibrosis in a model of NAFLD. *PLoS One* 7, e32785. <https://doi.org/10.1371/journal.pone.0032785>
- Paul, S. und Lal, G. (2017). The Molecular Mechanism of Natural Killer Cells Function and Its Importance in Cancer Immunotherapy. *Front Immunol* 8, 1124. <https://doi.org/10.3389/fimmu.2017.01124>

- Peng, H., Jiang, X., Chen, Y., Sojka, D.K., Wei, H., Gao, X., Sun, R., Yokoyama, W.M. und Tian, Z. (2013). Liver-resident NK cells confer adaptive immunity in skin-contact inflammation. *J Clin Invest* 123, 1444-1456. <https://doi.org/10.1172/JCI66381>
- Poisson, J., Lemoine, S., Boulanger, C., Durand, F., Moreau, R., Valla, D. und Rautou, P.E. (2017). Liver sinusoidal endothelial cells: Physiology and role in liver diseases. *J Hepatol* 66, 212-227. <https://doi.org/10.1016/j.jhep.2016.07.009>
- Poon, R.T., Ng, I.O., Lau, C., Yu, W.C., Yang, Z.F., Fan, S.T. und Wong, J. (2002). Tumor microvessel density as a predictor of recurrence after resection of hepatocellular carcinoma: a prospective study. *J Clin Oncol* 20, 1775-1785. <https://doi.org/10.1200/JCO.2002.07.089>
- Racanelli, V. und Rehmann, B. (2006). The liver as an immunological organ. *Hepatology* 43, S54-62. <https://doi.org/10.1002/hep.21060>
- Rasid, O., Ciulean, I.S., Fitting, C., Doyen, N. und Cavillon, J.M. (2016). Local Microenvironment Controls the Compartmentalization of NK Cell Responses during Systemic Inflammation in Mice. *J Immunol* 197, 2444-2454. <https://doi.org/10.4049/jimmunol.1601040>
- Ren, G., Zhao, X., Zhang, L., Zhang, J., L'Huillier, A., Ling, W., Roberts, A.I., Le, A.D., Shi, S., Shao, C., *et al.* (2010). Inflammatory cytokine-induced intercellular adhesion molecule-1 and vascular cell adhesion molecule-1 in mesenchymal stem cells are critical for immunosuppression. *J Immunol* 184, 2321-2328. <https://doi.org/10.4049/jimmunol.0902023>
- Reynders, N., Abboud, D., Baragli, A., Noman, M.Z., Rogister, B., Niclou, S.P., Heveker, N., Janji, B., Hanson, J., Szpakowska, M., *et al.* (2019). The Distinct Roles of CXCR3 Variants and Their Ligands in the Tumor Microenvironment. *Cells* 8. <https://doi.org/10.3390/cells8060613>
- Rieder, H., Ramadori, G., Allmann, K.H. und Meyer zum Buschenfelde, K.H. (1990). Prostanoid release of cultured liver sinusoidal endothelial cells in response to endotoxin and tumor necrosis factor. Comparison with umbilical vein endothelial cells. *J Hepatol* 11, 359-366. [https://doi.org/10.1016/0168-8278\(90\)90222-d](https://doi.org/10.1016/0168-8278(90)90222-d)
- Robinette, M.L., Fuchs, A., Cortez, V.S., Lee, J.S., Wang, Y., Durum, S.K., Gilfillan, S., Colonna, M. und Immunological Genome, C. (2015). Transcriptional programs define molecular characteristics of innate lymphoid cell classes and subsets. *Nat Immunol* 16, 306-317. <https://doi.org/10.1038/ni.3094>
- Romee, R., Rosario, M., Berrien-Elliott, M.M., Wagner, J.A., Jewell, B.A., Schappe, T., Leong, J.W., Abdel-Latif, S., Schneider, S.E., Willey, S., *et al.* (2016). Cytokine-induced memory-like natural killer cells exhibit enhanced responses against myeloid leukemia. *Sci Transl Med* 8, 357ra123. <https://doi.org/10.1126/scitranslmed.aaf2341>
- Rossetto, A., De Re, V., Steffan, A., Ravaioli, M., Miolo, G., Leone, P., Racanelli, V., Uzzau, A., Baccarani, U. und Cescon, M. (2019). Carcinogenesis and Metastasis in Liver: Cell Physiological Basis. *Cancers (Basel)* 11. <https://doi.org/10.3390/cancers11111731>
- Runge, A., Hu, J., Wieland, M., Bergeest, J.P., Mogler, C., Neumann, A., Geraud, C., Arnold, B., Rohr, K., Komljenovic, D., *et al.* (2014). An inducible hepatocellular carcinoma model for preclinical evaluation of antiangiogenic therapy in adult mice. *Cancer Res* 74, 4157-4169. <https://doi.org/10.1158/0008-5472.CAN-13-2311>
- Salazar-Mather, T.P., Ishikawa, R. und Biron, C.A. (1996). NK cell trafficking and cytokine expression in splenic compartments after IFN induction and viral infection. *J Immunol* 157, 3054-3064.



- Sathe, P., Delconte, R.B., Souza-Fonseca-Guimaraes, F., Seillet, C., Chopin, M., Vandenberg, C.J., Rankin, L.C., Mielke, L.A., Vikstrom, I., Kolesnik, T.B., *et al.* (2014). Innate immunodeficiency following genetic ablation of Mcl1 in natural killer cells. *Nat Commun* 5, 4539. <https://doi.org/10.1038/ncomms5539>
- Schaffner, F. und Poper, H. (1963). Capillarization of hepatic sinusoids in man. *Gastroenterology* 44, 239-242.
- Schildberg, F.A., Hegenbarth, S.I., Schumak, B., Scholz, K., Limmer, A. und Knolle, P.A. (2008). Liver sinusoidal endothelial cells veto CD8 T cell activation by antigen-presenting dendritic cells. *Eur J Immunol* 38, 957-967. <https://doi.org/10.1002/eji.200738060>
- Schurich, A., Berg, M., Stabenow, D., Bottcher, J., Kern, M., Schild, H.J., Kurts, C., Schuette, V., Burgdorf, S., Diehl, L., *et al.* (2010). Dynamic regulation of CD8 T cell tolerance induction by liver sinusoidal endothelial cells. *J Immunol* 184, 4107-4114. <https://doi.org/10.4049/jimmunol.0902580>
- Seki, E., Tsutsui, H., Nakano, H., Tsuji, N., Hoshino, K., Adachi, O., Adachi, K., Futatsugi, S., Kuida, K., Takeuchi, O., *et al.* (2001). Lipopolysaccharide-induced IL-18 secretion from murine Kupffer cells independently of myeloid differentiation factor 88 that is critically involved in induction of production of IL-12 and IL-1beta. *J Immunol* 166, 2651-2657. <https://doi.org/10.4049/jimmunol.166.4.2651>
- Shetty, S., Lalor, P.F. und Adams, D.H. (2018). Liver sinusoidal endothelial cells - gatekeepers of hepatic immunity. *Nat Rev Gastroenterol Hepatol* 15, 555-567. <https://doi.org/10.1038/s41575-018-0020-y>
- Shibuya, A., Campbell, D., Hannum, C., Yssel, H., Franz-Bacon, K., McClanahan, T., Kitamura, T., Nicholl, J., Sutherland, G.R., Lanier, L.L., *et al.* (1996). DNAM-1, a novel adhesion molecule involved in the cytolytic function of T lymphocytes. *Immunity* 4, 573-581. [https://doi.org/10.1016/s1074-7613\(00\)70060-4](https://doi.org/10.1016/s1074-7613(00)70060-4)
- Shibuya, M. und Claesson-Welsh, L. (2006). Signal transduction by VEGF receptors in regulation of angiogenesis and lymphangiogenesis. *Exp Cell Res* 312, 549-560. <https://doi.org/10.1016/j.yexcr.2005.11.012>
- Singhal, M., Gengenbacher, N., Abdul Pari, A.A., Kamiyama, M., Hai, L., Kuhn, B.J., Kallenberg, D.M., Kulkarni, S.R., Camilli, C., Preuss, S.F., *et al.* (2021). Temporal multi-omics identifies LRG1 as a vascular niche instructor of metastasis. *Sci Transl Med* 13, eabe6805. <https://doi.org/10.1126/scitranslmed.abe6805>
- Sojka, D.K., Plougastel-Douglas, B., Yang, L., Pak-Wittel, M.A., Artyomov, M.N., Ivanova, Y., Zhong, C., Chase, J.M., Rothman, P.B., Yu, J., *et al.* (2014). Tissue-resident natural killer (NK) cells are cell lineages distinct from thymic and conventional splenic NK cells. *Elife* 3, e01659. <https://doi.org/10.7554/eLife.01659>
- Sorensen, K.K., Simon-Santamaria, J., McCuskey, R.S. und Smedsrod, B. (2015). Liver Sinusoidal Endothelial Cells. *Compr Physiol* 5, 1751-1774. <https://doi.org/10.1002/cphy.c140078>
- Spiegel, A., Brooks, M.W., Houshyar, S., Reinhardt, F., Ardolino, M., Fessler, E., Chen, M.B., Krall, J.A., DeCock, J., Zervantonakis, I.K., *et al.* (2016). Neutrophils Suppress Intraluminal NK Cell-Mediated Tumor Cell Clearance and Enhance Extravasation of Disseminated Carcinoma Cells. *Cancer Discov* 6, 630-649. <https://doi.org/10.1158/2159-8290.CD-15-1157>
- Spits, H., Artis, D., Colonna, M., Diefenbach, A., Di Santo, J.P., Eberl, G., Koyasu, S., Locksley, R.M., McKenzie, A.N., Mebius, R.E., *et al.* (2013). Innate lymphoid cells - a proposal for uniform nomenclature. *Nat Rev Immunol* 13, 145-149. <https://doi.org/10.1038/nri3365>
- Srivastava, K., Hu, J., Korn, C., Savant, S., Teichert, M., Kapel, S.S., Jugold, M., Besemfelder, E., Thomas, M., Pasparakis, M., *et al.* (2014). Postsurgical adjuvant

- tumor therapy by combining anti-angiopoietin-2 and metronomic chemotherapy limits metastatic growth. *Cancer Cell* 26, 880-895. <https://doi.org/10.1016/j.ccell.2014.11.005>
- Stanietsky, N., Rovis, T.L., Glasner, A., Seidel, E., Tsukerman, P., Yamin, R., Enk, J., Jonjic, S. und Mandelboim, O. (2013). Mouse TIGIT inhibits NK-cell cytotoxicity upon interaction with PVR. *Eur J Immunol* 43, 2138-2150. <https://doi.org/10.1002/eji.201243072>
- Sun, H.C., Tang, Z.Y., Li, X.M., Zhou, Y.N., Sun, B.R. und Ma, Z.C. (1999). Microvessel density of hepatocellular carcinoma: its relationship with prognosis. *J Cancer Res Clin Oncol* 125, 419-426. <https://doi.org/10.1007/s004320050296>
- Sun, R. und Gao, B. (2004). Negative regulation of liver regeneration by innate immunity (natural killer cells/interferon-gamma). *Gastroenterology* 127, 1525-1539. <https://doi.org/10.1053/j.gastro.2004.08.055>
- Sun, X., Wu, J., Liu, L., Chen, Y., Tang, Y., Liu, S., Chen, H., Jiang, Y., Liu, Y., Yuan, H., *et al.* (2022). Transcriptional switch of hepatocytes initiates macrophage recruitment and T-cell suppression in endotoxemia. *J Hepatol* 77, 436-452. <https://doi.org/10.1016/j.jhep.2022.02.028>
- Suzuki, H., Duncan, G.S., Takimoto, H. und Mak, T.W. (1997). Abnormal development of intestinal intraepithelial lymphocytes and peripheral natural killer cells in mice lacking the IL-2 receptor beta chain. *J Exp Med* 185, 499-505. <https://doi.org/10.1084/jem.185.3.499>
- Szafranska, K., Kruse, L.D., Holte, C.F., McCourt, P. und Zapotoczny, B. (2021). The wHole Story About Fenestrations in LSEC. *Front Physiol* 12, 735573. <https://doi.org/10.3389/fphys.2021.735573>
- Takada, A., Yoshida, S., Kajikawa, M., Miyatake, Y., Tomaru, U., Sakai, M., Chiba, H., Maenaka, K., Kohda, D., Fugo, K., *et al.* (2008). Two novel NKG2D ligands of the mouse H60 family with differential expression patterns and binding affinities to NKG2D. *J Immunol* 180, 1678-1685. <https://doi.org/10.4049/jimmunol.180.3.1678>
- Takeda, K., Cretney, E., Hayakawa, Y., Ota, T., Akiba, H., Ogasawara, K., Yagita, H., Kinoshita, K., Okumura, K. und Smyth, M.J. (2005). TRAIL identifies immature natural killer cells in newborn mice and adult mouse liver. *Blood* 105, 2082-2089. <https://doi.org/10.1182/blood-2004-08-3262>
- Tang, L., Yang, J., Liu, W., Tang, X., Chen, J., Zhao, D., Wang, M., Xu, F., Lu, Y., Liu, B., *et al.* (2009). Liver sinusoidal endothelial cell lectin, LSECtin, negatively regulates hepatic T-cell immune response. *Gastroenterology* 137, 1498-1508 e1491-1495. <https://doi.org/10.1053/j.gastro.2009.07.051>
- Teng, M.W., Andrews, D.M., McLaughlin, N., von Scheidt, B., Ngiow, S.F., Moller, A., Hill, G.R., Iwakura, Y., Oft, M. und Smyth, M.J. (2010). IL-23 suppresses innate immune response independently of IL-17A during carcinogenesis and metastasis. *Proc Natl Acad Sci U S A* 107, 8328-8333. <https://doi.org/10.1073/pnas.1003251107>
- Thompson, T.W., Kim, A.B., Li, P.J., Wang, J., Jackson, B.T., Huang, K.T.H., Zhang, L. und Raulet, D.H. (2017). Endothelial cells express NKG2D ligands and desensitize antitumor NK responses. *Elife* 6. <https://doi.org/10.7554/eLife.30881>
- Thomson, A.W. und Knolle, P.A. (2010). Antigen-presenting cell function in the tolerogenic liver environment. *Nat Rev Immunol* 10, 753-766. <https://doi.org/10.1038/nri2858>
- Tian, Z., Chen, Y. und Gao, B. (2013). Natural killer cells in liver disease. *Hepatology* 57, 1654-1662. <https://doi.org/10.1002/hep.26115>
- Triantafyllou, E., Woollard, K.J., McPhail, M.J.W., Antoniadou, C.G. und Possamai, L.A. (2018). The Role of Monocytes and Macrophages in Acute and Acute-on-

- Chronic Liver Failure. *Front Immunol* 9, 2948. <https://doi.org/10.3389/fimmu.2018.02948>
- Tsilimigras, D.I., Brodt, P., Clavien, P.A., Muschel, R.J., D'Angelica, M.I., Endo, I., Parks, R.W., Doyle, M., de Santibanes, E. und Pawlik, T.M. (2021). Liver metastases. *Nat Rev Dis Primers* 7, 27. <https://doi.org/10.1038/s41572-021-00261-6>
- Tsou, C.L., Peters, W., Si, Y., Slaymaker, S., Aslanian, A.M., Weisberg, S.P., Mack, M. und Charo, I.F. (2007). Critical roles for CCR2 and MCP-3 in monocyte mobilization from bone marrow and recruitment to inflammatory sites. *J Clin Invest* 117, 902-909. <https://doi.org/10.1172/JCI29919>
- Uhrig, A., Banafsche, R., Kremer, M., Hegenbarth, S., Hamann, A., Neurath, M., Gerken, G., Limmer, A. und Knolle, P.A. (2005). Development and functional consequences of LPS tolerance in sinusoidal endothelial cells of the liver. *J Leukoc Biol* 77, 626-633. <https://doi.org/10.1189/jlb.0604332>
- Vignali, D.A. und Kuchroo, V.K. (2012). IL-12 family cytokines: immunological playmakers. *Nat Immunol* 13, 722-728. <https://doi.org/10.1038/ni.2366>
- Wald, O., Weiss, I.D., Wald, H., Shoham, H., Bar-Shavit, Y., Beider, K., Galun, E., Weiss, L., Flaishon, L., Shachar, I., *et al.* (2006). IFN-gamma acts on T cells to induce NK cell mobilization and accumulation in target organs. *J Immunol* 176, 4716-4729. <https://doi.org/10.4049/jimmunol.176.8.4716>
- Walzer, T., Chiossone, L., Chaix, J., Calver, A., Carozzo, C., Garrigue-Antar, L., Jacques, Y., Baratin, M., Tomasello, E. und Vivier, E. (2007). Natural killer cell trafficking in vivo requires a dedicated sphingosine 1-phosphate receptor. *Nat Immunol* 8, 1337-1344. <https://doi.org/10.1038/ni1523>
- Wang, P.L., O'Farrell, S., Clayberger, C. und Krensky, A.M. (1992). Identification and molecular cloning of tactile. A novel human T cell activation antigen that is a member of the Ig gene superfamily. *J Immunol* 148, 2600-2608.
- Warren, A., Le Couteur, D.G., Fraser, R., Bowen, D.G., McCaughan, G.W. und Bertolino, P. (2006). T lymphocytes interact with hepatocytes through fenestrations in murine liver sinusoidal endothelial cells. *Hepatology* 44, 1182-1190. <https://doi.org/10.1002/hep.21378>
- Weber, C., Weber, K.S., Klier, C., Gu, S., Wank, R., Horuk, R. und Nelson, P.J. (2001). Specialized roles of the chemokine receptors CCR1 and CCR5 in the recruitment of monocytes and T(H)1-like/CD45RO(+) T cells. *Blood* 97, 1144-1146. <https://doi.org/10.1182/blood.v97.4.1144>
- Weizman, O.E., Adams, N.M., Schuster, I.S., Krishna, C., Pritykin, Y., Lau, C., Degli-Esposti, M.A., Leslie, C.S., Sun, J.C. und O'Sullivan, T.E. (2017). ILC1 Confer Early Host Protection at Initial Sites of Viral Infection. *Cell* 171, 795-808 e712. <https://doi.org/10.1016/j.cell.2017.09.052>
- Wendel, M., Galani, I.E., Suri-Payer, E. und Cerwenka, A. (2008). Natural killer cell accumulation in tumors is dependent on IFN-gamma and CXCR3 ligands. *Cancer Res* 68, 8437-8445. <https://doi.org/10.1158/0008-5472.CAN-08-1440>
- Wiegand, C., Frenzel, C., Herkel, J., Kallen, K.J., Schmitt, E. und Lohse, A.W. (2005). Murine liver antigen presenting cells control suppressor activity of CD4+CD25+ regulatory T cells. *Hepatology* 42, 193-199. <https://doi.org/10.1002/hep.20756>
- Wisse, E., De Zanger, R.B., Charels, K., Van Der Smissen, P. und McCuskey, R.S. (1985). The liver sieve: considerations concerning the structure and function of endothelial fenestrae, the sinusoidal wall and the space of Disse. *Hepatology* 5, 683-692. <https://doi.org/10.1002/hep.1840050427>
- Wittlich, M., Dudek, M., Bottcher, J.P., Schanz, O., Hegenbarth, S., Bopp, T., Schmitt, E., Kurts, C., Garbers, C., Rose John, S., *et al.* (2017). Liver sinusoidal endothelial

- cell cross-priming is supported by CD4 T cell-derived IL-2. *J Hepatol* 66, 978-986. <https://doi.org/10.1016/j.jhep.2016.12.015>
- Wong, J., Johnston, B., Lee, S.S., Bullard, D.C., Smith, C.W., Beaudet, A.L. und Kubes, P. (1997). A minimal role for selectins in the recruitment of leukocytes into the inflamed liver microvasculature. *J Clin Invest* 99, 2782-2790. <https://doi.org/10.1172/JCI119468>
- Wu, J., Meng, Z., Jiang, M., Zhang, E., Trippler, M., Broering, R., Bucchi, A., Krux, F., Dittmer, U., Yang, D., *et al.* (2010). Toll-like receptor-induced innate immune responses in non-parenchymal liver cells are cell type-specific. *Immunology* 129, 363-374. <https://doi.org/10.1111/j.1365-2567.2009.03179.x>
- Wu, L.Q., Zhang, W.J., Niu, J.X., Ye, L.Y., Yang, Z.H., Grau, G.E. und Lou, J.N. (2008). Phenotypic and functional differences between human liver cancer endothelial cells and liver sinusoidal endothelial cells. *J Vasc Res* 45, 78-86. <https://doi.org/10.1159/000109079>
- Xu, B., Broome, U., Uzunel, M., Nava, S., Ge, X., Kumagai-Braesch, M., Hultenby, K., Christensson, B., Ericzon, B.G., Holgersson, J., *et al.* (2003). Capillarization of hepatic sinusoid by liver endothelial cell-reactive autoantibodies in patients with cirrhosis and chronic hepatitis. *Am J Pathol* 163, 1275-1289. [https://doi.org/10.1016/S0002-9440\(10\)63487-6](https://doi.org/10.1016/S0002-9440(10)63487-6)
- Yao, Z., Mates, J.M., Cheplowitz, A.M., Hammer, L.P., Maiseyeu, A., Phillips, G.S., Wewers, M.D., Rajaram, M.V., Robinson, J.M., Anderson, C.L., *et al.* (2016). Blood-Borne Lipopolysaccharide Is Rapidly Eliminated by Liver Sinusoidal Endothelial Cells via High-Density Lipoprotein. *J Immunol* 197, 2390-2399. <https://doi.org/10.4049/jimmunol.1600702>
- Yu, X., Harden, K., Gonzalez, L.C., Francesco, M., Chiang, E., Irving, B., Tom, I., Ivelja, S., Refino, C.J., Clark, H., *et al.* (2009). The surface protein TIGIT suppresses T cell activation by promoting the generation of mature immunoregulatory dendritic cells. *Nat Immunol* 10, 48-57. <https://doi.org/10.1038/ni.1674>
- Zabel, B.A., Wang, Y., Lewen, S., Berahovich, R.D., Penfold, M.E., Zhang, P., Powers, J., Summers, B.C., Miao, Z., Zhao, B., *et al.* (2009). Elucidation of CXCR7-mediated signaling events and inhibition of CXCR4-mediated tumor cell transendothelial migration by CXCR7 ligands. *J Immunol* 183, 3204-3211. <https://doi.org/10.4049/jimmunol.0900269>
- Zheng, M. und Tian, Z. (2019). Liver-Mediated Adaptive Immune Tolerance. *Front Immunol* 10, 2525. <https://doi.org/10.3389/fimmu.2019.02525>
- Zhu, J., Yamane, H. und Paul, W.E. (2010). Differentiation of effector CD4 T cell populations (\*). *Annu Rev Immunol* 28, 445-489. <https://doi.org/10.1146/annurev-immunol-030409-101212>
- Zlotnik, A. und Yoshie, O. (2000). Chemokines: a new classification system and their role in immunity. *Immunity* 12, 121-127. [https://doi.org/10.1016/s1074-7613\(00\)80165-x](https://doi.org/10.1016/s1074-7613(00)80165-x)
- Zwirner, N.W. und Domaica, C.I. (2010). Cytokine regulation of natural killer cell effector functions. *Biofactors* 36, 274-288. <https://doi.org/10.1002/biof.107>

## 8 ABBREVIATIONS

7-AAD	7-aminoactinomycin D
ACK	Ammonium-chloride-potassium buffer
Ahr	Aryl hydrocarbon receptor
APC	Allophycocyanin
APC	Antigen presenting cell
APC-Cy7	Allophycocyanin conjugated with cyanine7
BCR	B cell receptor
BV	Brilliant violet
CCL	CC motif chemokine ligand
CCl <sub>4</sub>	Carbon tetrachloride
CCR	CC motif chemokine receptor
CD	Cluster of differentiation
cDNA	complementary DNA
CHILP	Common helper-like ILC progenitor
CILP	Common ILC progenitor
CSF	Colony-stimulating factor
CXCL	CXC motif chemokine ligand
CXCR	CXC motif chemokine receptor
DAMP	Damage-associated molecular pattern
DMSO	Dimethylsulphoxide
DNA	Deoxyribonucleic acid
DNAM-1	DNAX accessory molecule-1
EC	Endothelial cells
ELISA	Enzyme-linked immunosorbent assay
Eomes	Eomesodermin
FACS	Fluorescence-activated cell sorting
FITC	Fluorescein isothiocyanate
Flox	Flanked by LoxP
FoxP3	Forkhead box P3
FSC-A	Forward scatter area
GATA3	GATA-binding protein 3
h	Hour(s)

HCC	Hepatocellular carcinoma
HSC	Hepatic stellate cell
IFN	Interferon
IFN- $\gamma$	Interferon gamma
IL	Interleukin
ILCs	Innate lymphoid cells
Iso	Isotype
KC	Kupffer cell
KO	Knockout
LPS	Lipopolysaccharide
LSECs	Liver sinusoidal endothelial cells
MACS	Magnetic-activated cell sorting
MCMV	Mouse Cytomegalovirus
MFI	Mean fluorescence intensity
MHC	Major histocompatibility complex
MIF	Macrophage migration inhibitory factor
min	Minute(s)
Mono	Monocyte
NASH	Non-alcoholic steatohepatitis
n.s.	Not significant
NK cells	Natural killer cells
NKT	Natural Killer T cell
PAMP	Pathogen-associated molecular pattern
PBS	Phosphate-buffered saline
PCR	Polymerase chain reaction
PD-1	Programmed cell death protein 1
PD-L1	Programmed death-ligand 1
PE	Phycoerythrin
PE-Cy7	Phycoerythrin conjugated with cyanine7
PRR	Pattern recognition receptor
p-value	Probability value
rpm	revolutions per minute
RT	Room temperature
RT-PCR	Real time polymerase chain reaction

s	Second(s)
SEM	Standard error of the mean
SSC-A	Side scatter area
Tbet	T-box protein expressed in T cells
TCR	T cell receptor
TGF- $\beta$	Transforming growth factor beta
Th1	Type 1 helper T cell
Th17	Type 17 helper T cell
Th2	Type 2 helper T cell
TLR	Toll-like receptor
TNF- $\alpha$	Tumor necrosis factor alpha
TRAIL	TNF-related apoptosis-inducing ligand
Treg	Regulatory T cell
VEGF	Vascular growth factor
WT	Wild type
XCL	XC motif chemokine ligand





## 9 CURRICULUM VITAE

### PERSONAL INFORMATION

Name and Surname	Sophia Georgia Paraskevi Papaioannou
Date of birth	12.03.1994
Place of birth	Mainz, Germany
Nationality	German

### EDUCATION

08/2019 – Today	<b>Promotion, Dr. sc. hum. (scientiarum humanarum)</b> Majored in Immunology Medical Faculty of Mannheim University of Heidelberg, Germany Thesis: Interaction of endothelial cells and innate lymphoid cells in hepatic inflammation and cancer
09/2017 – 04/2019	<b>Master of Science</b> in Molecular Medicine Georg-August University of Göttingen, Germany Thesis: The role of CD2AP and EpCAM on exosomal composition and their influence on the tumor microenvironment
09/2013 – 02/2017	<b>Bachelor of Science</b> in Bio Science and Health Hochschule Rhein-Waal, Kleve, Germany Thesis: ADAM10 and ADAM17 as potential molecular switches of dendritic cell migration
2004 - 2013	<b>Allgemeine Hochschulreife</b> Gymnasium am Römerkastell, Alzey, Germany

## WORKING EXPERIENCE

05/2017 – 09/2017      Research Assistant  
University Medical Center Mainz, Germany  
Institute for Molecular Medicine

## PUBLICATIONS

**Papaioannou, S.\***, See, J. X.\*, Jeong, M., De La Torre, C., Ast, V., Reiners-Koch, P. S., Sati, A., Mogler, C., Platten, M., Cerwenka, A., & Stojanovic, A. (2023). Liver sinusoidal endothelial cells orchestrate NK cell recruitment and activation in acute inflammatory liver injury. *Cell Reports*, 42(8), 112836. <https://doi.org/10.1016/j.celrep.2023.112836>. \*equal contribution

See, J. X.\*, **Papaioannou, S.\***, (...), Cerwenka, A., & Stojanovic, A. Protocol for the isolation and purification of murine liver sinusoidal endothelial cells for in vitro culture and functional assays. STAR Protoc. *In preparation*. \*equal contribution

See, J. X.\*, **Papaioannou, S.\***, (...), Cerwenka, A., & Stojanovic, A. Innate lymphocyte-derived IFN- $\gamma$  maintains MHC II expression on LSECs and KCs for CD4<sup>+</sup> T cell homeostasis in the liver. *In preparation*. \*equal contribution

## 10 ACKNOWLEDGEMENTS

First, I would like to thank Prof. Dr. Adelheid Cerwenka for giving me the opportunity to conduct my PhD in her lab, for her support and organization of collaborations that were driving the project forward. Next, I would like to express my deepest gratitude to my supervisor Dr. Ana Stojanovic for her guidance, support, and insightful feedback throughout the journey of this research. Her expertise, encouragement, and patience have been instrumental in shaping this project, the publication and this thesis. Thank you for trusting me with my experimental ideas, for your help in the lab, late-night sorts, sharing your antibodies and a great Oslo trip.

I am also thankful to Prof. Dr. Umansky for being a member of my examination committee and my thesis advisory committee, thereby guiding me and my project. I am grateful to Prof. Dr. Dieterich and Prof. Dr. Geraud for agreeing to be members of my examination committee. Thank you to Prof. Dr. Reiners-Koch for being a member of my thesis advisory committee, the great collaboration and advices on LSECs.

My sincere appreciation extends to my colleagues and friends of the IBC lab. Special thanks to mouse team, Uncle Jia and Mingeuma, for always supporting me during experiments, introducing me to the Asian cuisine to train my spicy food tolerance, and spending the best birthday in 2022 with me. Thank you Jia, my second unofficial supervisor, for teaching me all your knowledge on LSECs and ILCs, fun times during long experiments and outside of the lab. Many thanks to Mingeuma, for many many hugs, Christmas market magic, sharing awesome Korean snacks and sweets, and making unforgettable memories in and outside of Germany. I am truly grateful to Irene, for always encouraging and motivating me, for supporting me during the ups and downs of PhD, puzzle and movie nights, and even more hugs. Thank you Tomato for providing me with an endless supply of mandarines, cookies and marlenka. Next, I would like to thank Francesco, Sebastiano, Bianca, Silvina, Helen and Andi for the fun times in the lab and during outings.

I would also like to thank Sina, the technicians, especially Petra, and all other members of the lab for their support and assistance during my PhD.

Ein besonderer Dank geht an Fabi und Tory, für ermutigende Worte und Geduld, wenn ich mich überwältigt gefühlt habe. Tory, danke für deine unermüdlichen side-eyes und die beste Stadt-Land-WG; Figures 4.22+4.23 sind für Dich. Mein Dank geht auch an die Prinzessinnen, und an all die anderen Freunde, die mich mit ihrer positiven Energie unterstützt haben.

Zuletzt, aber keineswegs am wenigsten, bin ich meiner Familie zutiefst dankbar für ihre Liebe, Ermutigung und ihr Verständnis während meines Studiums. Danke Mama, deine Unterstützung war meine größte Stärke und Motivation.